

Supporting Information

Synthesis of Chiral 1,4-Oxazepane-5-Carboxylic Acids from Polymer-Supported Homoserine

Petra Králová,¹ Barbora Lemrová,¹ Michal Maloň,² and Miroslav Soural^{1,3*}

¹ Department of Organic Chemistry, Faculty of Science, Palacký University, 771 46 Olomouc, Czech Republic

² JEOL (U.K.) Ltd., JEOL House, Silver Court, Watchmead, Welwyn Garden City, Hertfordshire AL7 1LT, United Kingdom

³ Institute of Molecular and Translational Medicine, Faculty of Medicine and Dentistry, Palacký University, Hněvotínská 5, 779 00 Olomouc, Czech Republic

*Corresponding author. E-mail: miroslav.soural@upol.cz

Content

Analytical Data (NMR, IR, HRMS and optical rotation) of Prepared Derivatives	S2
(-)-(S)-2-nitro-N-(2-oxo-2-phenethyl)-N-(2-oxotetrahydrofuran-3-yl)benzenesulfonamide 5a	S2
(-)-ammonium (2R,5S)-2-phenyl-4-tosyl-1,4-oxazepane-5-carboxylate 6g	S9
(-)-(2R,5S)-4-((2-aminophenyl)sulfonyl)-2-phenyl-1,4-oxazepane-5-carboxylic acid 7a	S11
(-)-(2R,5S)-4-((2-aminophenyl)sulfonyl)-2-phenyl-1,4-oxazepane-5-carboxamide 7b^{2R}	S18
(+)-(2S,5S)-4-((2-aminophenyl)sulfonyl)-2-phenyl-1,4-oxazepane-5-carboxamide 7b^{2S}	S20
(-)-(2R,5S)-4-((2-amino-4-methoxyphenyl)sulfonyl)-2-phenyl-1,4-oxazepane-5-carboxylic acid 7e	S25
(-)-(2RS,5S)-4-((2-amino-4-chlorophenyl)sulfonyl)-2-phenyl-1,4-oxazepane-5-carboxylic acid 7f^{2RS}	S27
(-)-(2R,5S)-4-((2-aminophenyl)sulfonyl)-2-(2-fluorophenyl)-1,4-oxazepane-5-carboxylic acid 7i^{2R}	S29
(-)-(2S,5S)-4-((2-aminophenyl)sulfonyl)-2-(2-fluorophenyl)-1,4-oxazepane-5-carboxylic acid 7i^{2S}	S31
(-)-(2R,5S)-4-((2-aminophenyl)sulfonyl)-2-(3-fluorophenyl)-1,4-oxazepane-5-carboxylic acid 7k	S33
(+)-(2R,5S)-4-((2-aminophenyl)sulfonyl)-2-(p-tolyl)-1,4-oxazepane-5-carboxylic acid 7m	S35
(+)-(2R,5S)-4-((2-aminophenyl)sulfonyl)-2-(4-fluorophenyl)-1,4-oxazepane-5-carboxylic acid 7o	S37
(-)-(2R,5S)-4-((2-aminophenyl)sulfonyl)-2-(4-(trifluoromethyl)phenyl)-1,4-oxazepane-5-carboxylic acid 7q	S39
(-)-(2R,5S)-4-((2-aminophenyl)sulfonyl)-2-(thiophen-3-yl)-1,4-oxazepane-5-carboxylic acid 7t	S41
(-)-(S)-3-(1,1-dioxo-4-(o-tolyl)benzo[f][1,2,5]thiadiazepin-2(5H)-yl)dihydrofuran-2(3H)-one 9h	S43
(-)-(S)-3-(4-(2-bromophenyl)-1,1-dioxobenzof[f][1,2,5]thiadiazepin-2(5H)-yl)dihydrofuran-2(3H)-one 9j	S45
(+)-(S)-((2-aminophenyl)sulfonyl)-L-homoserine 10r	S47
(-)-(S)-N-(4-methoxyphenethyl)-2-nitro-N-(2-oxotetrahydrofuran-3-yl)benzenesulfonamide 11n	S50

Analytical Data (NMR, IR, HRMS and optical rotation) of Prepared Derivatives

(-)-(S)-2-nitro-N-(2-oxo-2-phenethyl)-N-(2-oxotetrahydrofuran-3-yl)benzenesulfonamide **5a**

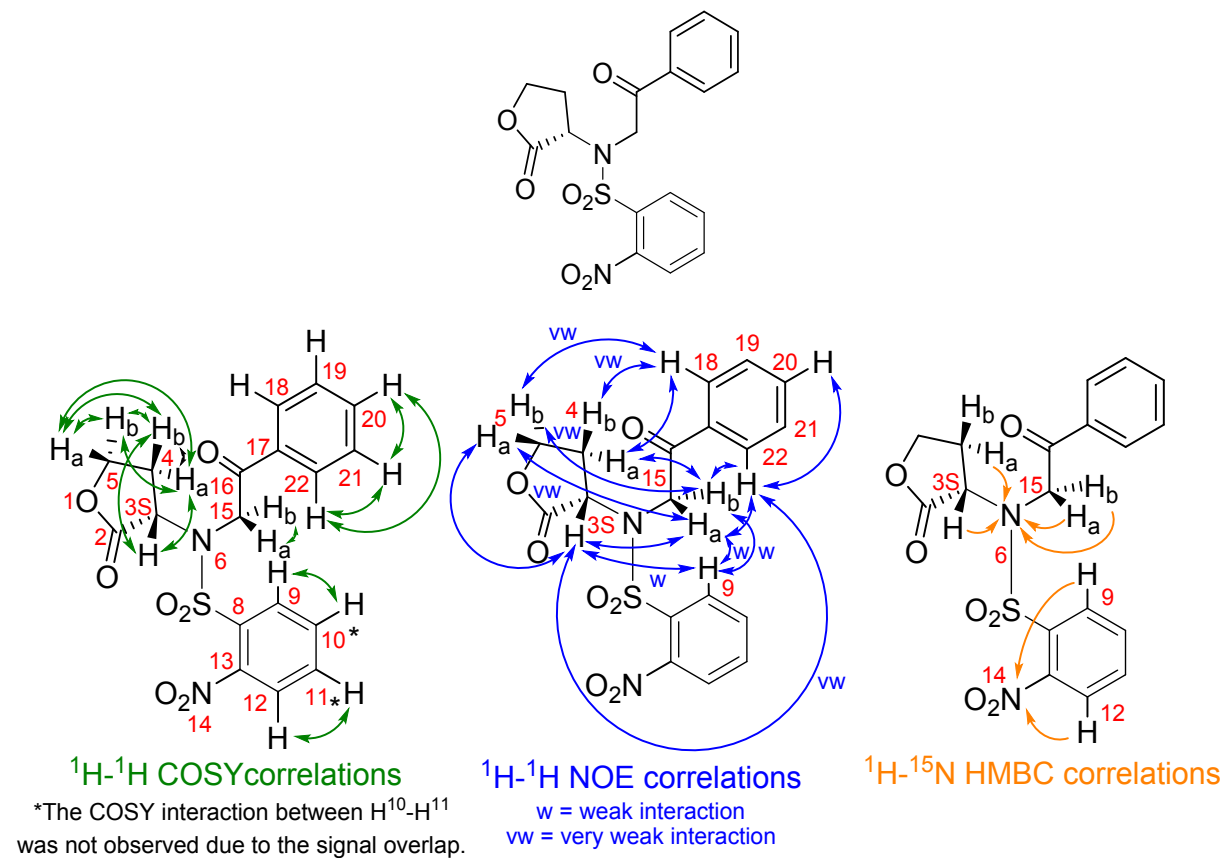


Figure S1. Detailed COSY, NOE and ^1H - ^{15}N HMBC NMR analysis of lactone **5a**

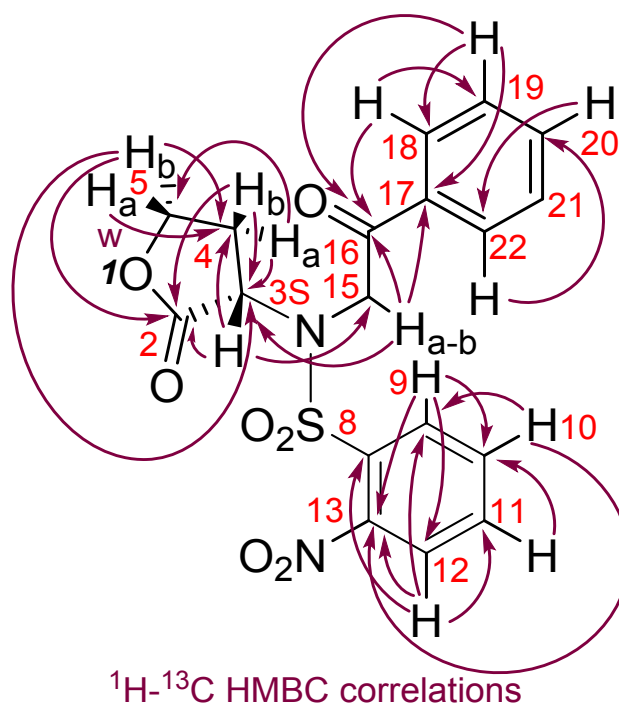


Figure S2. Detailed ^1H - ^{13}C HMBC NMR analysis of lactone **5a**

Table S1. ^1H NMR (500 MHz) and $^{13}\text{C}\{^1\text{H}\}$ NMR (126 MHz) data, including detailed COSY, ^1H - ^{13}C HMBC and NOE correlations for lactone **5a**^a

position	^1H NMR δ_{H} [ppm] ^b	splitting pattern, J [Hz], integration	$^{13}\text{C}\{^1\text{H}\}$ NMR δ_{C} [ppm]	COSY correlations	^1H - ^{13}C HMBC correlations	NOE correlations
2	-	-	174.4	-	-	-
3	5.05	dd, $J = 12.4, 8.7$ Hz, 1H	58.6	$\text{H}_a^4, \text{H}_b^4$	28.4, 53.2, 174.4	H_a^5, H^9 (weak int.), $\text{H}_a^{15}, \text{H}^{18,22}$ (very weak int.)
4	H_a : 2.29	dddd, $J = 12.5, 12.5, 11.2, 9.0$ Hz, 1H	28.4	$\text{H}^3, \text{H}_a^5, \text{H}_b^5$	58.6, 66.2	$\text{H}_b^{15}, \text{H}^{18,22}$
	H_b : 2.57	dddd, $J = 12.7, 8.7, 5.8, 1.0$ Hz, 1H		$\text{H}^3, \text{H}_a^5, \text{H}_b^5$ (weak int.)	58.6, 174.4	$\text{H}^{18,22}$ (very weak int.)
5	H_a : 4.24	ddd, $J = 11.2, 9.0, 5.8$ Hz, 1H	66.7	$\text{H}_a^4, \text{H}_b^4, \text{H}_b^5$ $\text{H}_a^4, \text{H}_b^4$ (weak int.), H_a^5	28.4 (weak int.)	$\text{H}^3, \text{H}_a^{15}$
	H_b : 4.31	ddd, $J = 9.0, 9.0, 1.0$ Hz, 1H		$\text{H}_a^5,$	28.4, 58.6, 174.4	H_a^{15} (very weak int.), $\text{H}^{18,22}$ (very weak int.)
8	-	-	133.8	-	-	-
9	8.26	dd, $J = 7.7, 1.6$ Hz, 1H	131.6	H^{10}	125.4, 135.4, 148.9	$\text{H}^{11}, \text{H}^{12}$
10	7.81	m, 1H	125.1	H^9	131.6, 148.9	H^{12}
11	7.77	m, 1H	133.3	H^{12}	125.4	H^9
12	7.75	m, 1H	135.4	H^{11}	131.6, 133.3, 133.8, 148.9	$\text{H}^9, \text{H}^{10}$
13	-	-	148.9	-	-	-
15	H_a : 5.25	$J = 19.2$ Hz, 1H	53.2	H_b^{15}	58.6, 135.5, 194.7	H^3, H_a^5 (very weak int.), H^9 (weak int.), $\text{H}^{18,22}$
	H_b : 4.60	d, $J = 19.2$ Hz, 1H		H_a^{15}	58.6, 135.5, 194.7	$\text{H}_a^4, \text{H}_b^5$ (very weak int.), H^9 (weak int.), $\text{H}^{18,22}$
16	-	-	194.7	-	-	-
17	-	-	135.5	-	-	-
18,22	7.94-7.96	m, 2H	128.9	$\text{H}^{19,21}$	129.8, 134.9, 194.7	H^{20}
19,21	7.50-7.54	m, 2H	129.8	$\text{H}^{18,22}, \text{H}^{20}$	128.9, 135.5, 194.7	-
20	7.63-7.67	m, 1H	134.9	H^{21}	128.9	$\text{H}^{18,22}$

^aAssignments are based on extensive 1D and 2D NMR analysis (^1H - ^1H COSY, ^1H - ^{13}C HMQC, ^1H - ^{13}C HMBC and ^1H - ^1H NOESY); measured in MeCN- d_3 ; int. = interaction.

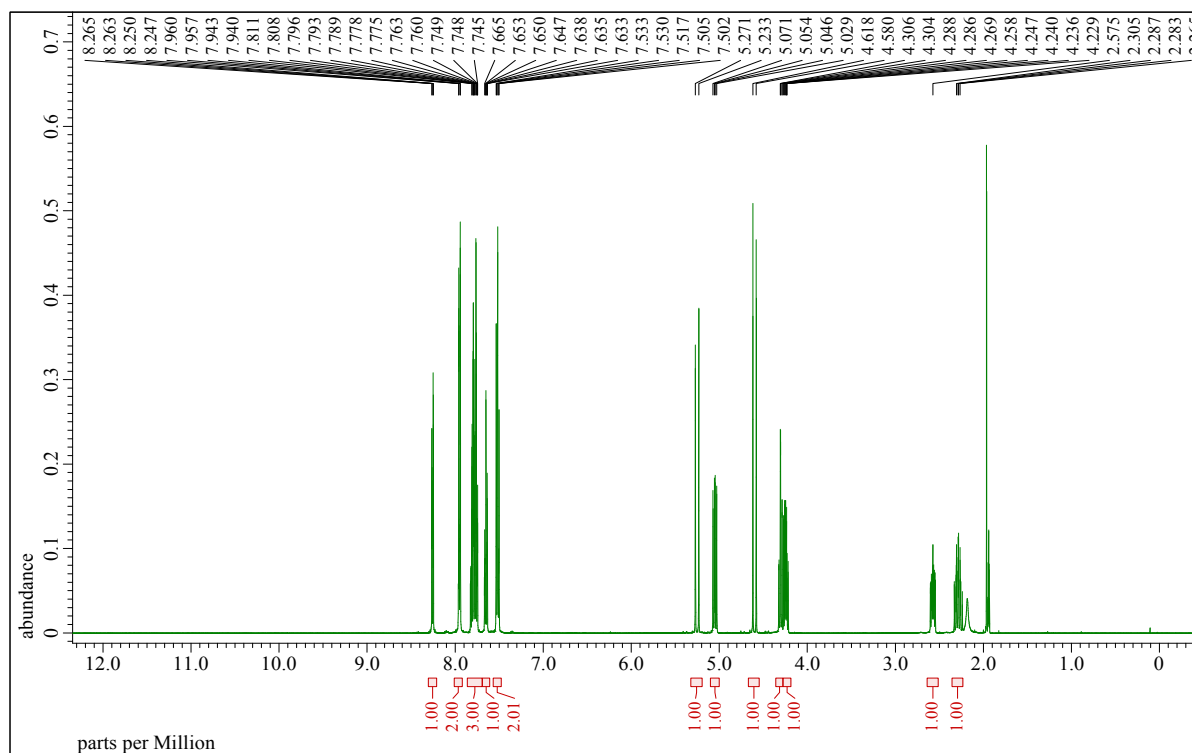


Figure S3. ^1H NMR spectrum of **5a** (500 MHz, $\text{MeCN-}d_3$); note: the signal of non-deuterated MeCN at 1.96 ppm and $\text{MeCN-}d_3$ at 1.94 ppm in ratio 62:38 in ^1H NMR

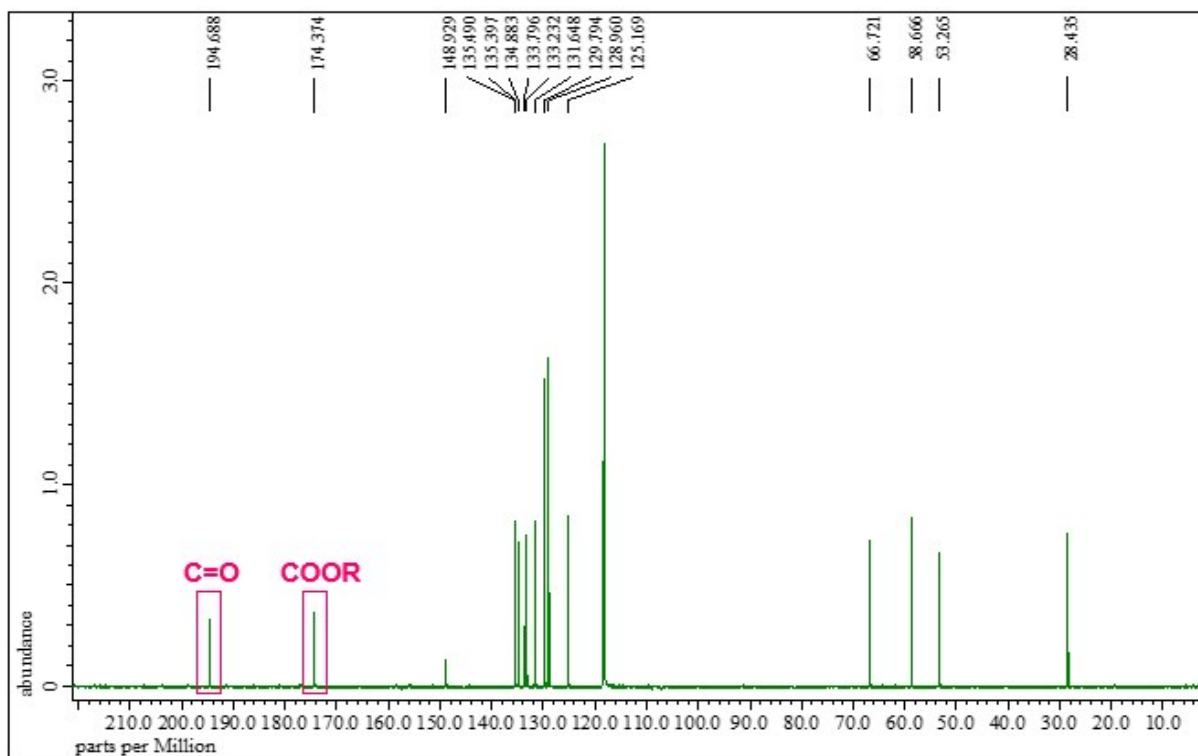


Figure S4. $^{13}\text{C}\{^1\text{H}\}$ NMR spectrum of **5a** (126 MHz, $\text{MeCN-}d_3$)

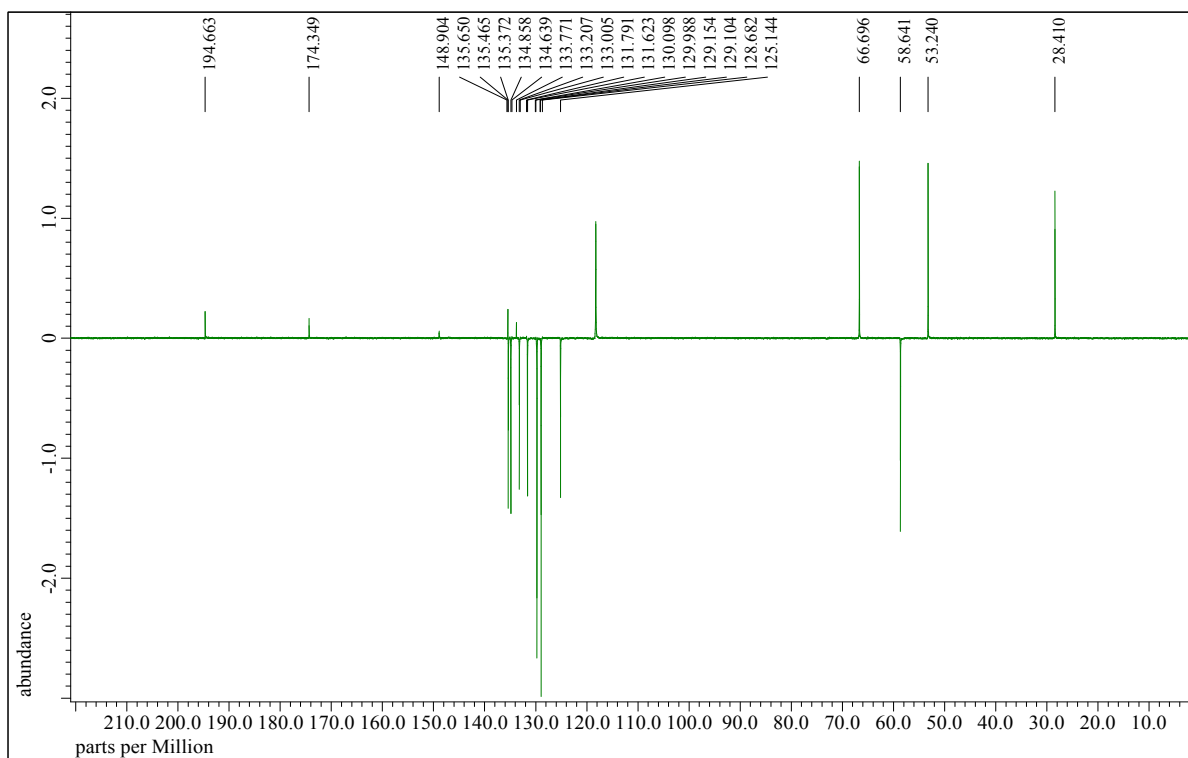


Figure S5. ¹³C APT NMR spectrum of **5a** (126 MHz, MeCN-*d*₃)

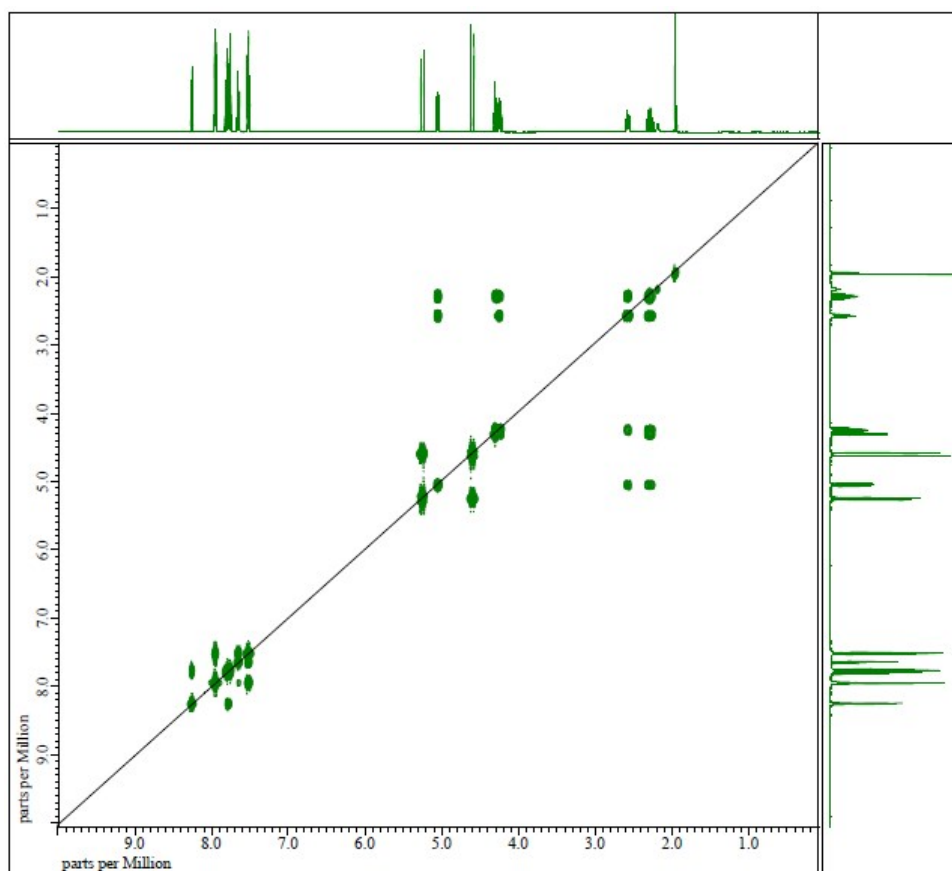


Figure S6. ¹H-¹H COSY NMR spectrum of **5a** (500 MHz, MeCN-*d*₃)

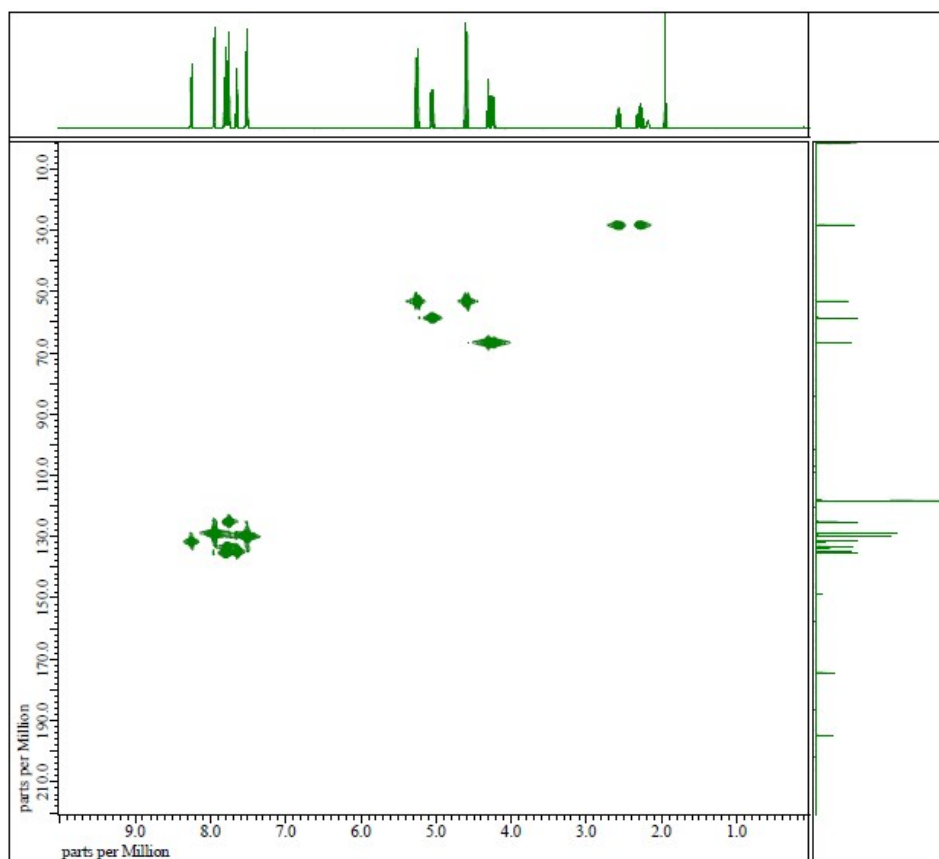


Figure S7. ^1H - ^{13}C HMQC NMR spectrum of **5a** ($\text{MeCN-}d_3$)

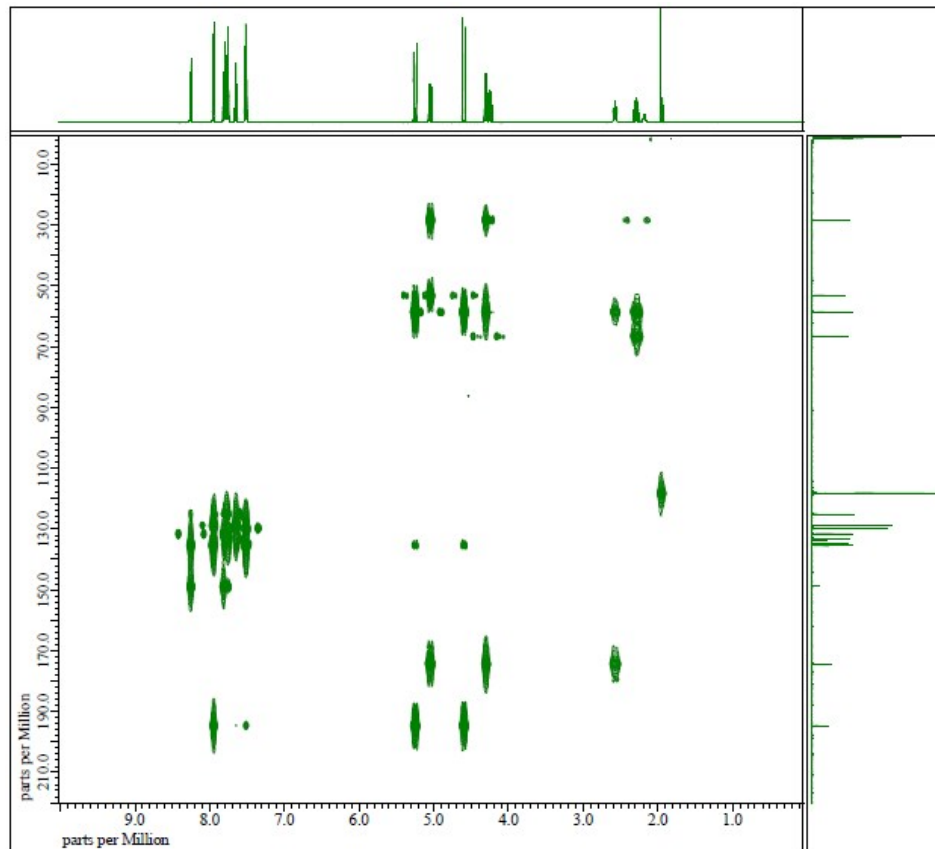


Figure S8. ^1H - ^{13}C HMBC NMR spectrum of **5a** ($\text{MeCN-}d_3$)

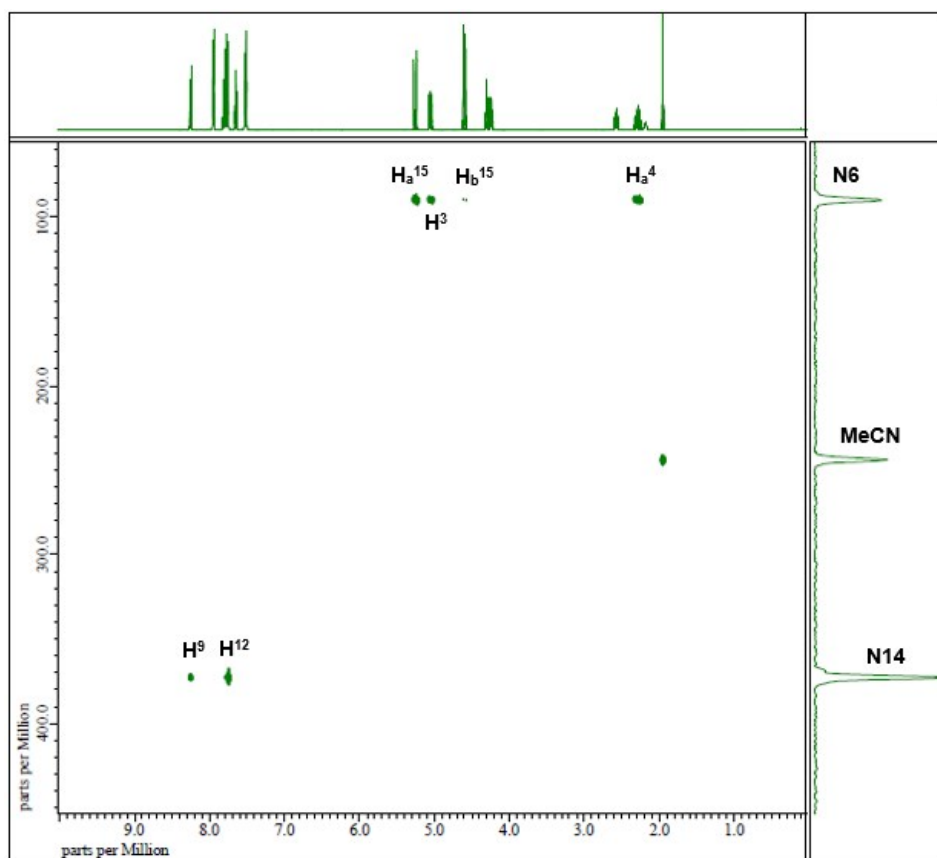


Figure S9. ^1H - ^{15}N HMBC NMR spectrum of **5a** ($\text{MeCN-}d_3$)

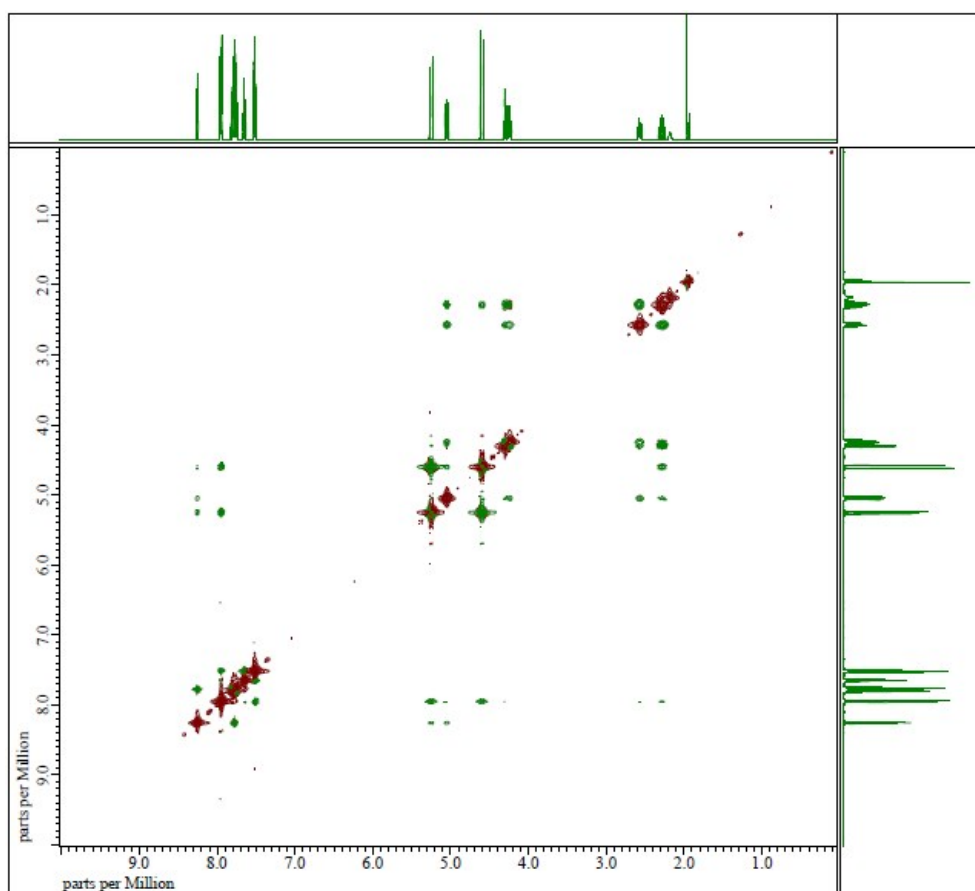


Figure S10. ^1H - ^1H NOESY NMR spectrum of **5a** ($\text{MeCN-}d_3$)

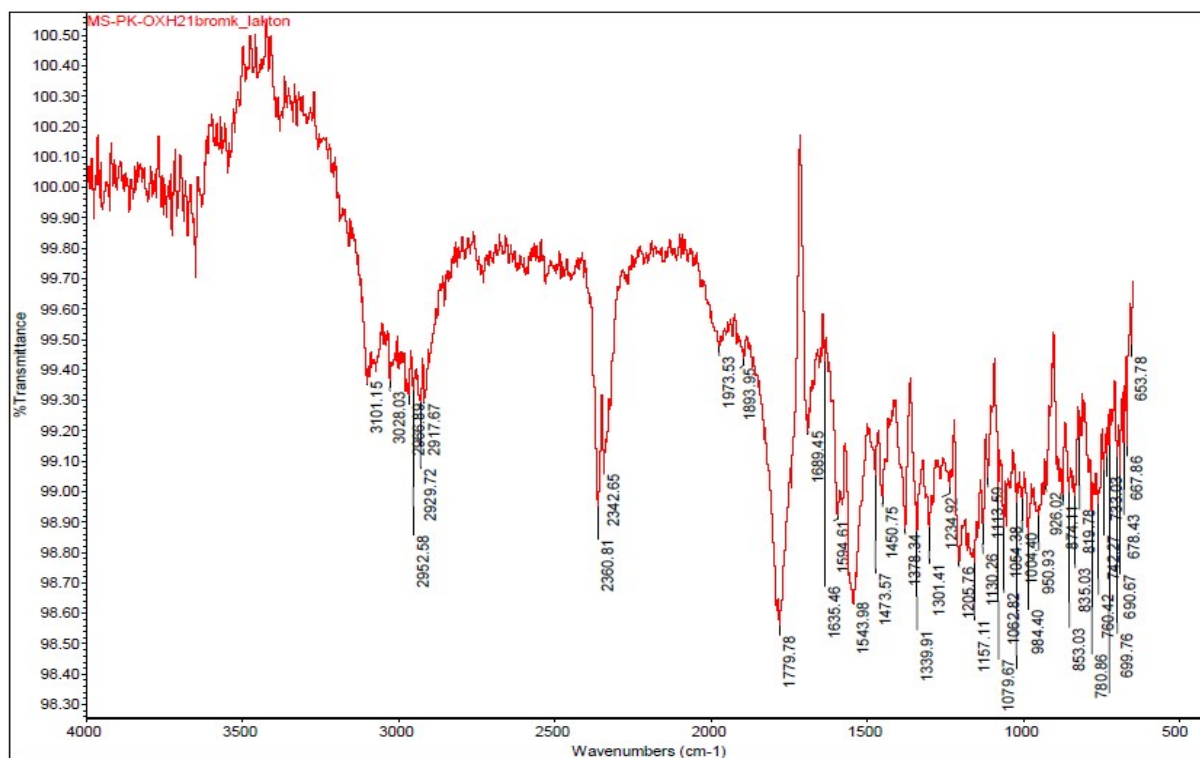


Figure S11. IR spectrum of 5a

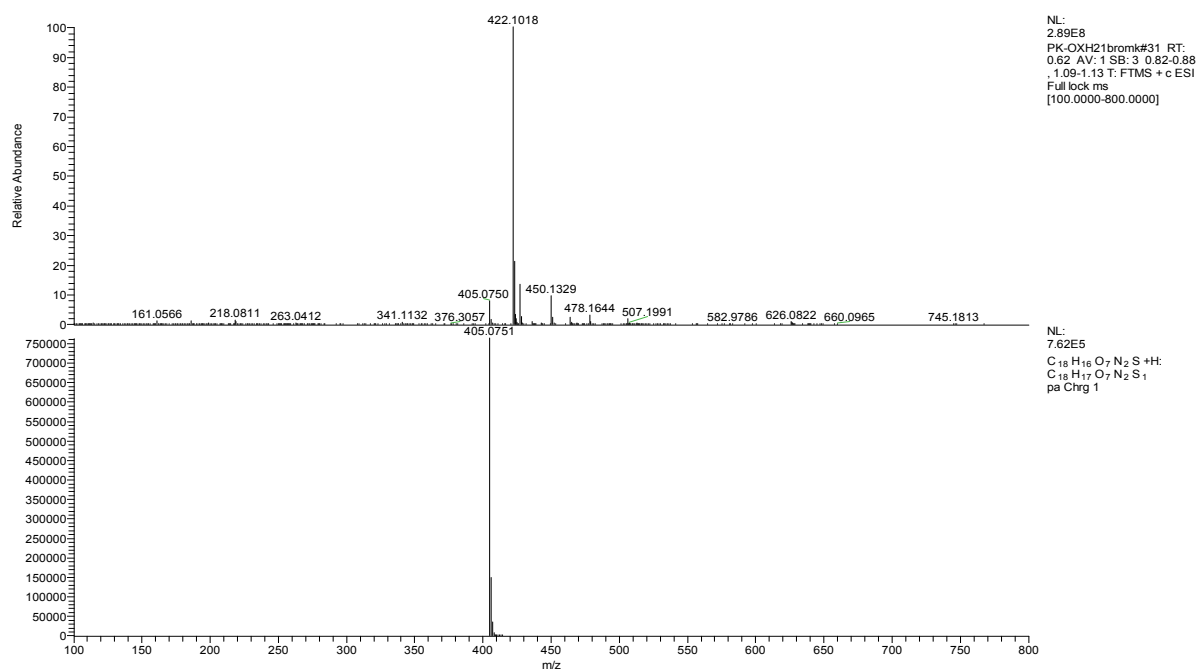


Figure S12. HRMS spectrum of 5a. Note: ion 422 belongs to the ammonium adduct originating from mobile phase.

(-)-ammonium (2*R*,5*S*)-2-phenyl-4-tosyl-1,4-oxazepane-5-carboxylate **6g**

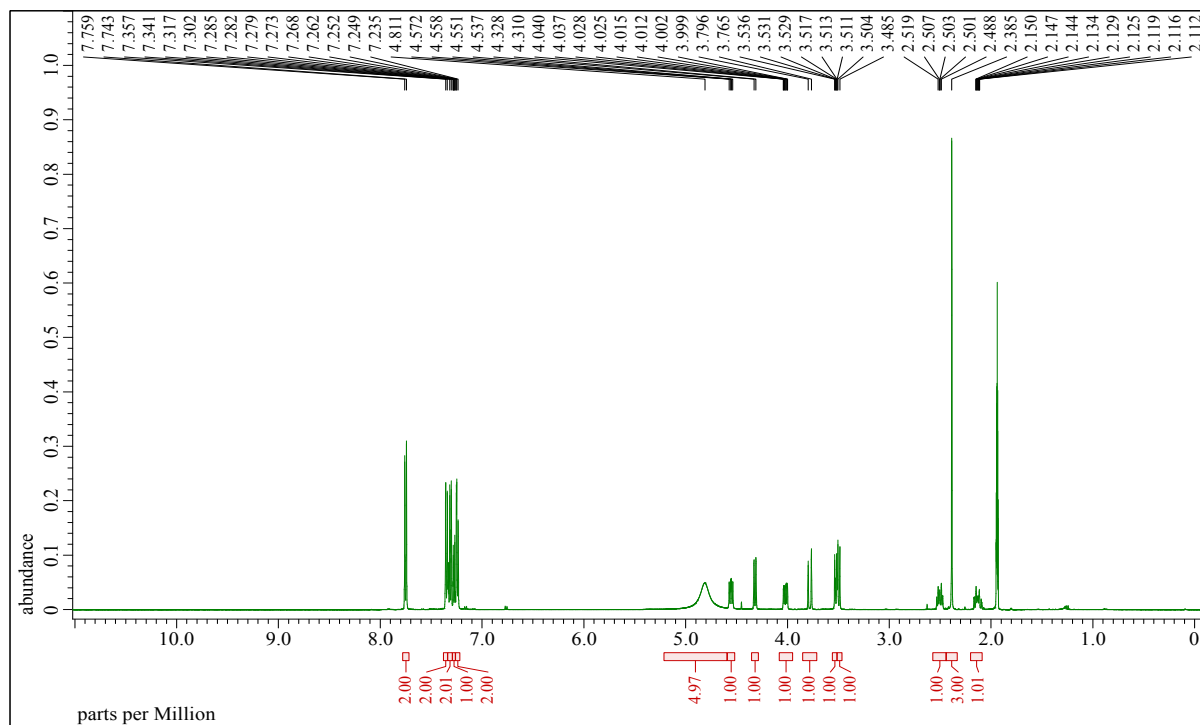
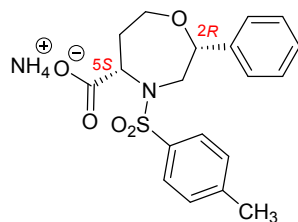


Figure S13. ^1H NMR spectrum of **6g** (500 MHz, $\text{MeCN-}d_3$). Note: The broad signal observed at 4.81 ppm represents ammonium ion and residual water.

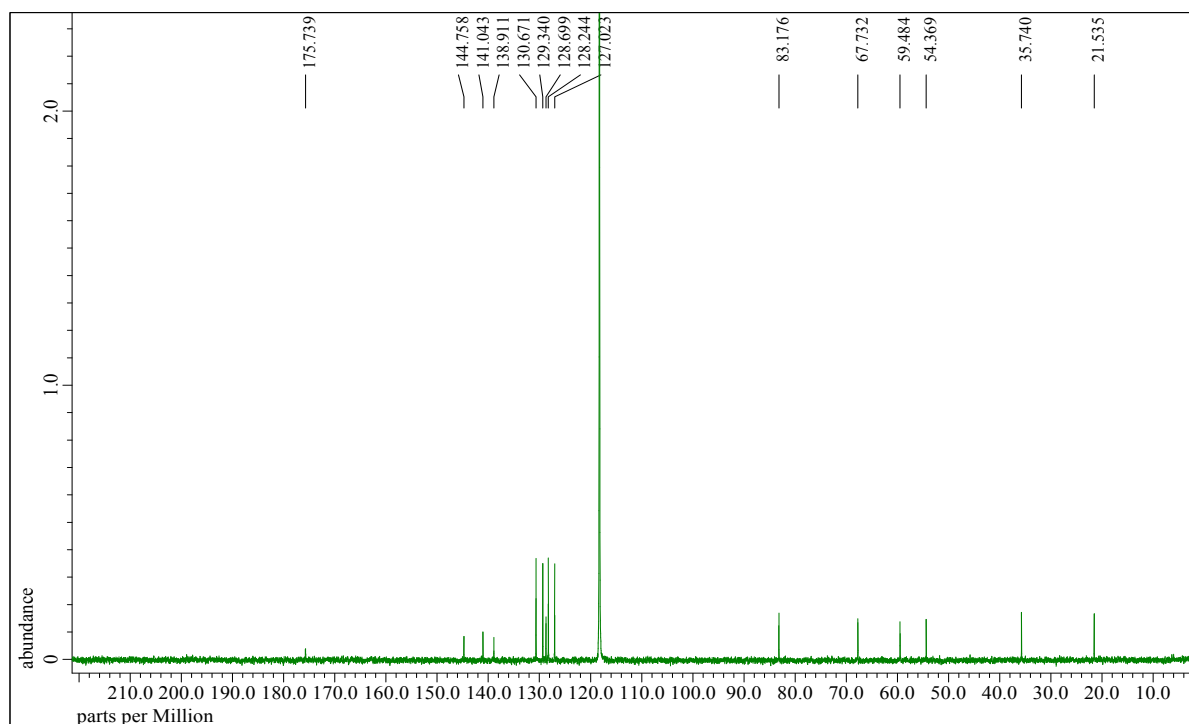


Figure S14. $^{13}\text{C}\{^1\text{H}\}$ NMR spectrum of **6g** (126 MHz, $\text{MeCN-}d_3$)

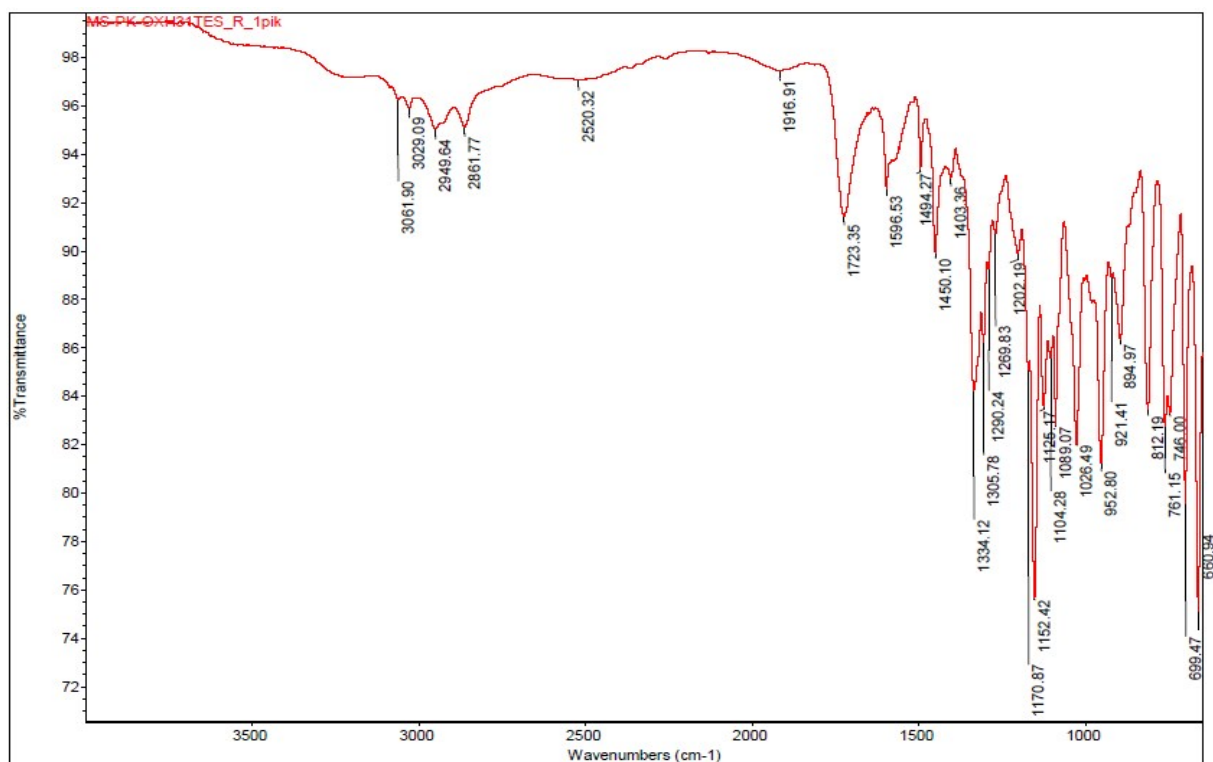


Figure S15. IR spectrum of 6g

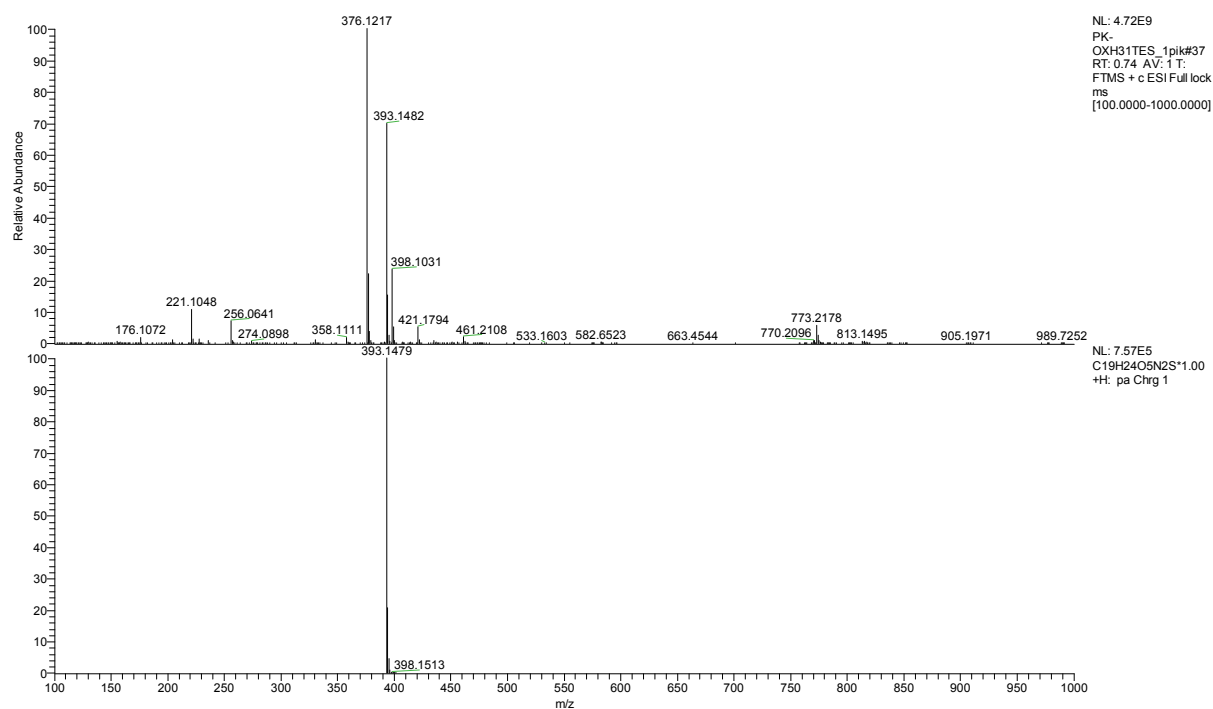


Figure S16. HRMS spectrum of 6g

(-)-(2R,5S)-4-((2-aminophenyl)sulfonyl)-2-phenyl-1,4-oxazepane-5-carboxylic acid 7a

The analytical data are identical for **7a** prepared from Wang resin or Wang-piperazine resin.

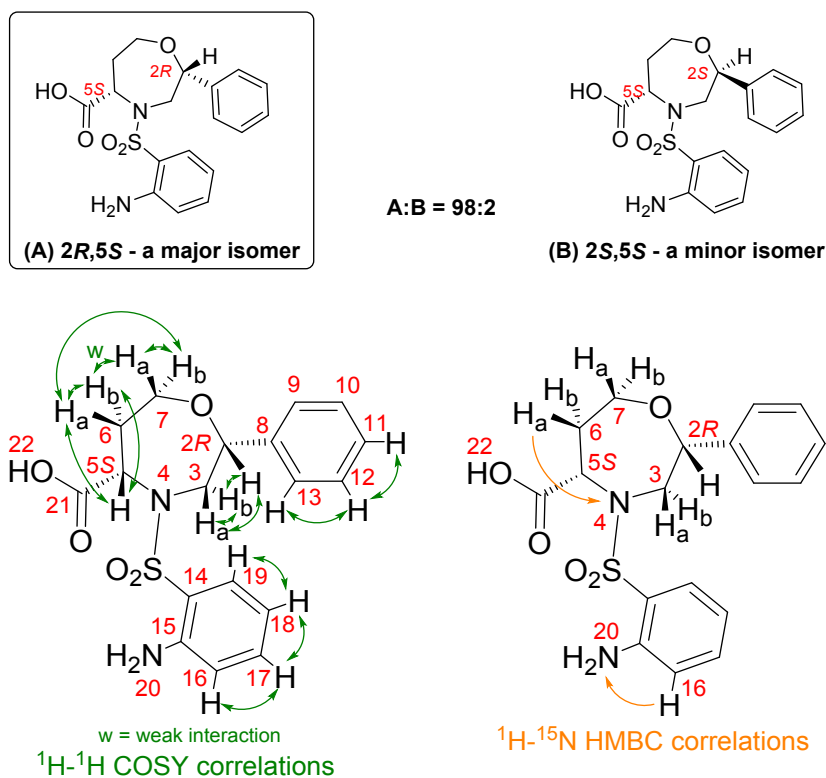


Figure S17. Detailed COSY and ^1H - ^{15}N HMBC NMR analysis of 1,4-oxazepane **7a**

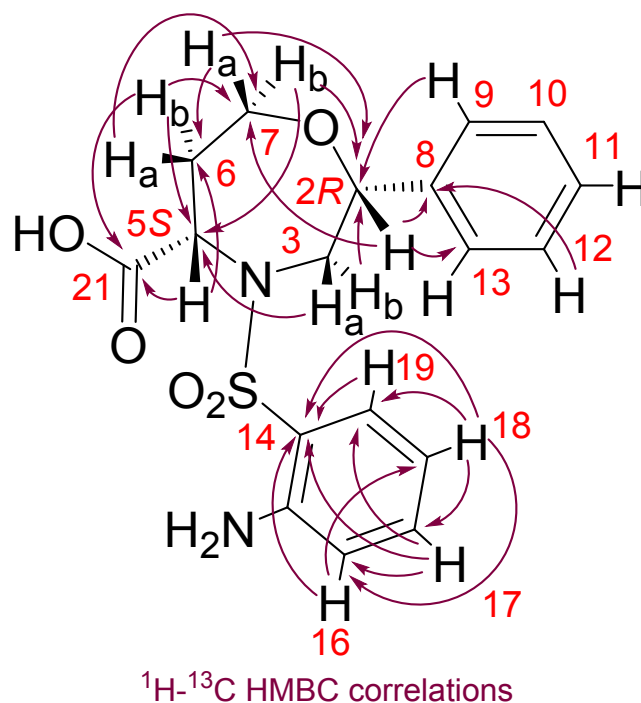


Figure S18. Detailed ^1H - ^{13}C HMBC NMR analysis of 1,4-oxazepane **7a**

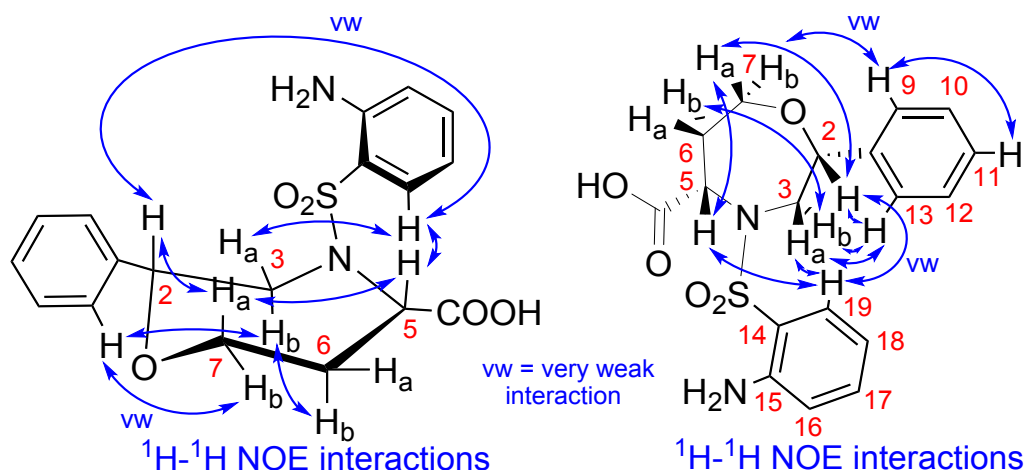


Figure S19. Detailed ¹H-¹H NOE NMR analysis of 1,4-oxazepane **7a**

Table S2. ¹H NMR (500 MHz) and ¹³C{¹H} NMR (126 MHz) data, including detailed COSY, ¹H-¹³C HMBC and NOE correlations for 1,4-oxazepane **7a**^a

position	¹ H NMR δ_{H} [ppm] ^b	splitting pattern, J [Hz], integration	¹³ C{ ¹ H} NMR δ_{C} [ppm]	COSY correlation s	¹ H- ¹³ C HMBC correlations	NOE correlations
2	4.16	d, $J = 9.5$ Hz, 1H	82.7	H _b ³	67.5, 127.1, 141.0	H _a ⁷ , H ^{9,13} , H ¹⁹ (weak int.)
3	H _a : 3.70	d, $J = 16.1$ Hz, 1H,	54.1	H _b ³	59.1	H ^{9,13} , H ¹⁹
	H _b : 3.50	dd, $J = 16.1, 9.5$ Hz, 1H		H ² , H _a ³	59.1 (weak int.), 82.7	H _b ⁶ , H ^{9,13}
5	4.66	dd, $J = 10.4, 7.1$ Hz, 1H	59.1	H _a ⁶ , H _b ⁶	35.6, 174.8	H _a ⁷ , H ¹⁹
6	H _a : 2.54	ddd, $J = 15.4, 7.1,$ 6.3 Hz, 1H	35.6	H ⁵ , H _b ⁶ , H _b ⁷	67.5	-
	H _b : 2.16	dddd, $J = 15.4,$ 10.4, 8.9, 1.1 Hz, 1H		H ⁵ , H _a ⁶ , H _a ⁷	59.1, 67.5, 174.8	H _b ³
7	H _a : 3.65	dd, $J = 12.7, 8.9$ Hz, 1H	67.5	H _b ⁶ , H _b ⁷	35.6, 59.1, 82.7	H ² , H ⁵ ,
	H _b : 4.02	ddd, $J = 12.7, 6.3,$ 1.1 Hz, 1H		H _a ⁶ , H _a ⁷	59.1, 82.7	H ^{9,13} (very weak int.)
8	-	-	141.0	-	-	-
9,13	7.15	m, 2H	127.1	H ^{10,12}	82.7, 128.7, 129.3	H ² , H _a ³ , H _b ³ , H _b ⁷ (very weak int.)
10,12	7.27-7.31	m, 2H	129.3	H ^{9,13} , H ¹¹	127.1, 128.7, 141.0	-
11	7.23-7.27	m, 1H	128.7	H ^{10,12}	127.1, 129.3	-
14	-	-	121.9	-	-	-
15	-	-	147.5	-	-	-
16	6.84	dd, $J = 8.3, 1.0$ Hz, 1H	118.6	H ¹⁷	117.7, 121.9	-
17	7.34	ddd, $J = 8.3, 7.2,$ 1.5 Hz, 1H	135.4	H ¹⁶ , H ¹⁸ ,	118.6, 131.0, 147.5	-
18	6.75	ddd, $J = 8.1, 7.2,$ 1.0 Hz, 1H	117.7	H ¹⁷ , H ¹⁹	121.9, 131.0, 135.4	-
19	7.66	dd, $J = 8.1, 1.5$ Hz, 1H	131.0	H ¹⁸	135.4, 147.5	H ² (very weak int.), H _a ³ , H ⁵
21	-	-	174.8	-	-	-

^aAssignments are based on extensive 1D and 2D NMR analysis (¹H-¹H COSY, ¹H-¹³C HMQC, ¹H-¹³C HMBC and ¹H-¹H NOESY); measured in MeCN-*d*₃; int. = interaction.

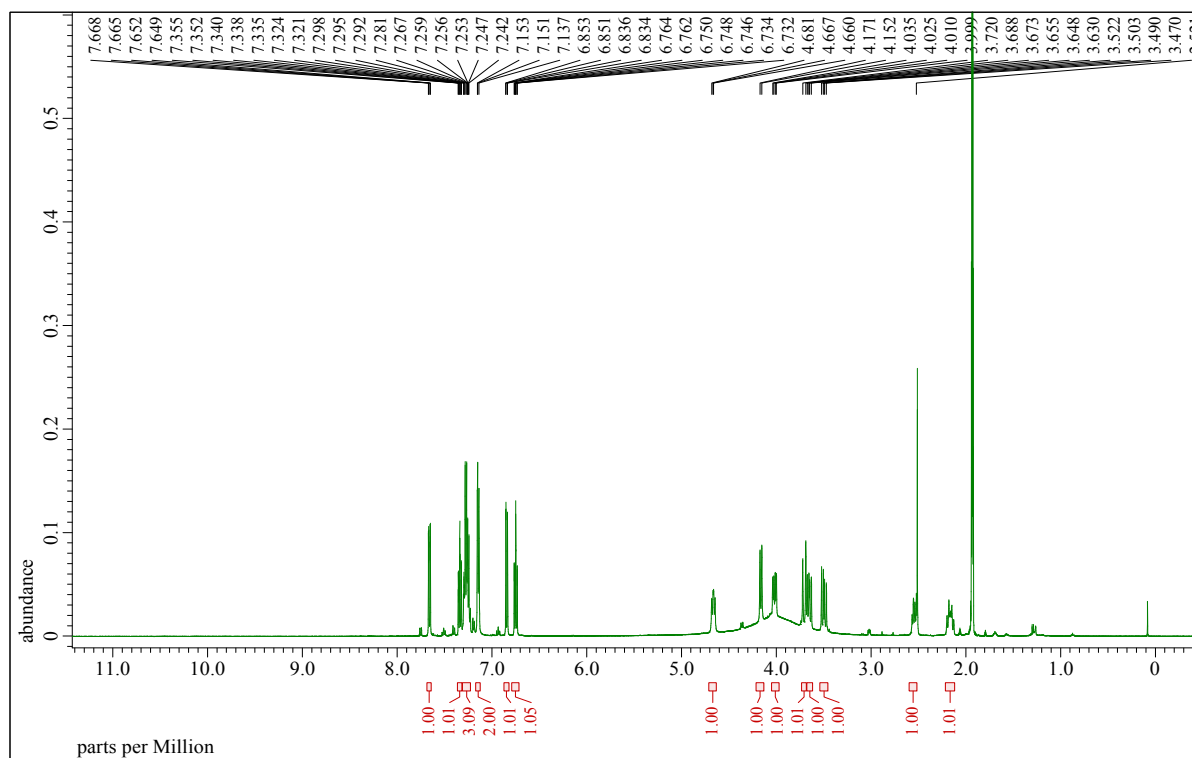


Figure S20. ^1H NMR spectrum of **7a** (500 MHz, $\text{MeCN-}d_3$)

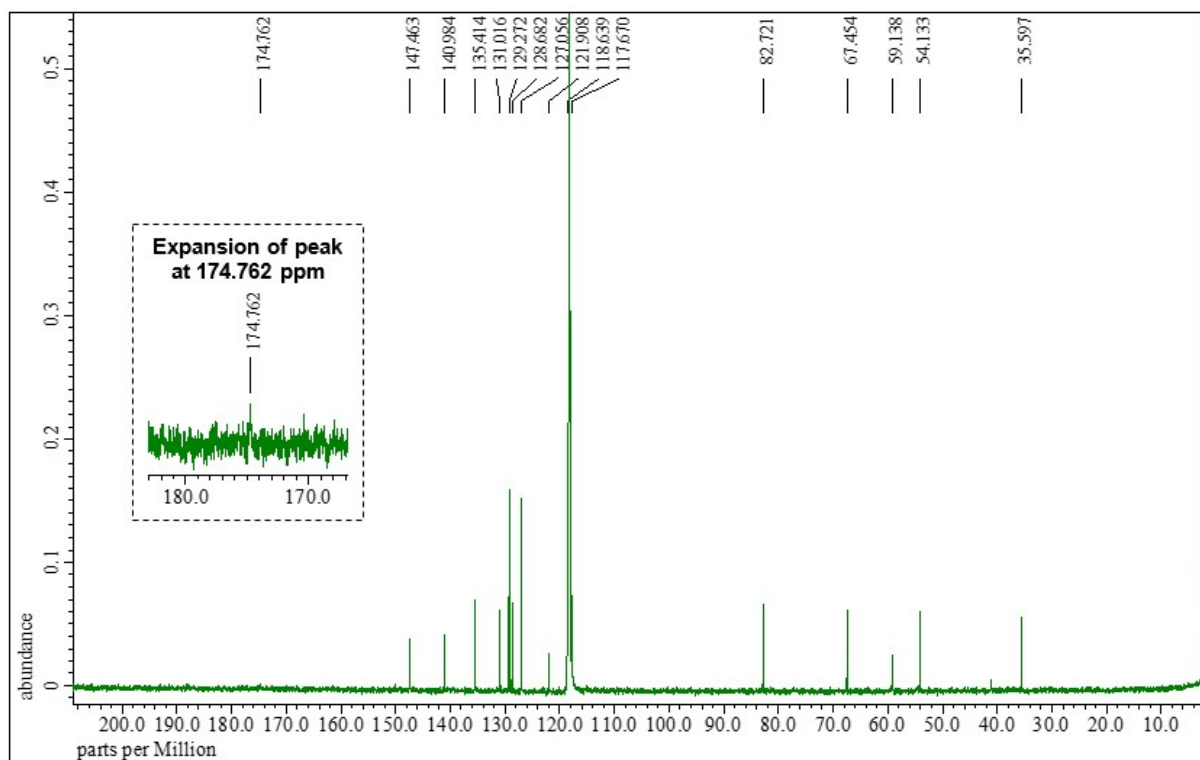


Figure S21. $^{13}\text{C}\{^1\text{H}\}$ NMR spectrum of **7a** (126 MHz, $\text{MeCN-}d_3$)

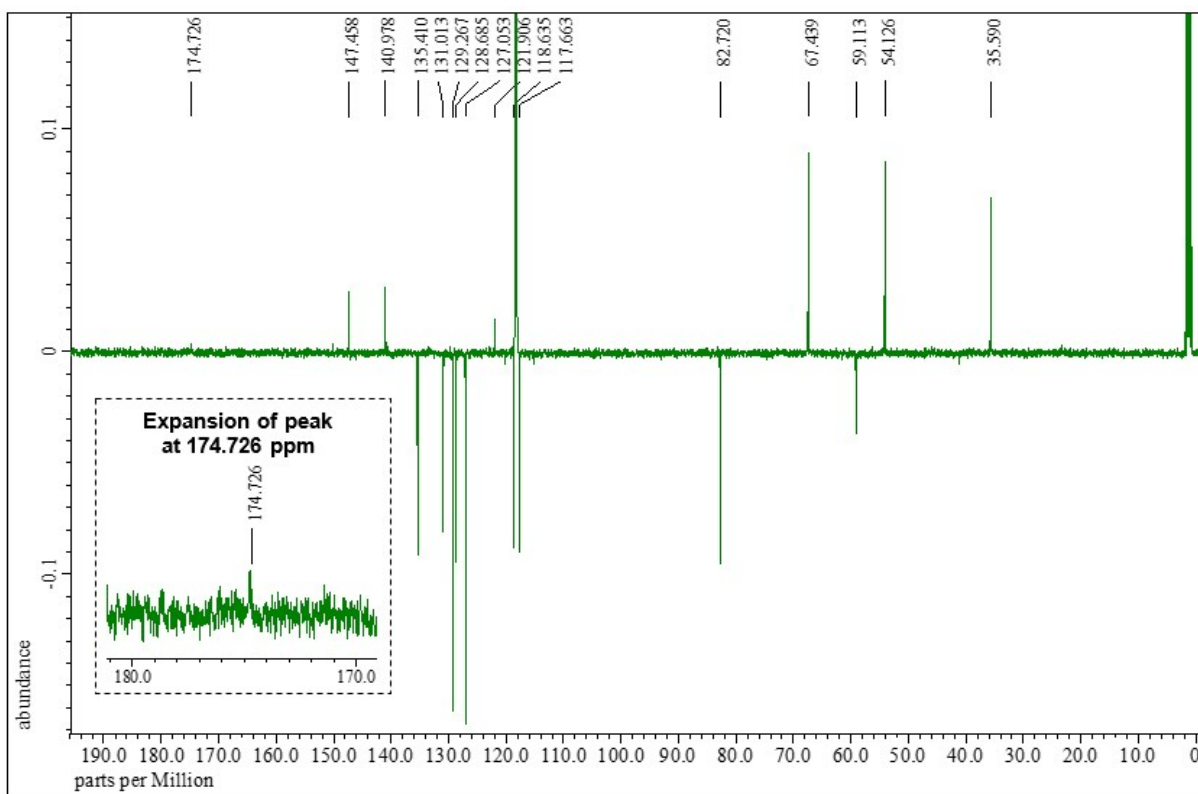


Figure S22. ^{13}C APT NMR spectrum of **7a** (126 MHz, $\text{MeCN-}d_3$)

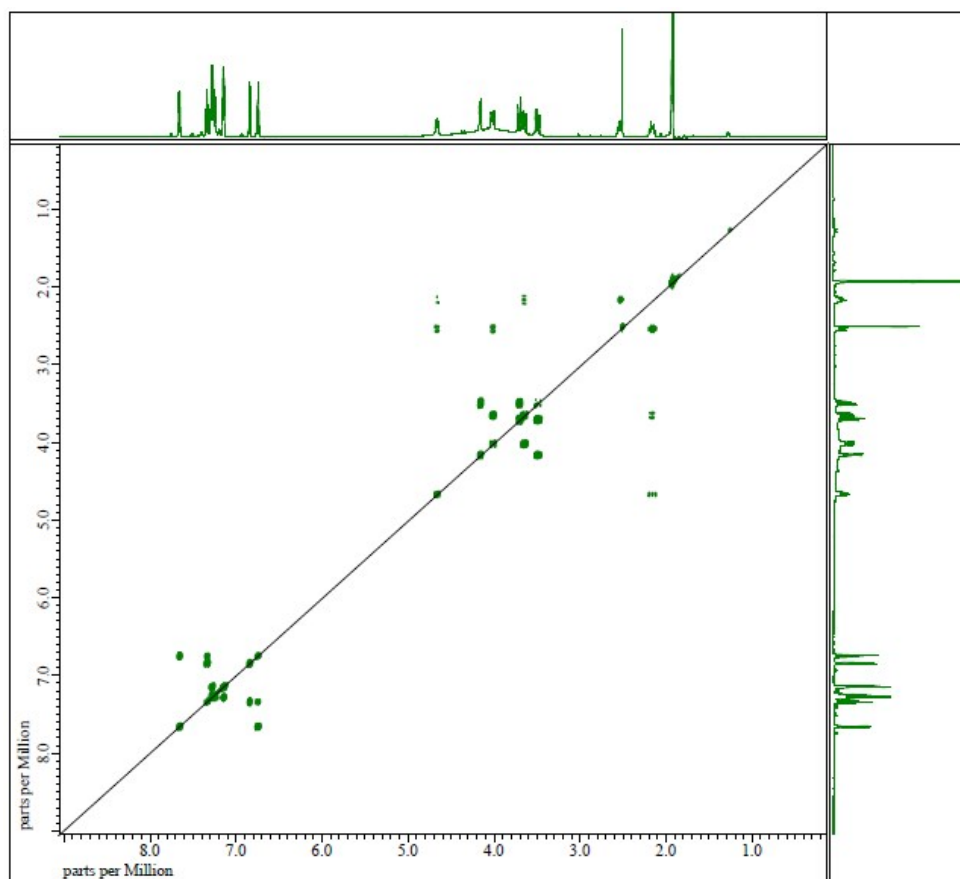


Figure S23. $^1\text{H-}^1\text{H}$ COSY NMR spectrum of **7a** (500 MHz, $\text{MeCN-}d_3$)

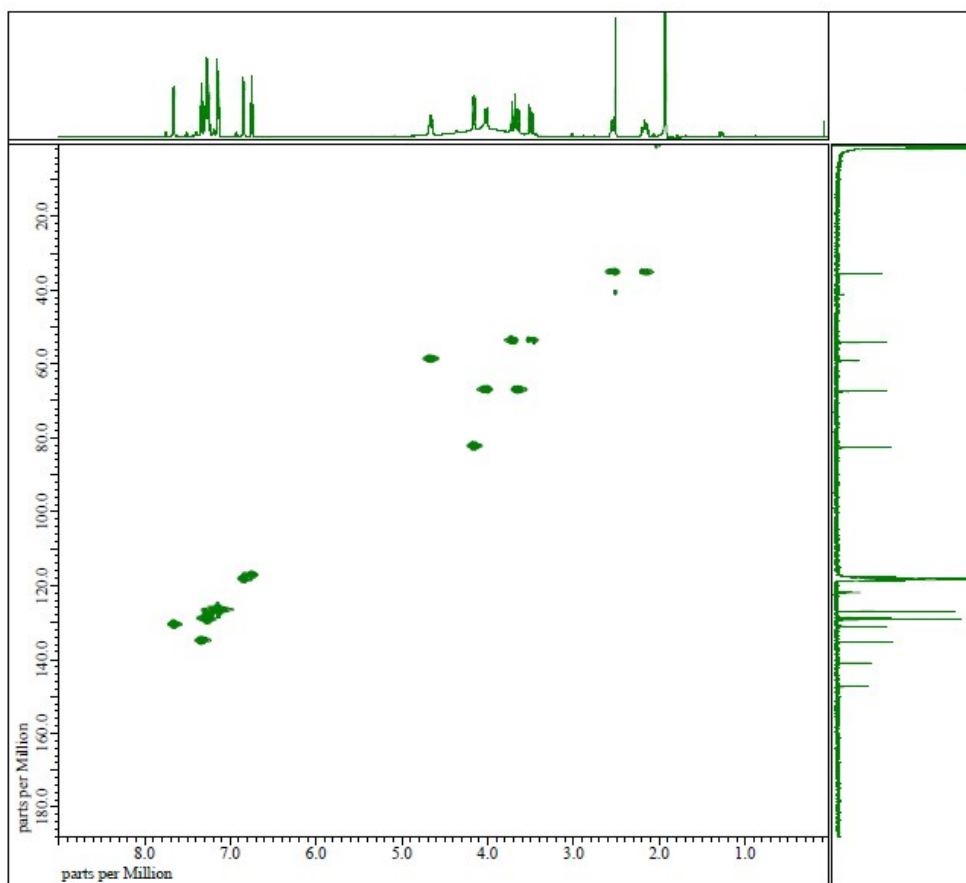


Figure S24. ^1H - ^{13}C HMQC NMR spectrum of **7a** ($\text{MeCN-}d_3$)

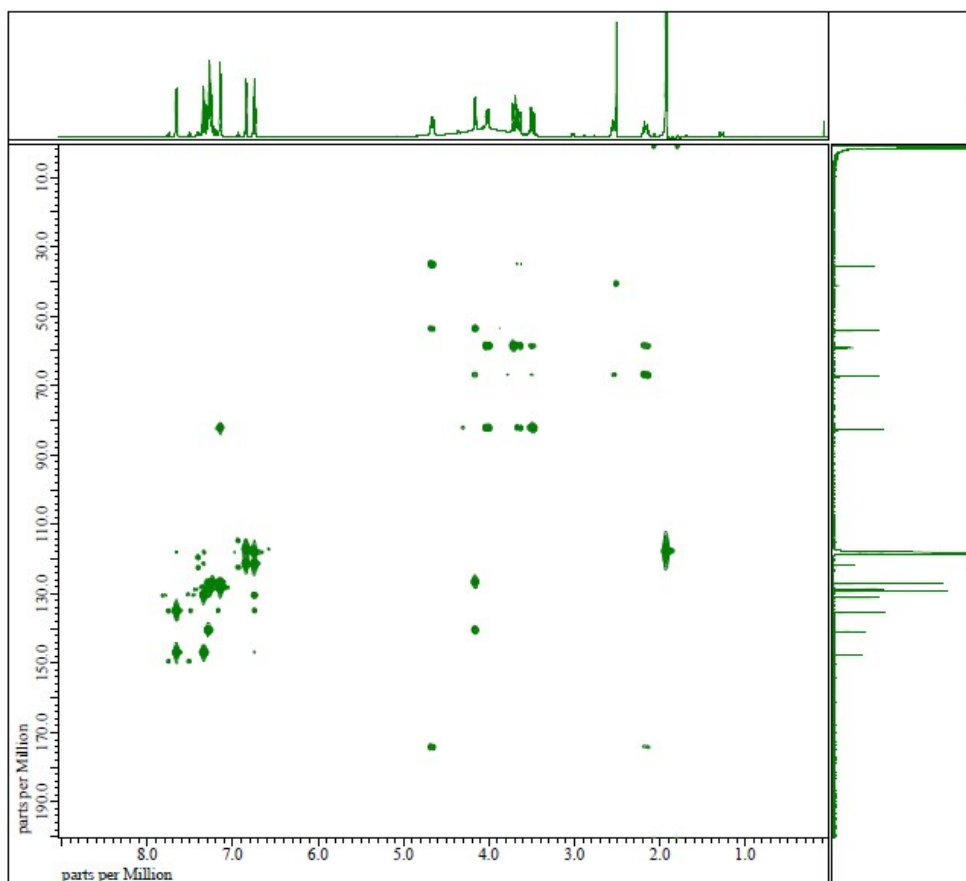


Figure S25. ^1H - ^{13}C HMBC NMR spectrum of **7a** ($\text{MeCN-}d_3$)

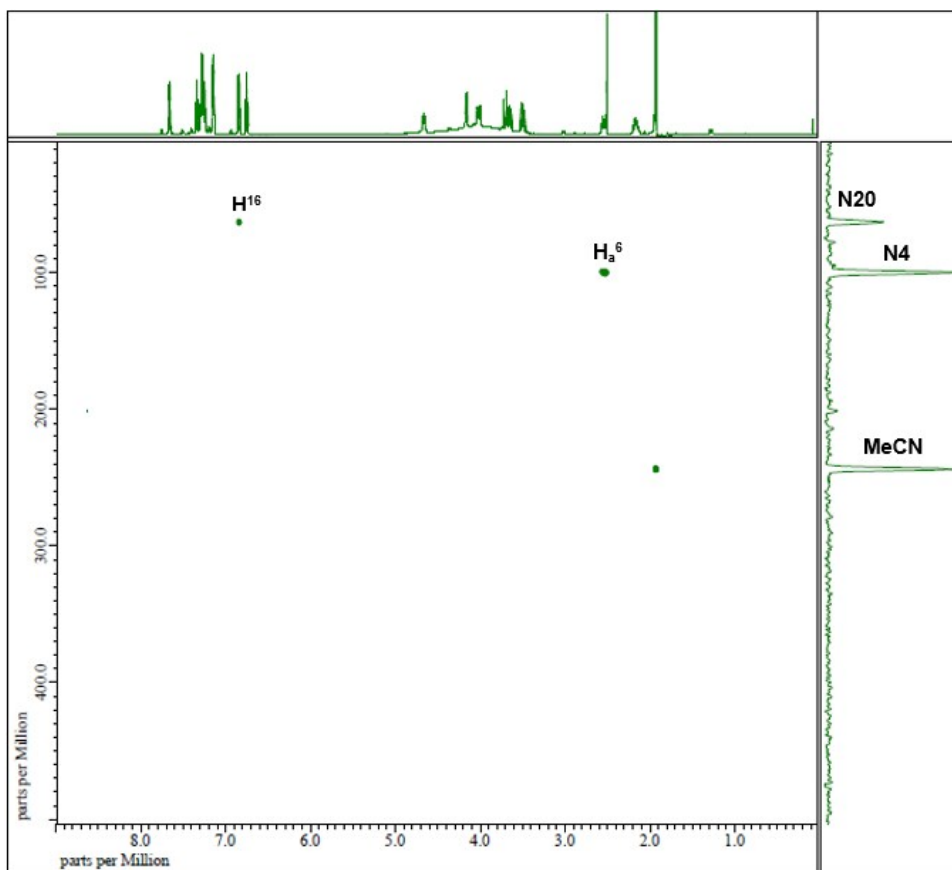


Figure S26. ^1H - ^{15}N HMBC NMR spectrum of **7a** ($\text{MeCN-}d_3$)

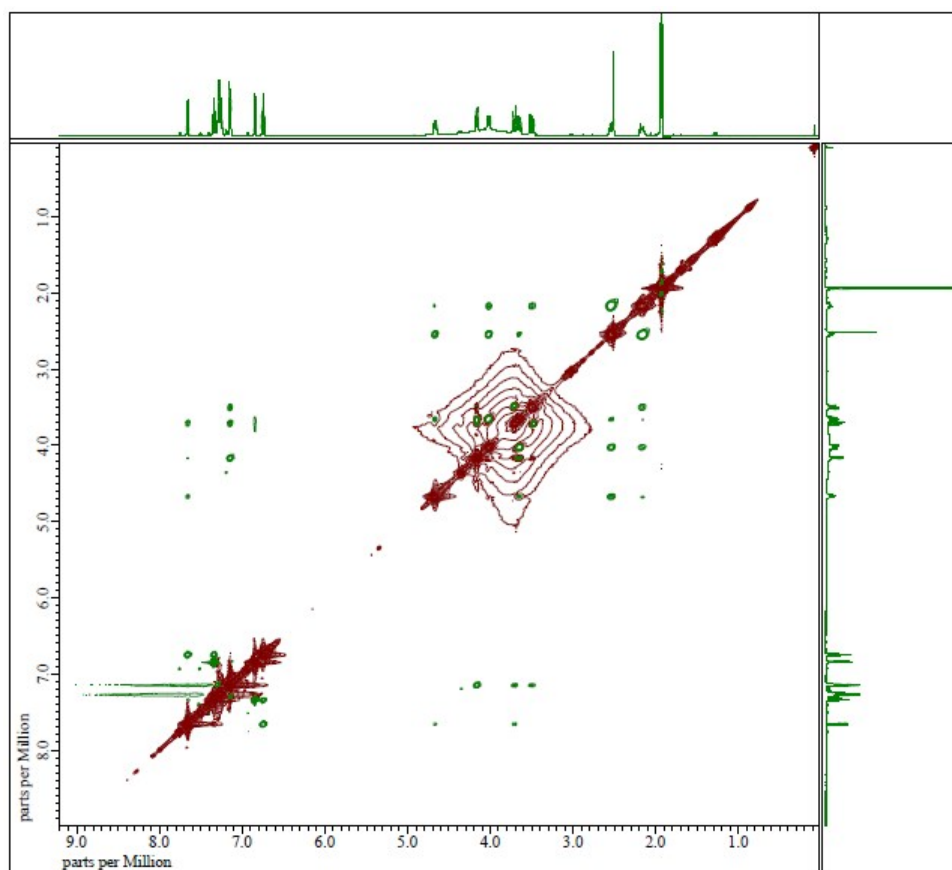


Figure S27. ^1H - ^1H NOESY NMR spectrum of **7a** ($\text{MeCN-}d_3$)

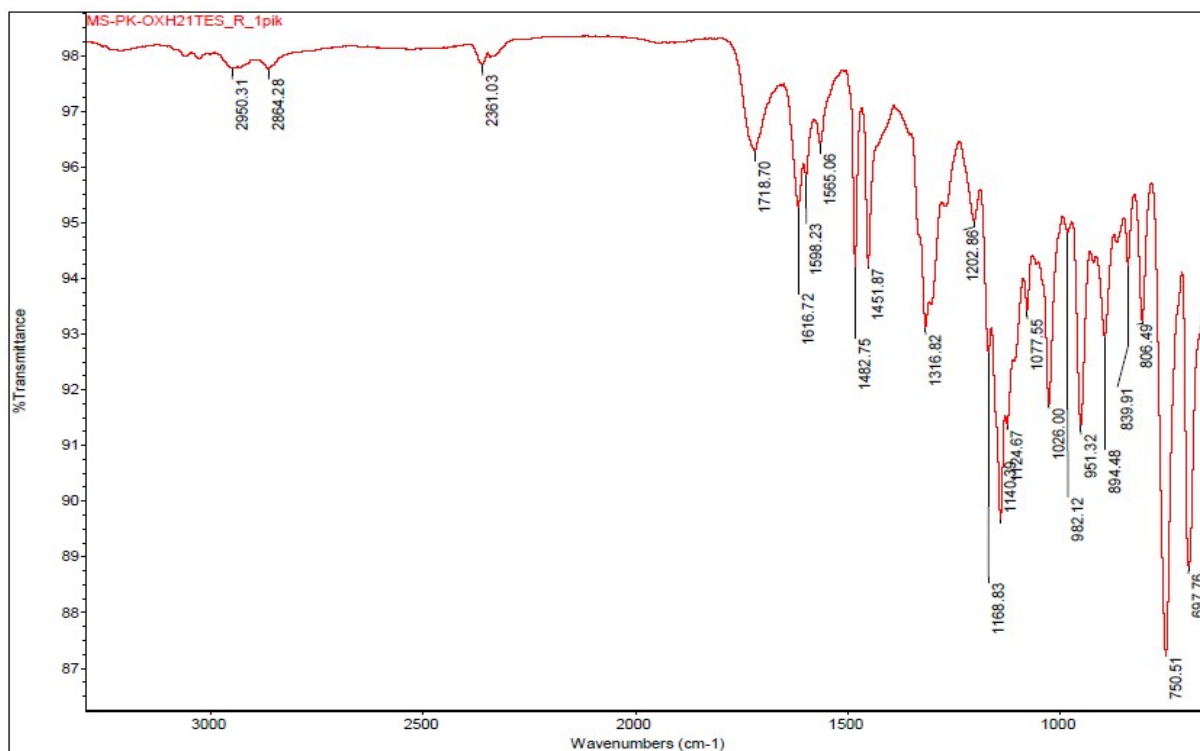


Figure S28. IR spectrum of 7a

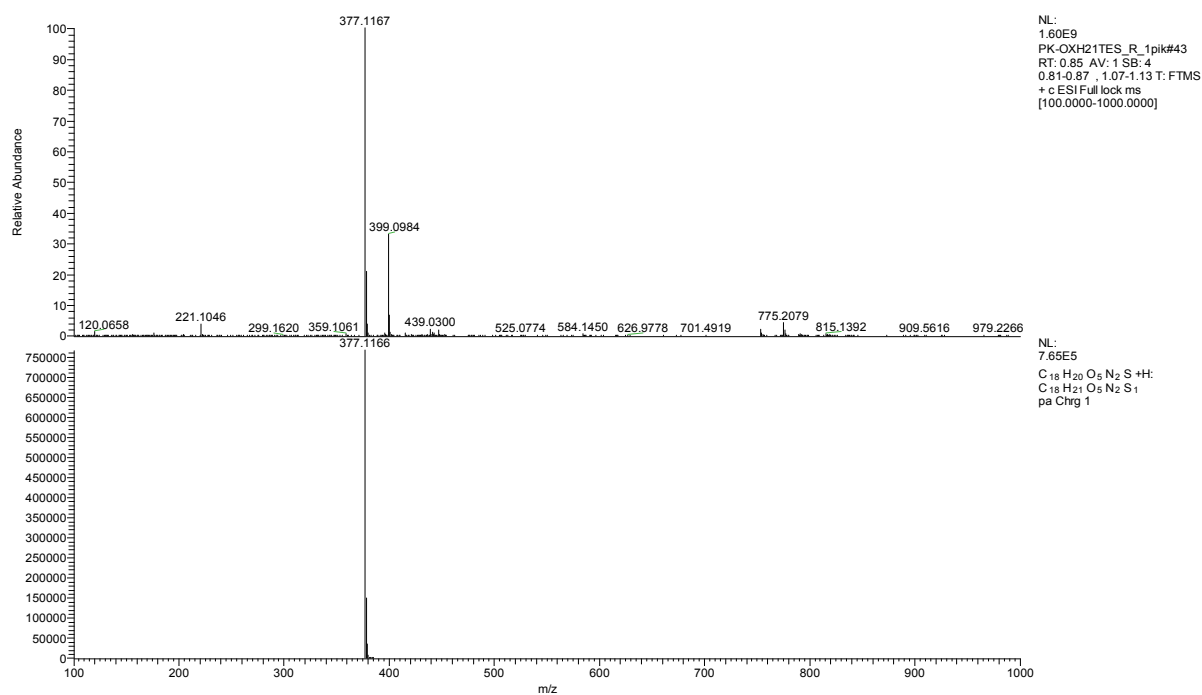


Figure S29. HRMS spectrum of 7a

(-)-(2R,5S)-4-((2-aminophenyl)sulfonyl)-2-phenyl-1,4-oxazepane-5-carboxamide 7b^{2R}

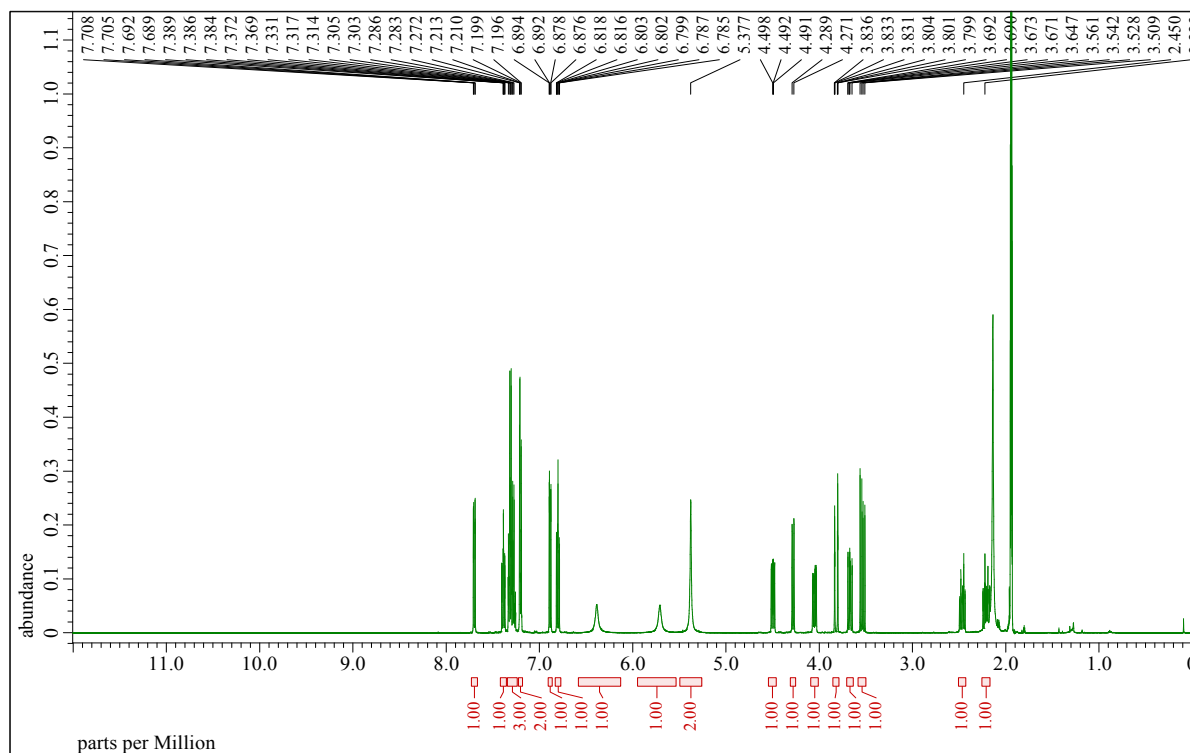
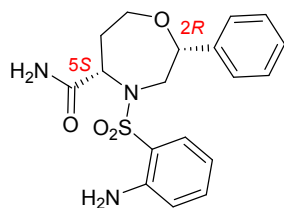


Figure S30. ¹H NMR spectrum of **7b^{2R}** (500 MHz, MeCN-*d*₃)

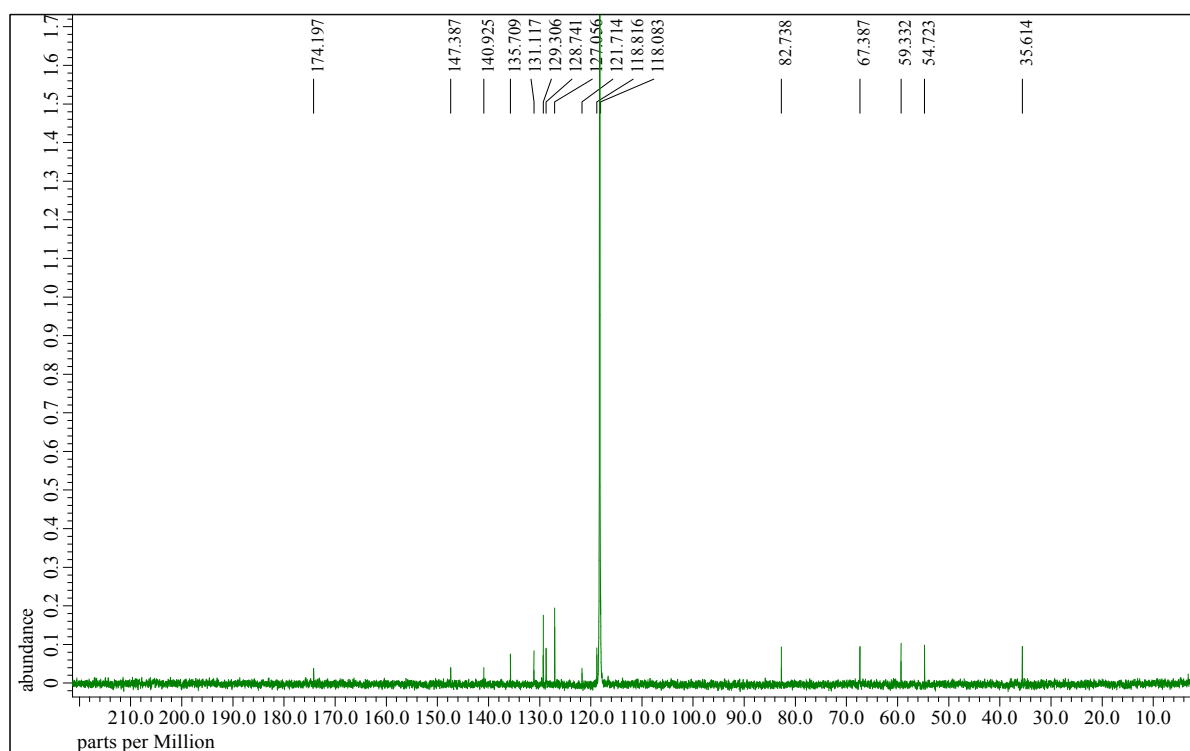


Figure S31. ¹³C{¹H} NMR spectrum of **7b^{2R}** (126 MHz, MeCN-*d*₃)

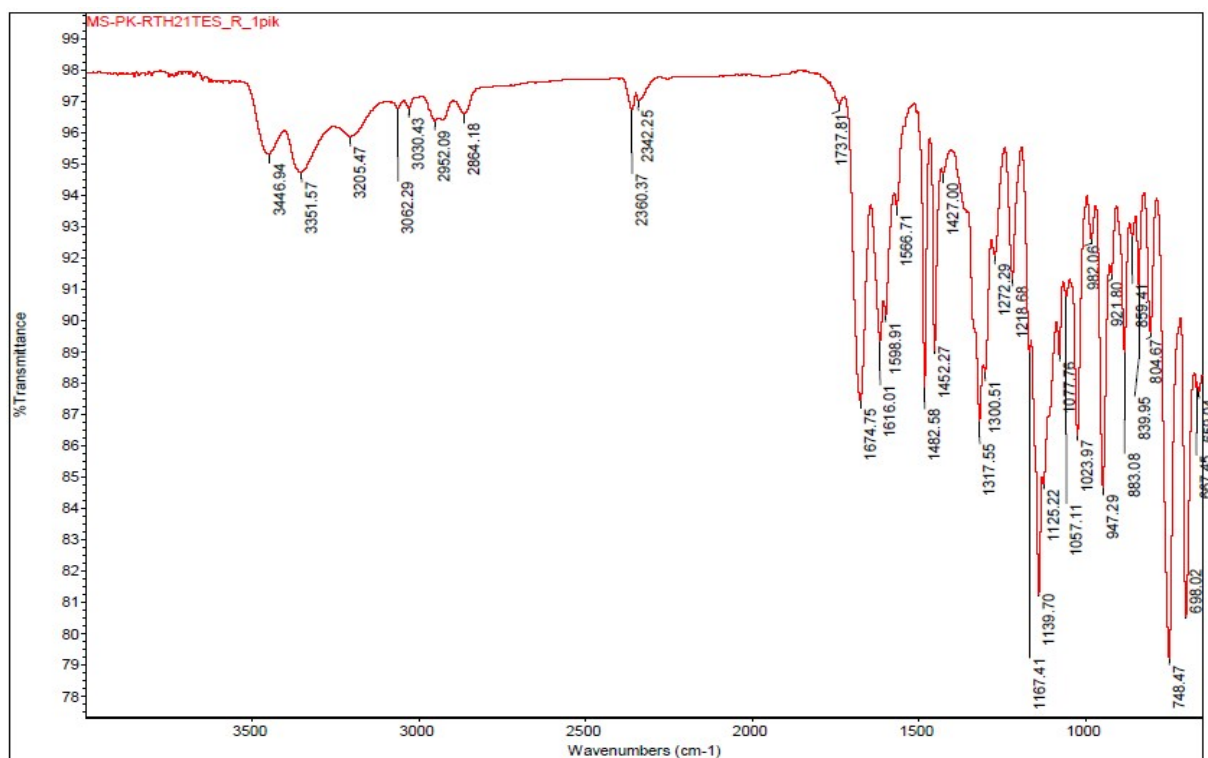


Figure S32. IR spectrum of **7b^{2R}**

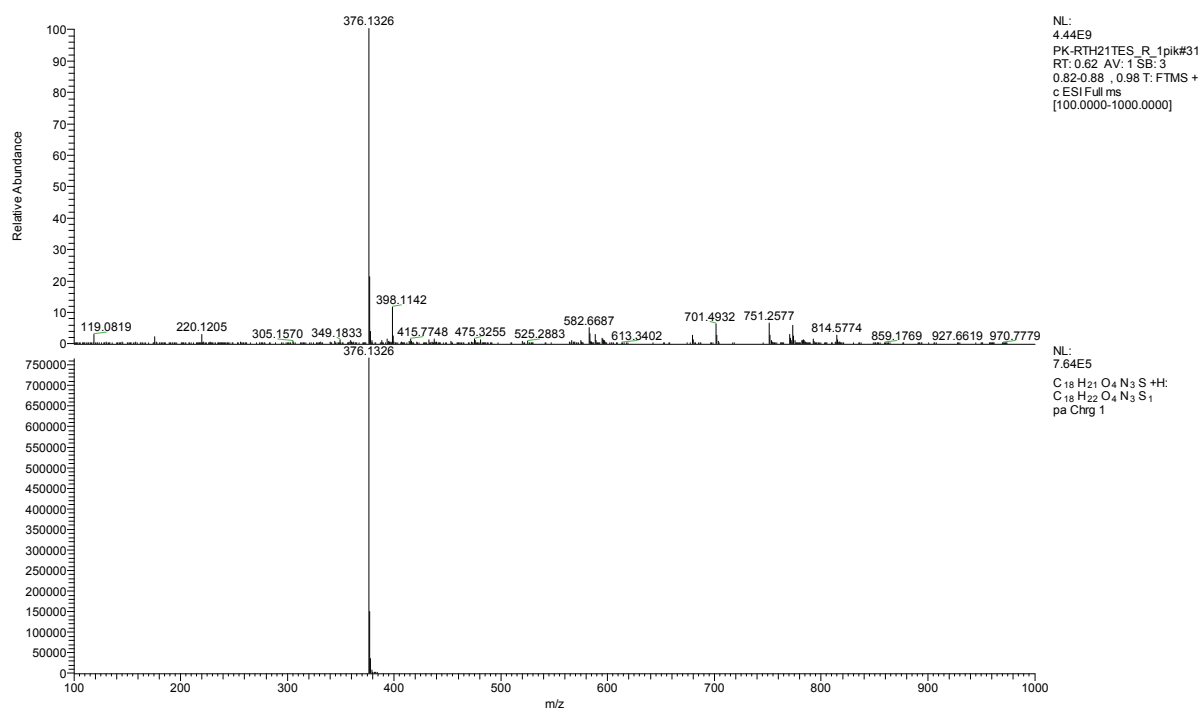


Figure S33. HRMS spectrum of **7b^{2R}**

(+)-(2*S*,5*S*)-4-((2-aminophenyl)sulfonyl)-2-phenyl-1,4-oxazepane-5-carboxamide **7b^{2*S*}**

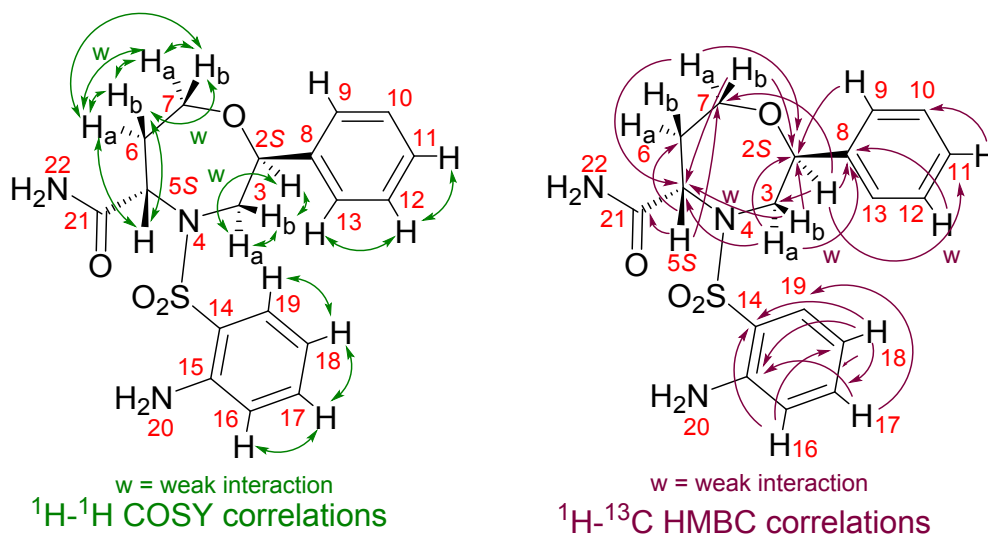
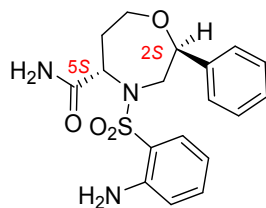


Figure S34. Detailed COSY and ¹H-¹³C HMBC NMR analysis of 1,4-oxazepane **7b**^{2*S*}

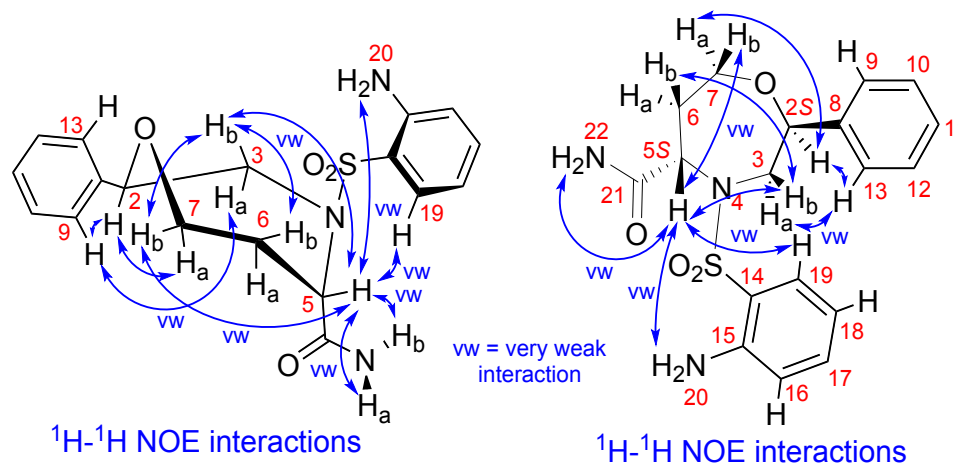


Figure S35. Detailed ¹H-¹H NOE NMR analysis of 1,4-oxazepane **7b**^{2*S*}

Table S3. ^1H NMR (500 MHz) and $^{13}\text{C}\{^1\text{H}\}$ NMR (126 MHz) spectral data, including detailed COSY, ^1H - ^{13}C HMBC and NOE correlations for 1,4-oxazepane **7b**^{2Sa}

position	^1H NMR δ_{H} [ppm] ^b	splitting pattern, J [Hz], integration	$^{13}\text{C}\{^1\text{H}\}$ NMR δ_{C} [ppm]	COSY correlations	^1H - ^{13}C HMBC correlations	NOE correlations
2	4.64	dd, $J = 8.7, 1.6$ Hz, 1H	81.4	$\text{H}_a^3, \text{H}_b^3$	56.8, 126.6, 128.6 (weak int.), 141.9	$\text{H}_a^7, \text{H}^{9,13}$
3	H_a : 3.63	dd, $J = 14.2, 1.6$ Hz, 1H,	56.8	H^2, H_b^3	59.4, 81.4	$\text{H}^{9,13}$ (very weak int.)
	H_b : 3.43	dd, $J = 14.2, 8.7$ Hz, 1H		H^2, H_a^3	59.4 (weak int.), 81.4, 141.9 (weak int.)	H^5, H_b^6
5	4.59	dd, $J = 4.5, 4.5$ Hz, 1H	59.4	$\text{H}_a^6, \text{H}_b^6$	33.0 (weak int.), 66.9, 174.3	$\text{H}_b^3, \text{H}_b^7$ (very weak int.), H^{19} (very weak int.), $\text{H}^{20}, \text{H}^{22}$ (very weak int.)
6	H_a : 2.30	dddd, $J = 15.8, 4.9, 4.5, 1.6$ Hz, 1H	33.0	$\text{H}^5, \text{H}_b^6, \text{H}_a^7$ (weak int.), H_b^7	-	-
	H_b : 2.10	dddd, $J = 15.8, 11.0, 4.5, 3.0$ Hz, 1H		$\text{H}^5, \text{H}_a^6, \text{H}_a^7, \text{H}_b^7$ (weak int.)	-	H_b^3
7	H_a : 3.78	ddd, $J = 12.8, 11.0, 1.6$ Hz, 1H	67.0	H_a^6 (weak int.), $\text{H}_b^6, \text{H}_b^7$	59.4, 81.4	H^2
	H_b : 3.94	ddd, $J = 12.8, 4.5, 3.0$ Hz, 1H		$\text{H}_a^6, \text{H}_b^6$ (weak int.), H_a^7	59.4, 81.4	H^5 (very weak int.)
8	-	-	141.9	-	-	-
9,13	7.18-7.19	m, 2H	126.6	$\text{H}^{10,12}$	81.4, 128.6	H^2, H_a^3 (weak int.)
10,12	7.27-7.30	m, 2H	129.3	$\text{H}^{9,13}, \text{H}^{11}$	141.9	-
11	7.24-7.27	m, 1H	128.6	$\text{H}^{10,12}$	126.6, 129.3	-
14	-	-	119.1	-	-	-
15	-	-	148.0	-	-	-
16	6.85	dd, $J = 8.5, 1.1$ Hz, 1H	118.7	H^{17}	117.5, 119.1	-
17	7.35	ddd, $J = 8.5, 7.2, 1.6$ Hz, 1H	135.7	$\text{H}^{16}, \text{H}^{18}$,	131.3, 148.0	-
18	6.70	ddd, $J = 8.2, 7.2, 1.1$ Hz, 1H	117.5	$\text{H}^{17}, \text{H}^{19}$	118.7, 119.1, 148.0	-
19	7.58	dd, $J = 8.1, 1.6$ Hz, 1H	131.3	H^{18}	135.7	H^5 (very weak int.)
20	5.62	br. s, 2H	-	-	-	H^5
21	-	-	174.4	-	-	-
22	H_a : 5.99	br. s, 1H	-	-	-	H^5 (very weak int.)
	H_b : 6.75	br.s, 1H				H^5 (very weak int.)

^aAssignments are based on extensive 1D and 2D NMR analysis (^1H - ^1H COSY, ^1H - ^{13}C HMQC, ^1H - ^{13}C HMBC and ^1H - ^1H NOESY); measured in MeCN- d_3 ; int. = interaction.

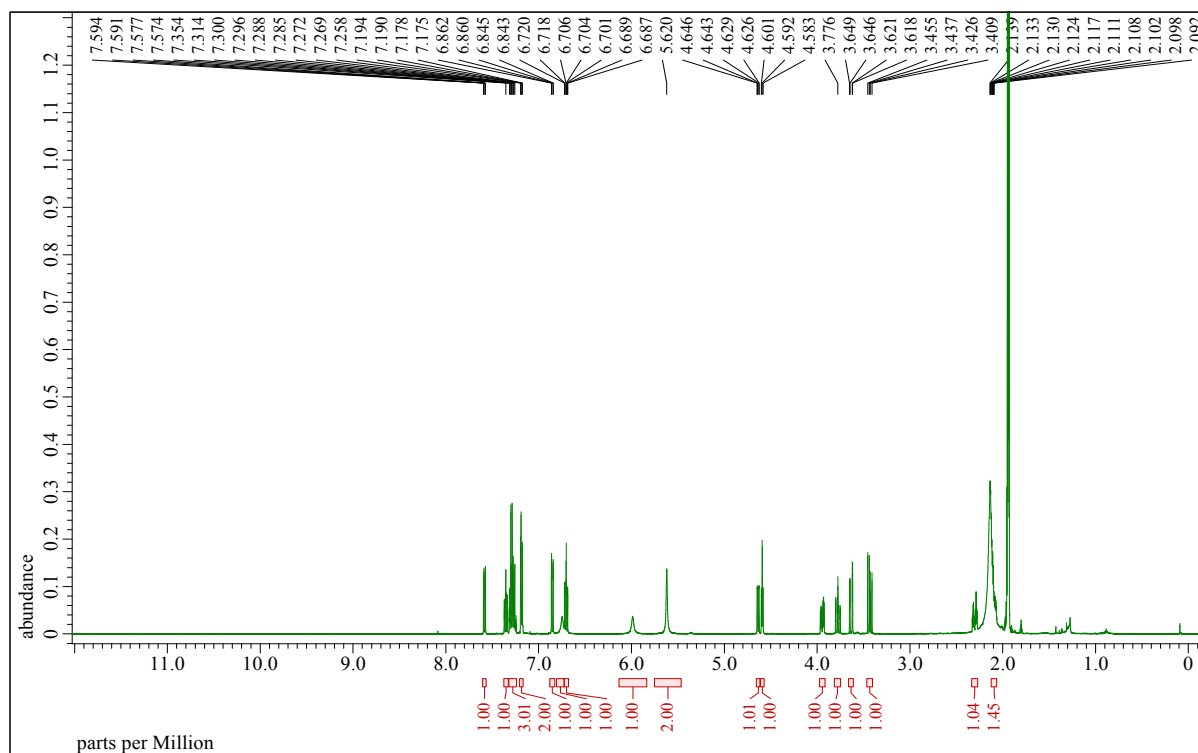


Figure S36. ^1H NMR spectrum of $7\text{b}^{2\text{S}}$ (500 MHz, $\text{MeCN-}d_3$)

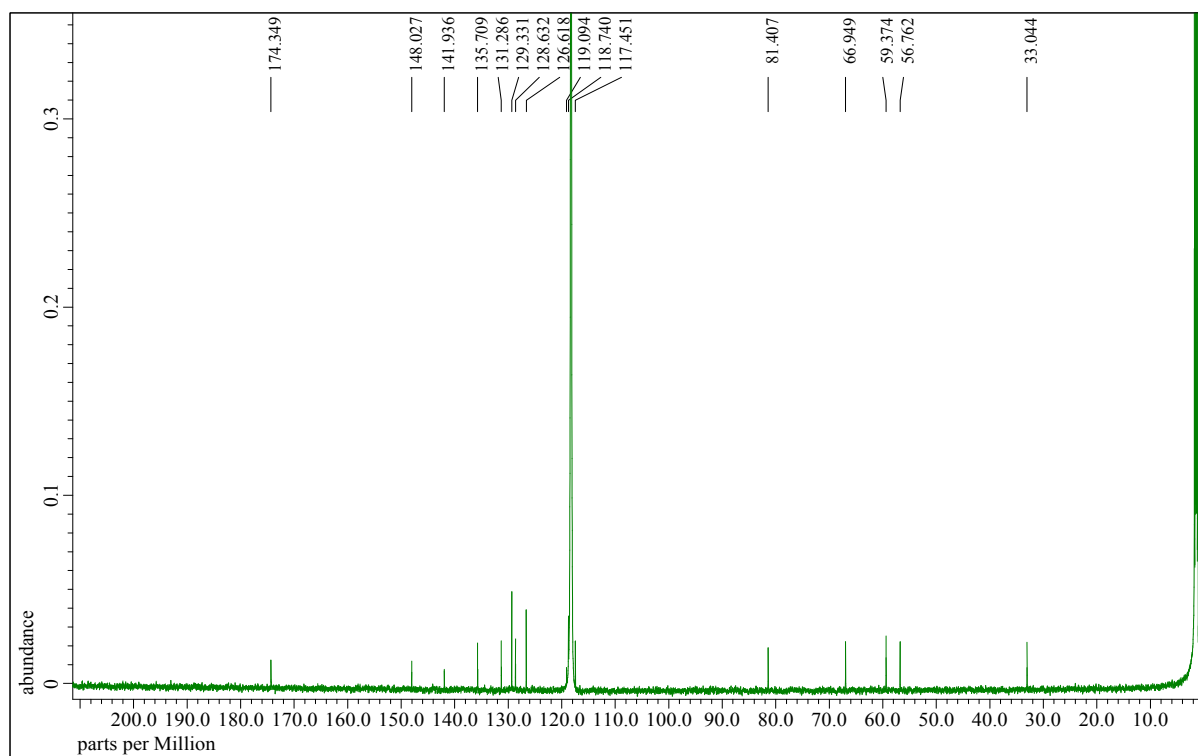


Figure S37. $^{13}\text{C}\{^1\text{H}\}$ NMR spectrum of $7\text{b}^{2\text{S}}$ (126 MHz, $\text{MeCN-}d_3$)

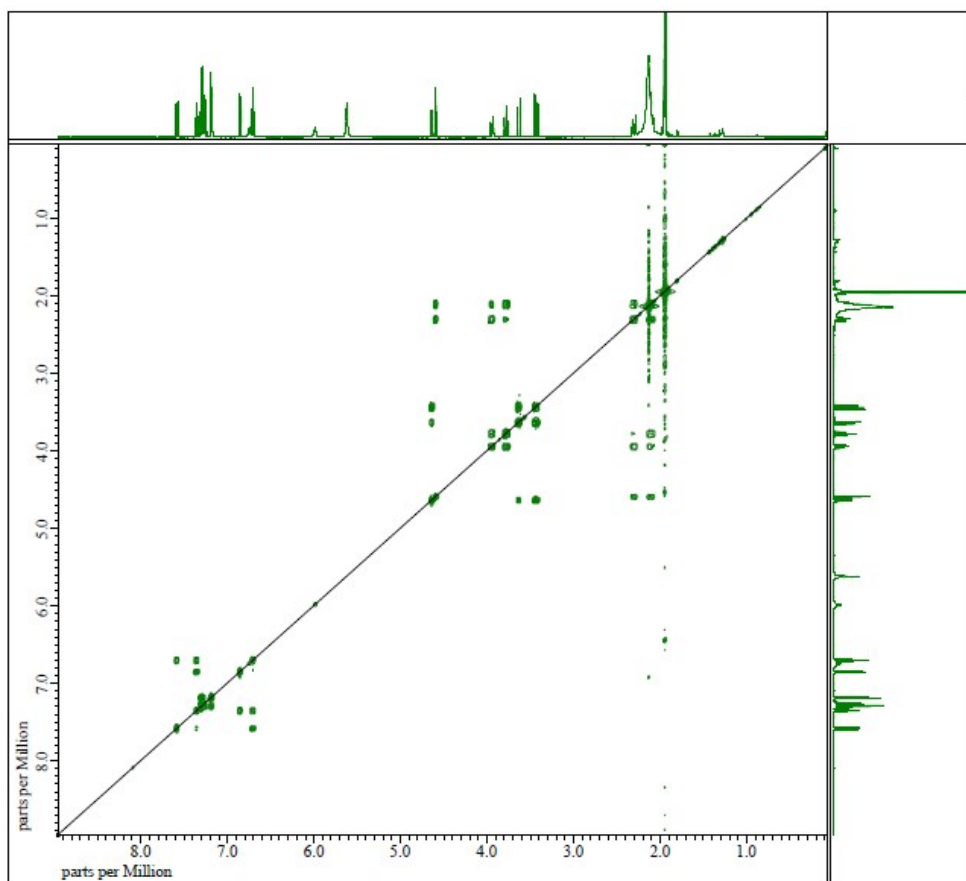


Figure S38. ^1H - ^1H COSY NMR spectrum of **7b^{2S}** (500 MHz, MeCN- d_3)

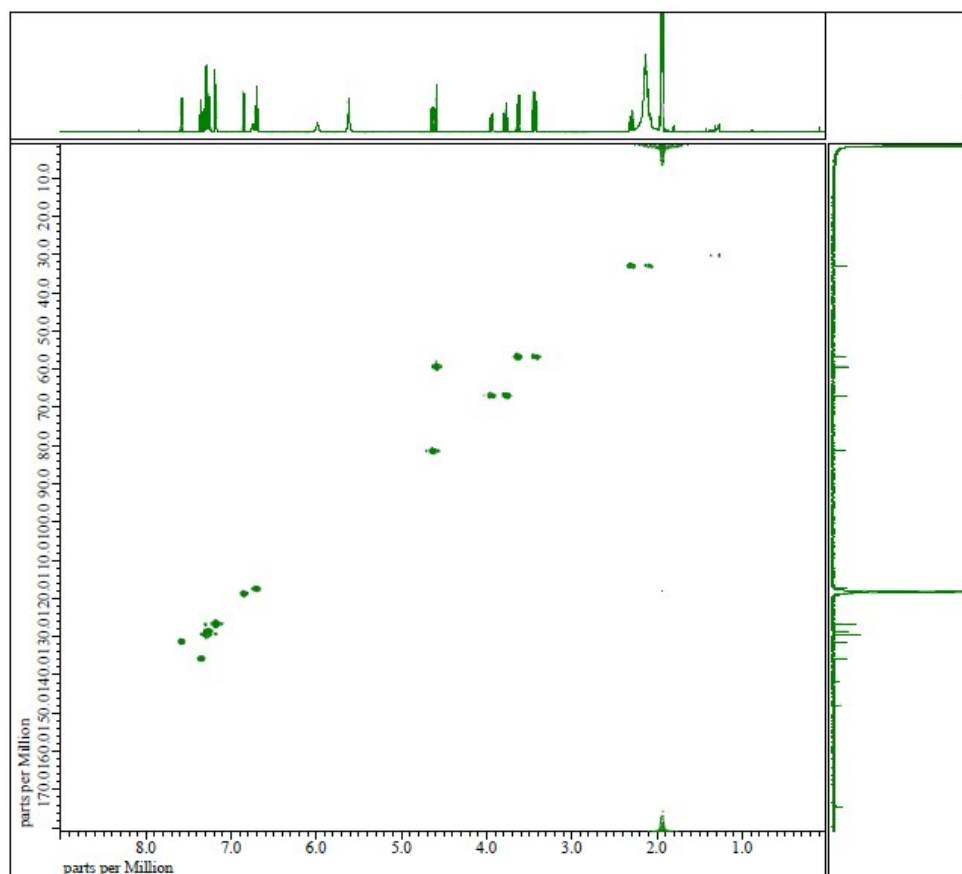


Figure S39. ^1H - ^{13}C HMQC NMR spectrum of **7b^{2S}** (MeCN- d_3)

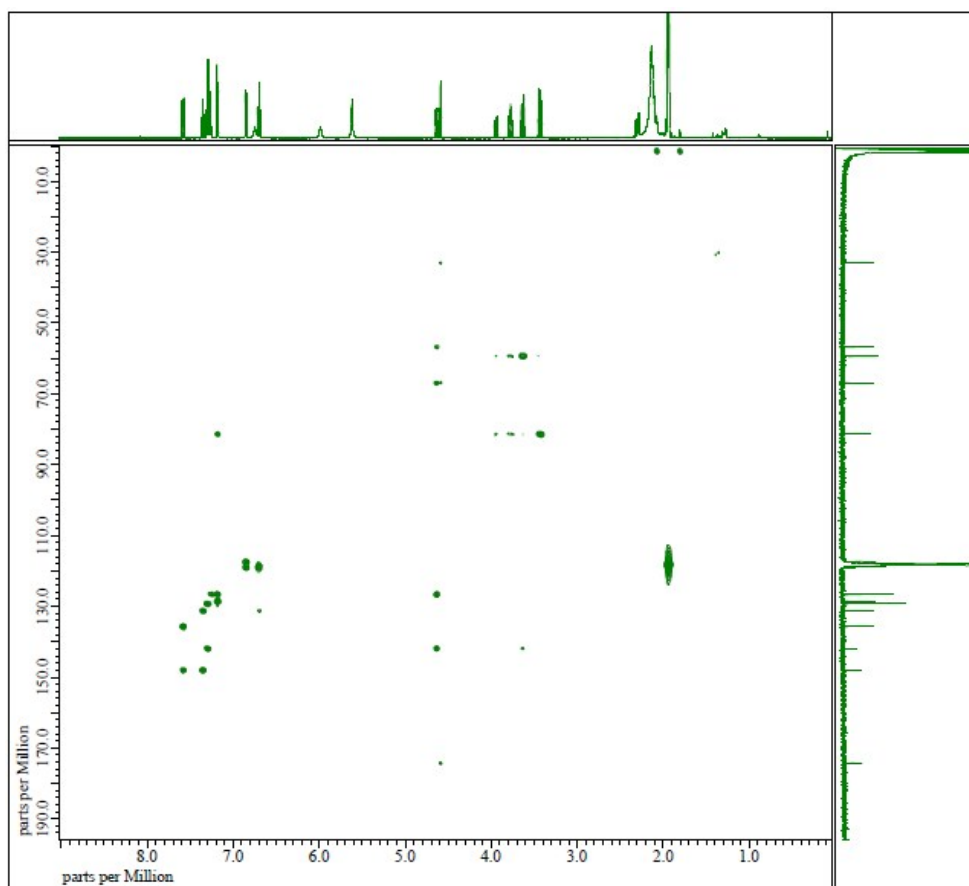


Figure S40. ^1H - ^{13}C HMBC NMR spectrum of **7b^{2S}** (MeCN- d_3)

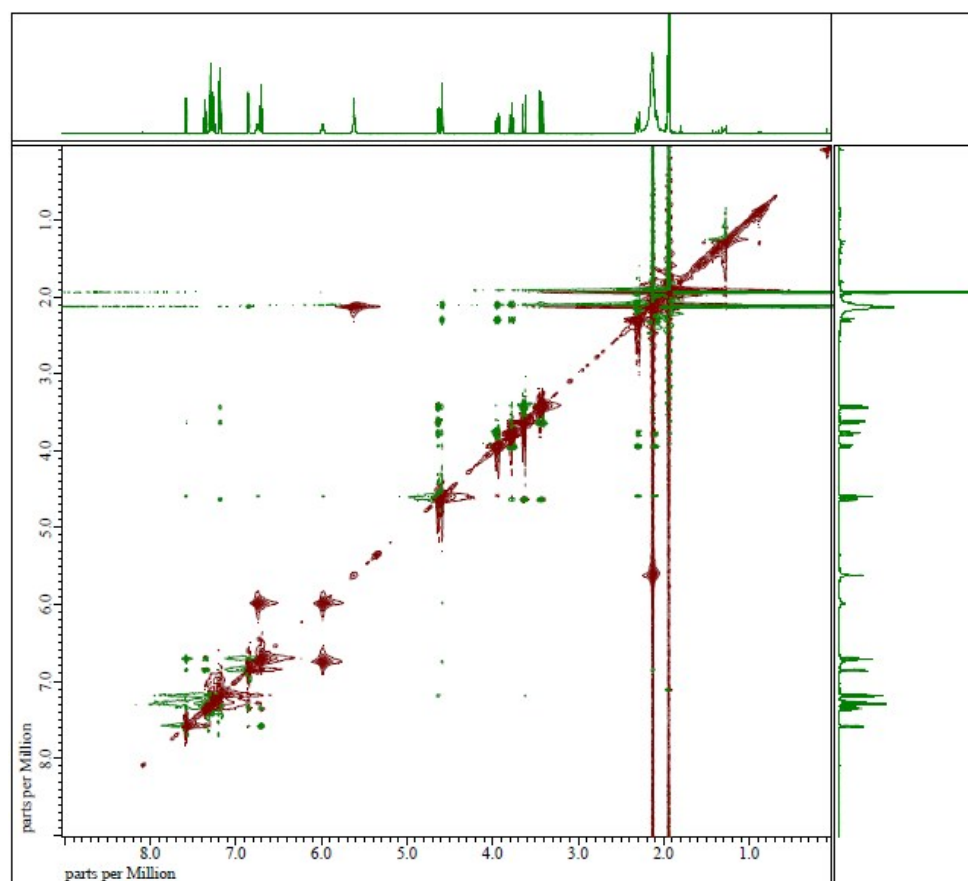


Figure S41. ^1H - ^1H NOESY NMR spectrum of **7b^{2S}** (MeCN- d_3)

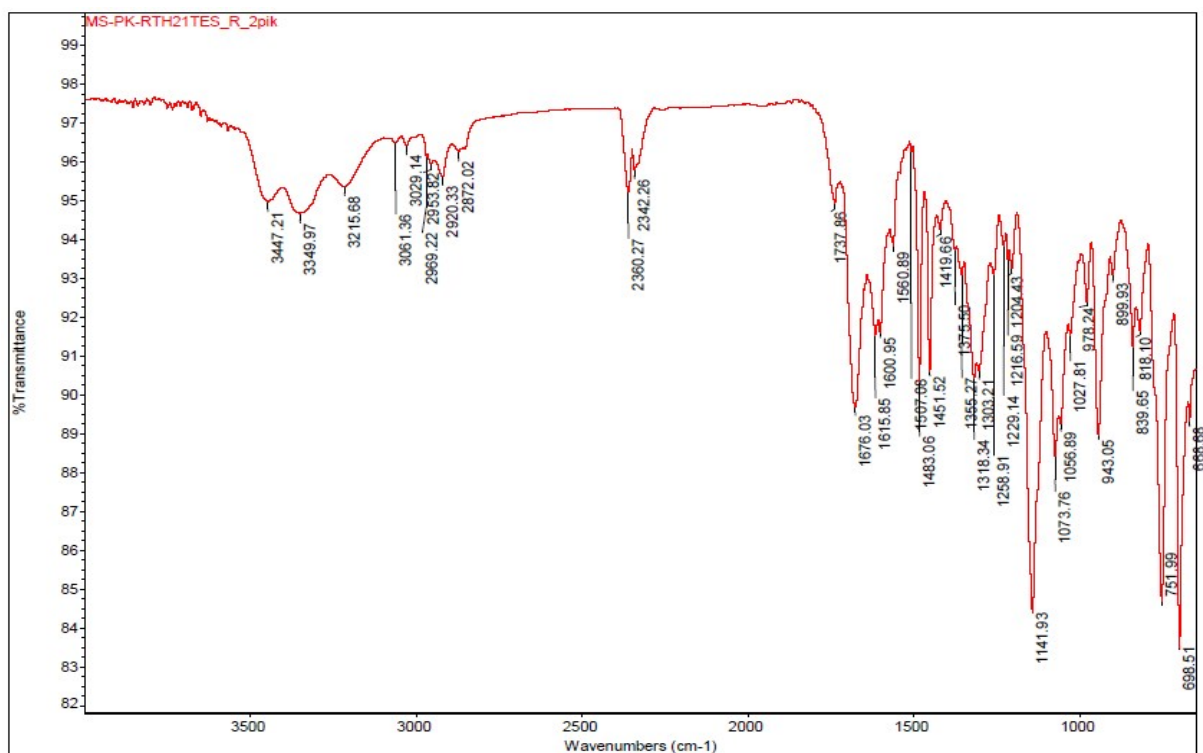


Figure S42. IR spectrum of **7b^{2S}**

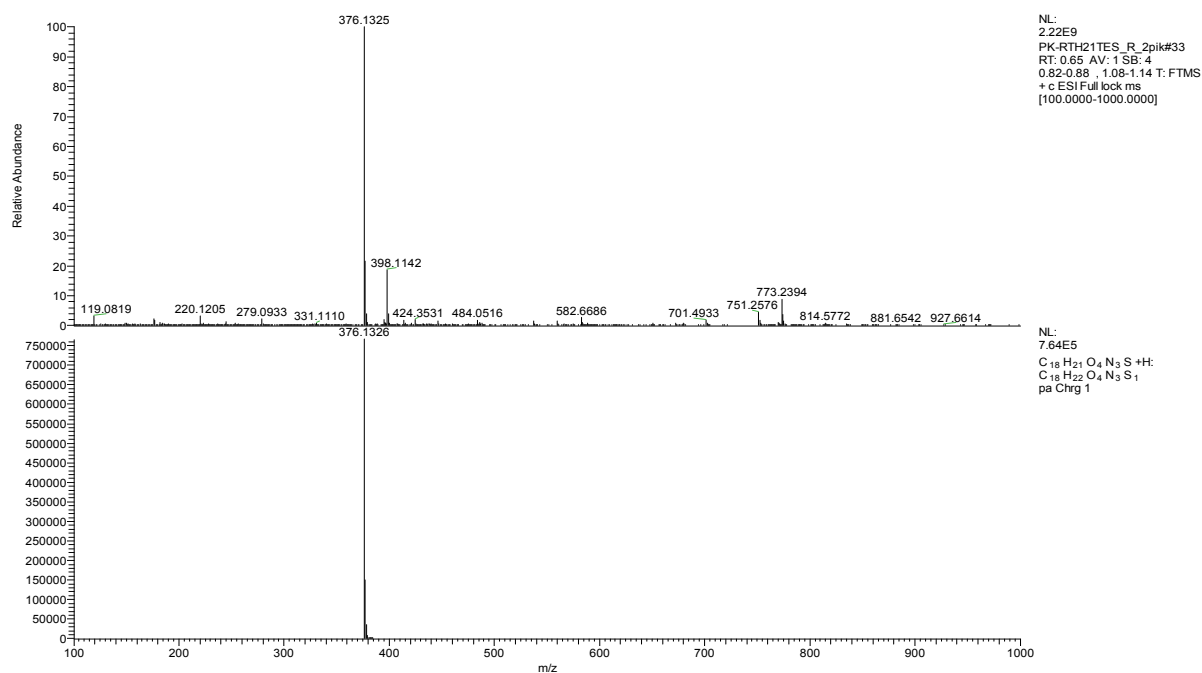
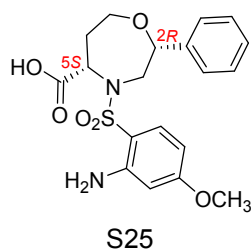


Figure S43. HRMS spectrum of **7b^{2S}**

(-)-(2R,5S)-4-((2-amino-4-methoxyphenyl)sulfonyl)-2-phenyl-1,4-oxazepane-5-carboxylic acid 7e



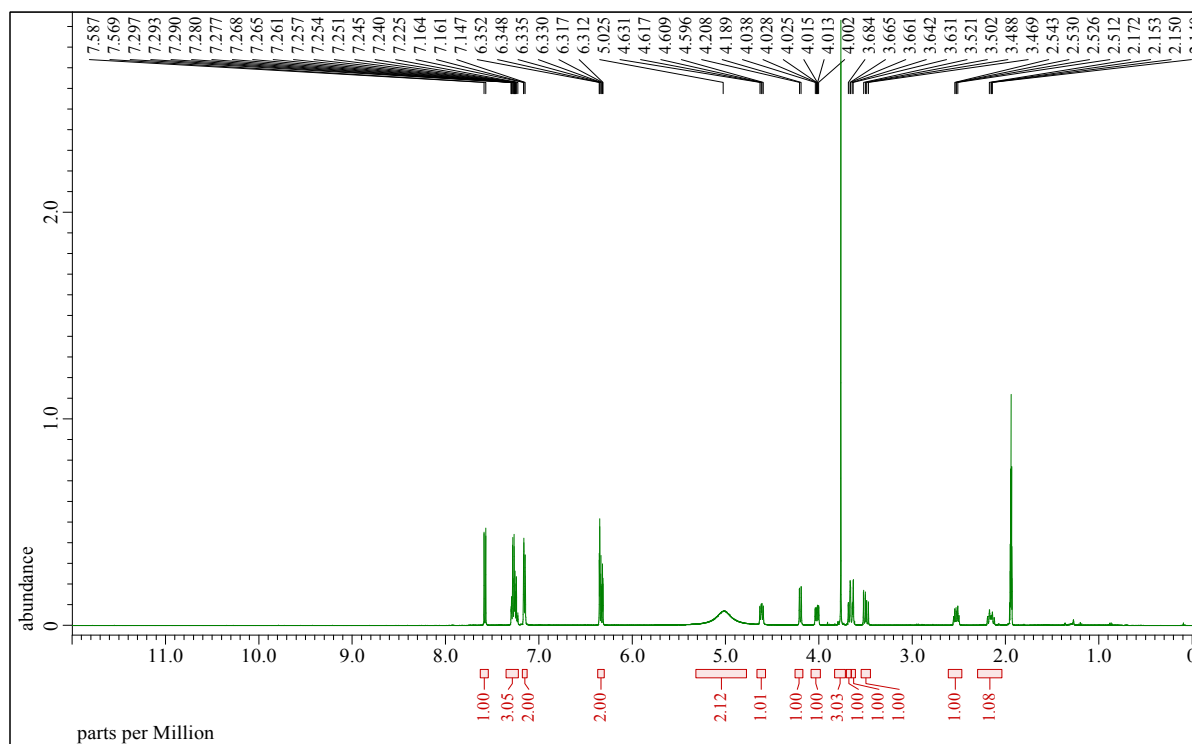


Figure S44. ^1H NMR spectrum of **7e** (500 MHz, $\text{MeCN-}d_3$)

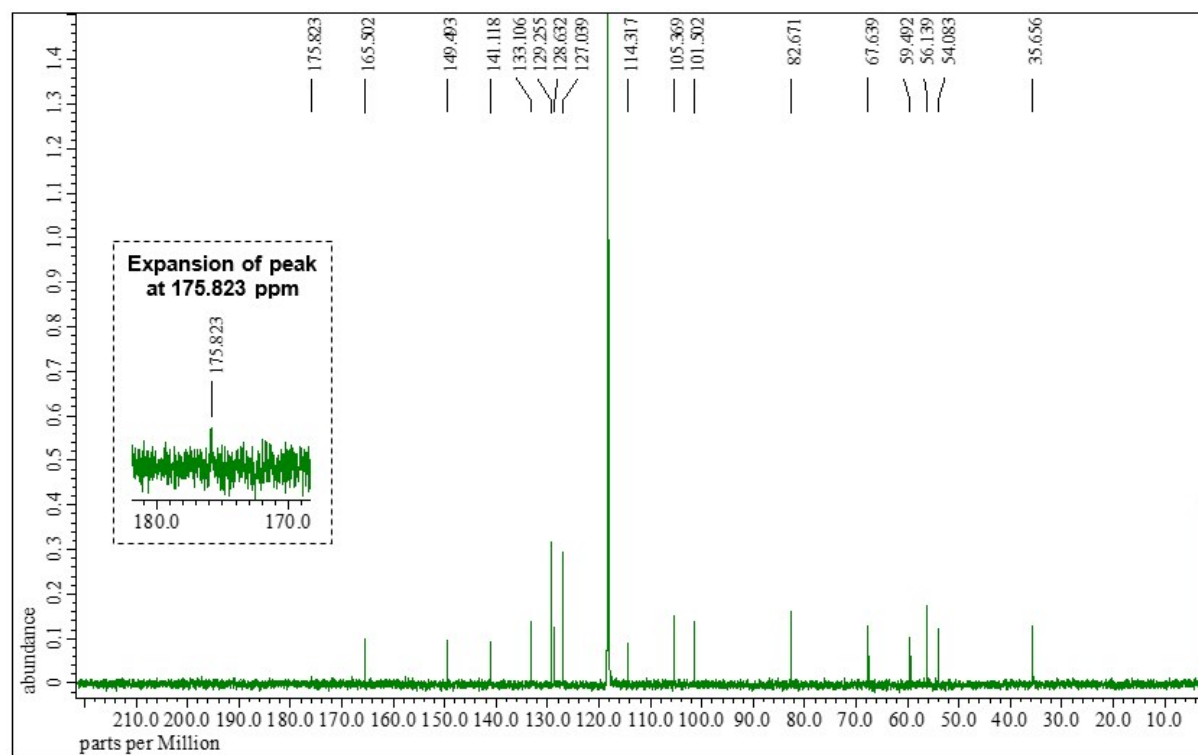


Figure S45. $^{13}\text{C}\{^1\text{H}\}$ NMR spectrum of **7e** (126 MHz, $\text{MeCN-}d_3$)

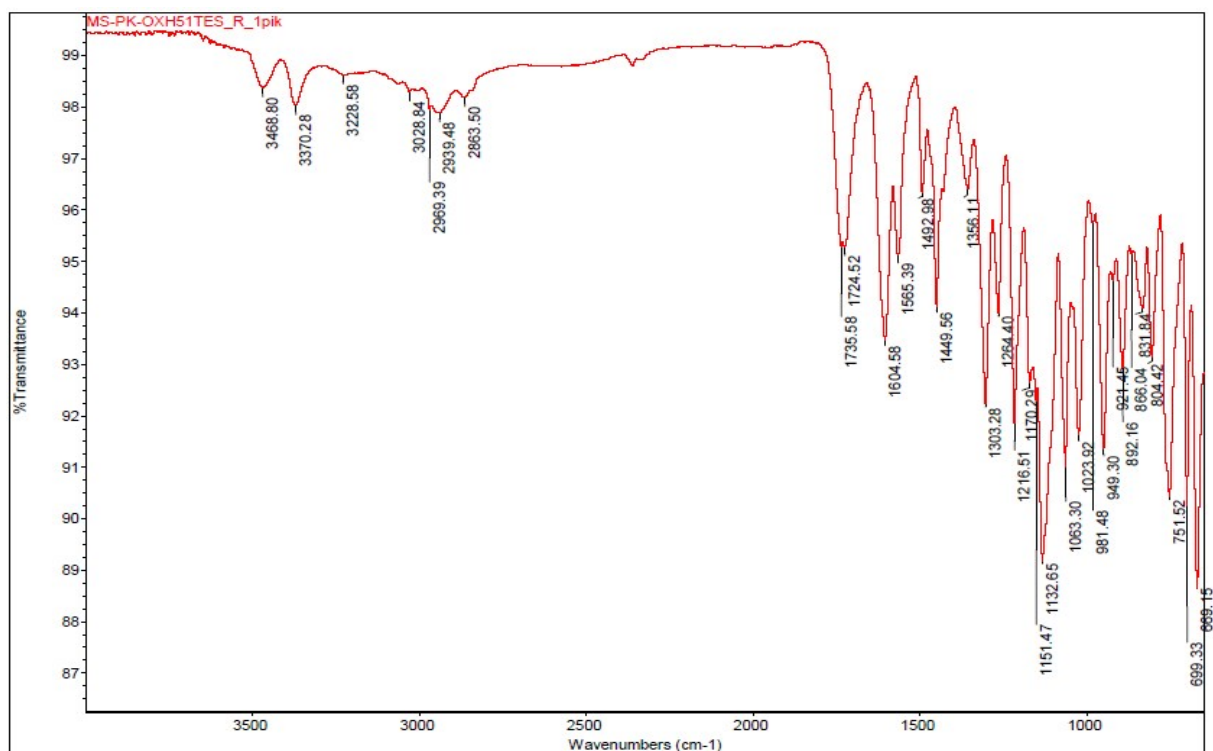


Figure S46. IR spectrum of 7e

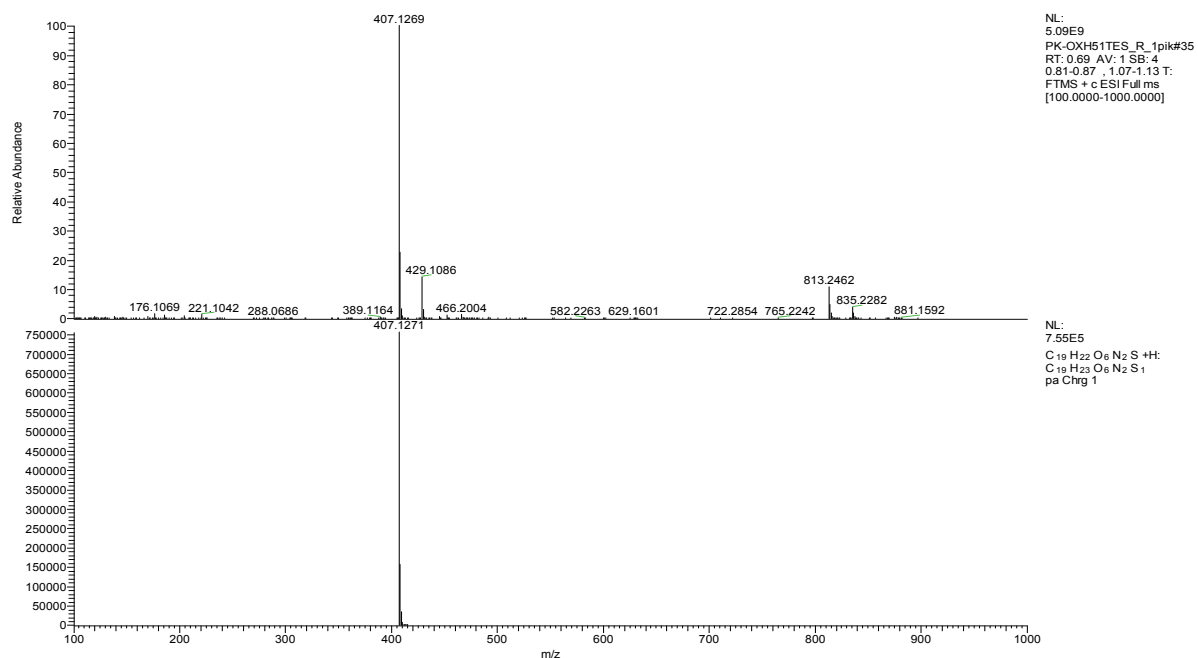
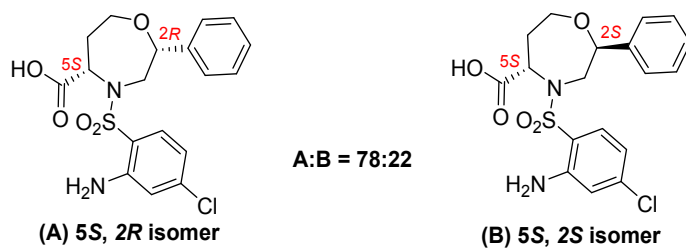


Figure S47. HRMS spectrum of 7e

(-)-(2*RS*,5*S*)-4-((2-amino-4-chlorophenyl)sulfonyl)-2-phenyl-1,4-oxazepane-5-carboxylic acid 7f^{2RS}



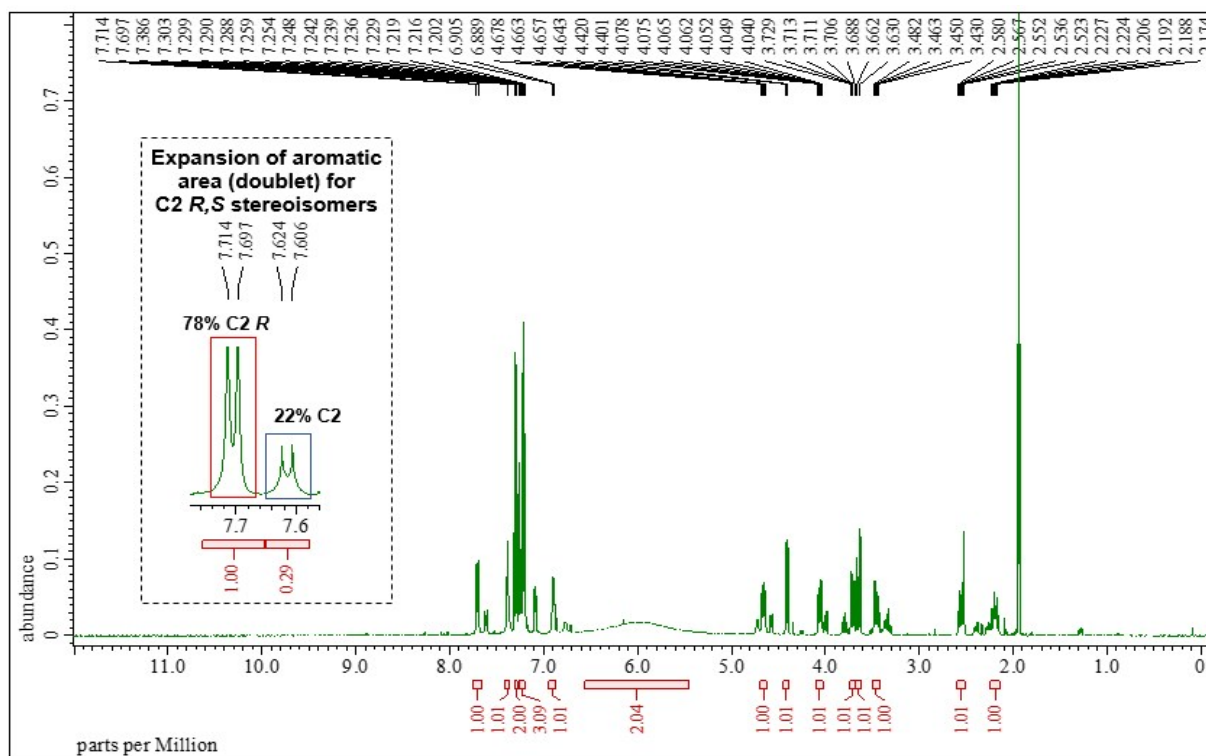


Figure S48. ^1H NMR spectrum of $7f^{2RS}$ (500 MHz, $\text{MeCN-}d_3$). Note: Only the signals belonging to the major diastereomer were analyzed.

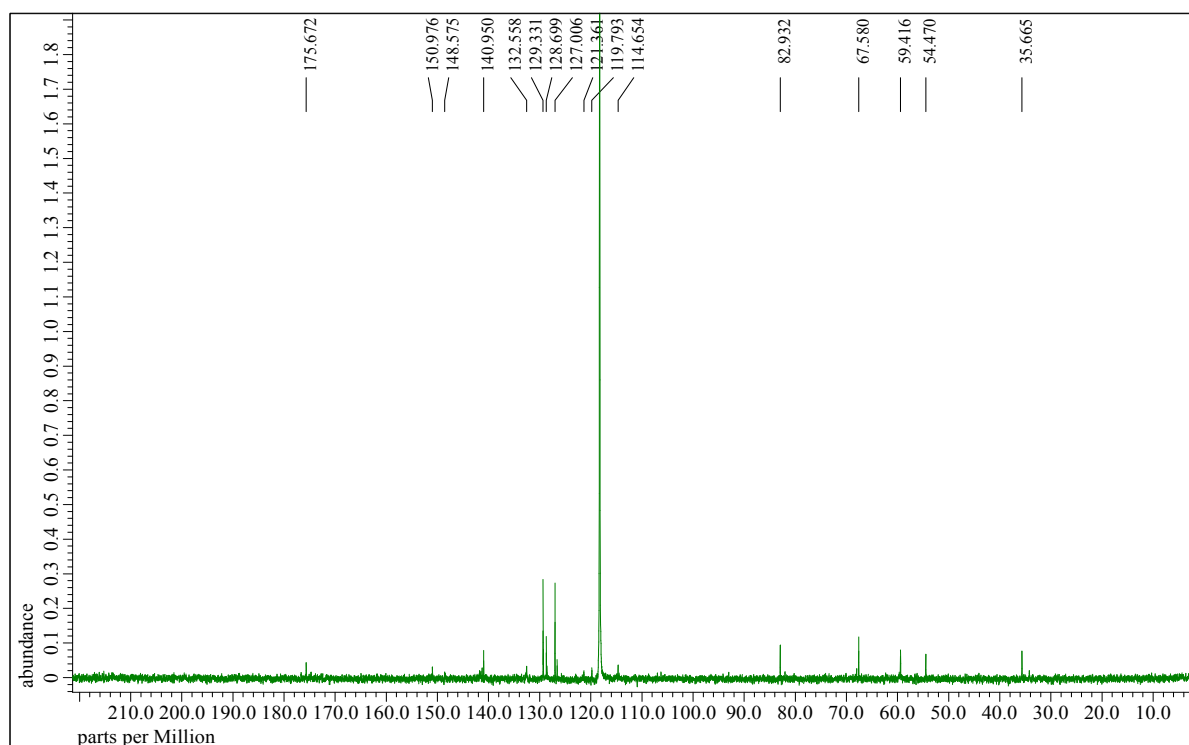


Figure S49. $^{13}\text{C}\{^1\text{H}\}$ NMR spectrum of $7f^{2RS}$ (126 MHz, $\text{MeCN-}d_3$). Note: Only the signals belonging to the major diastereomer were analyzed.

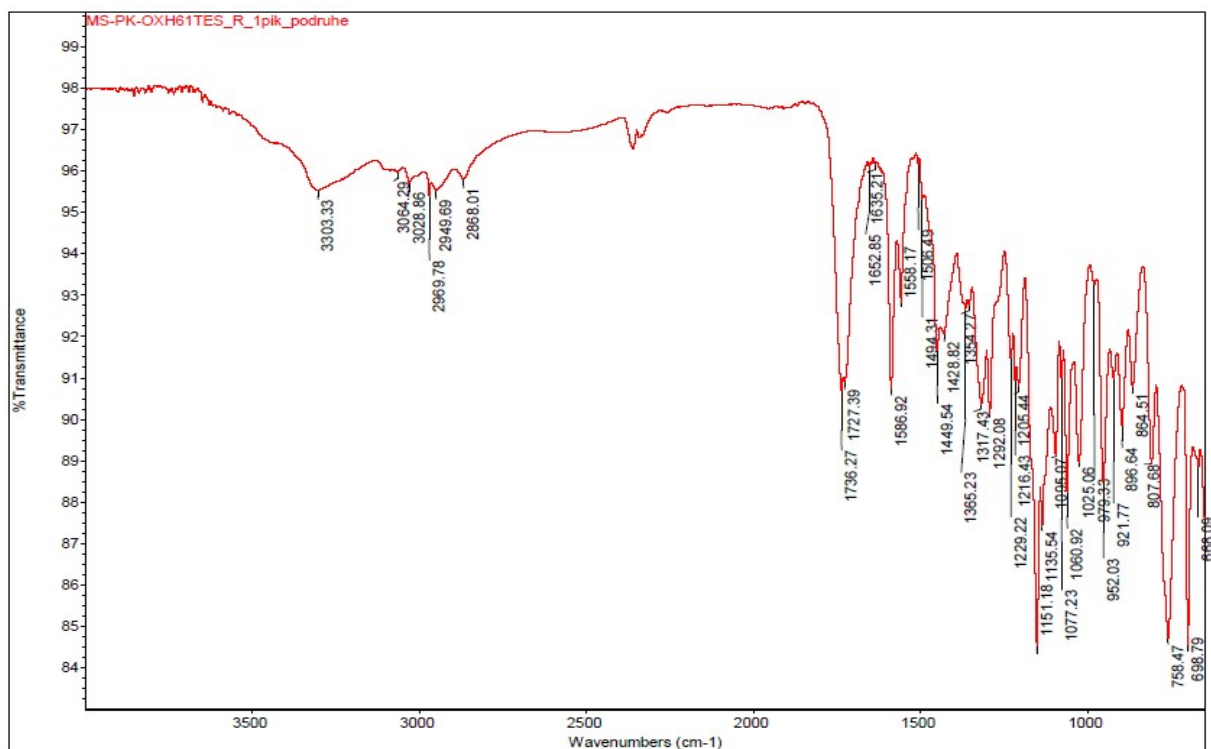


Figure S50. IR spectrum of **7f^{2RS}**

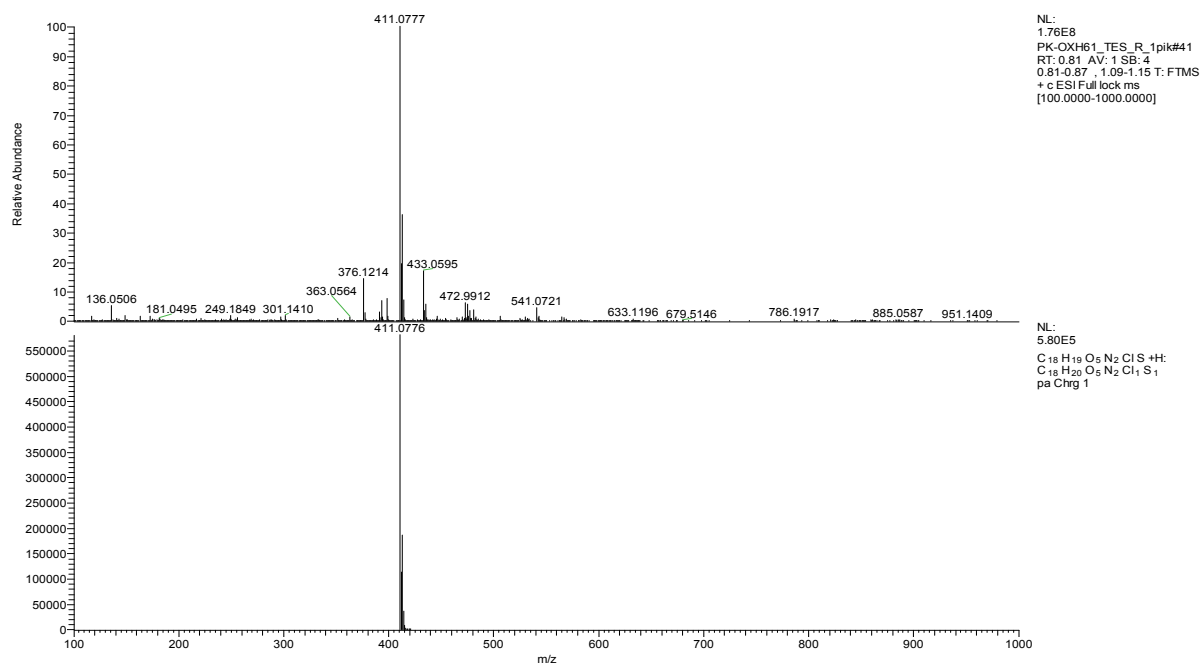
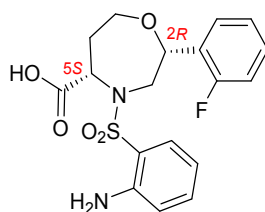


Figure S51. HRMS spectrum of **7f^{2RS}**

(-)-(2R,5S)-4-((2-aminophenyl)sulfonyl)-2-(2-fluorophenyl)-1,4-oxazepane-5-carboxylic acid 7i^{2R}



S29

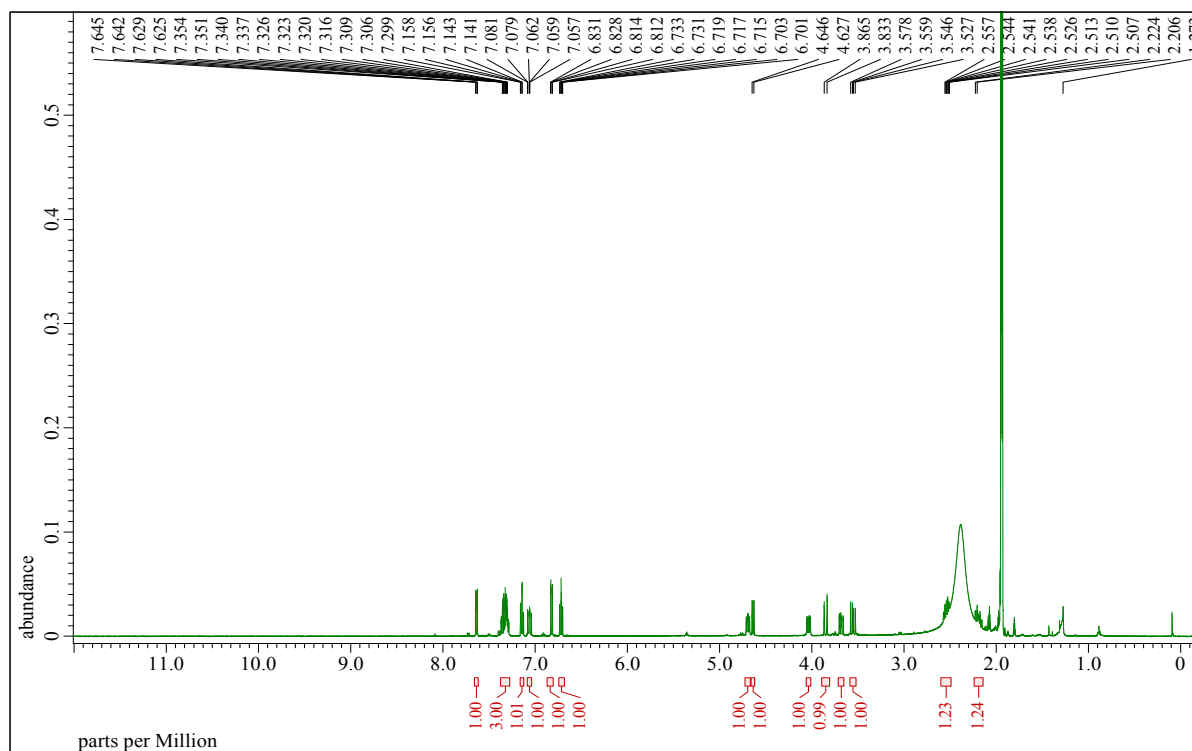


Figure S52. ^1H NMR spectrum of $7i^{2R}$ (500 MHz, $\text{MeCN-}d_3$)

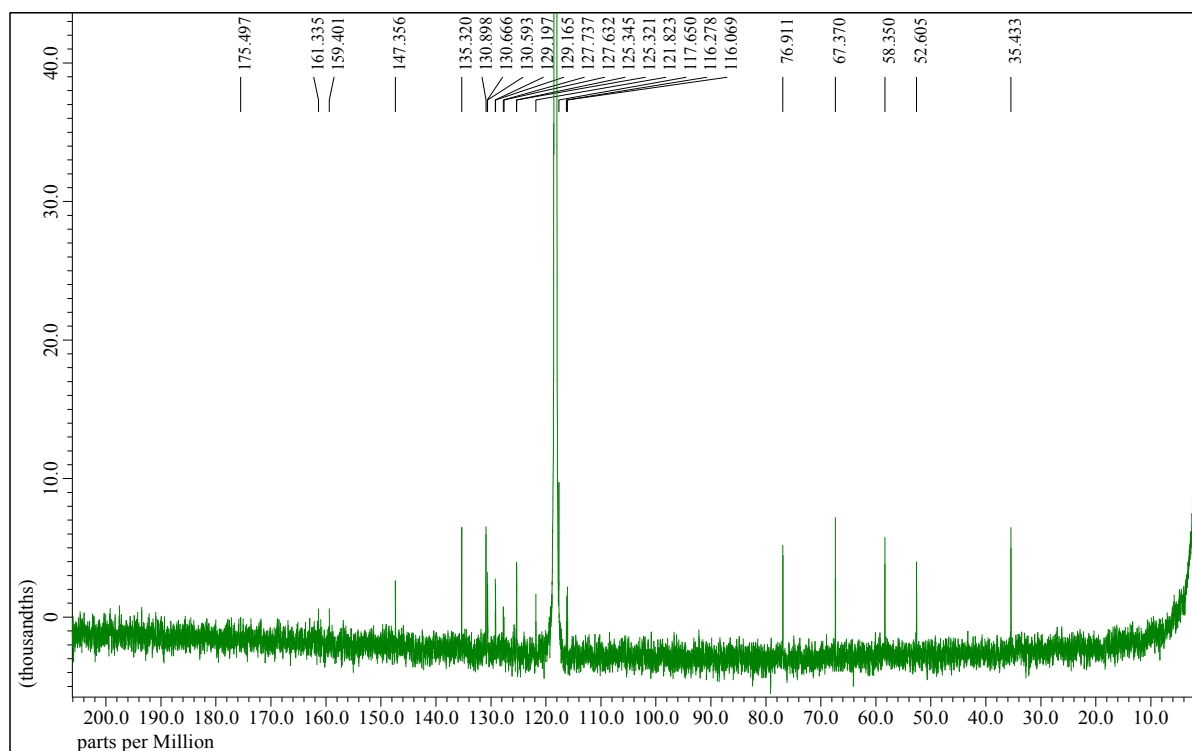


Figure S53. $^{13}\text{C}\{^1\text{H}\}$ NMR spectrum of $7i^{2R}$ (126 MHz, $\text{MeCN-}d_3$)

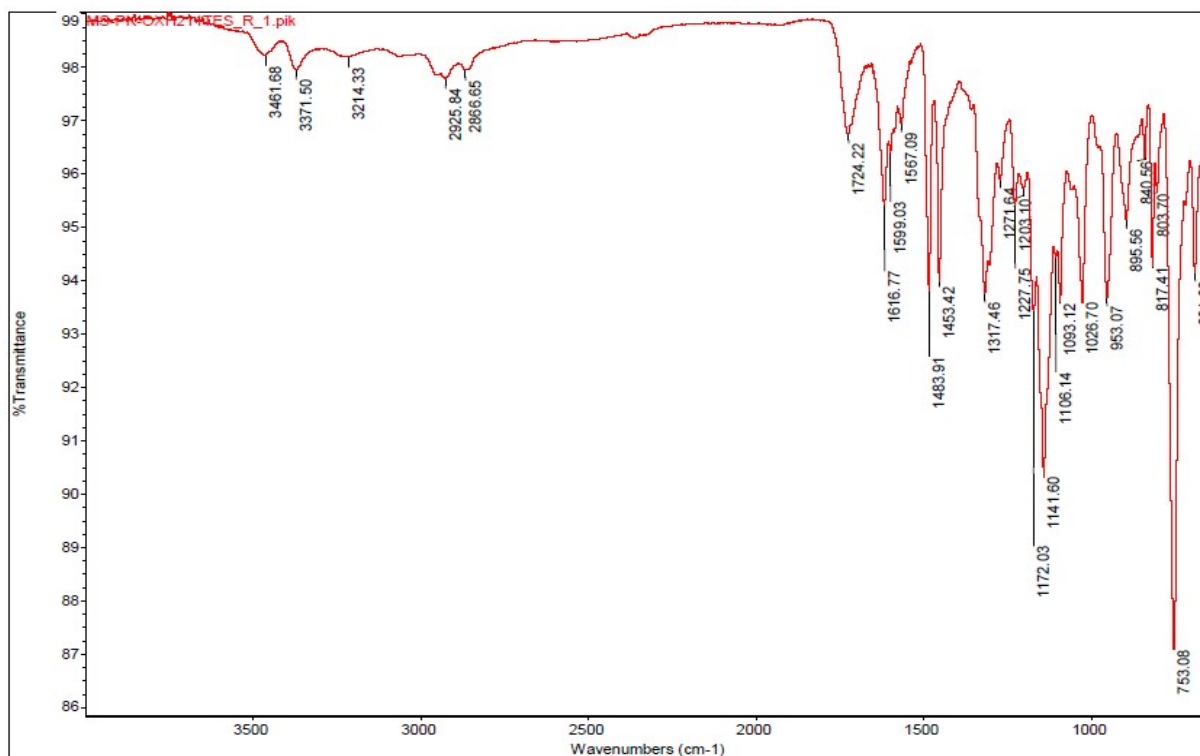


Figure S54. IR spectrum of **7i^{2R}**

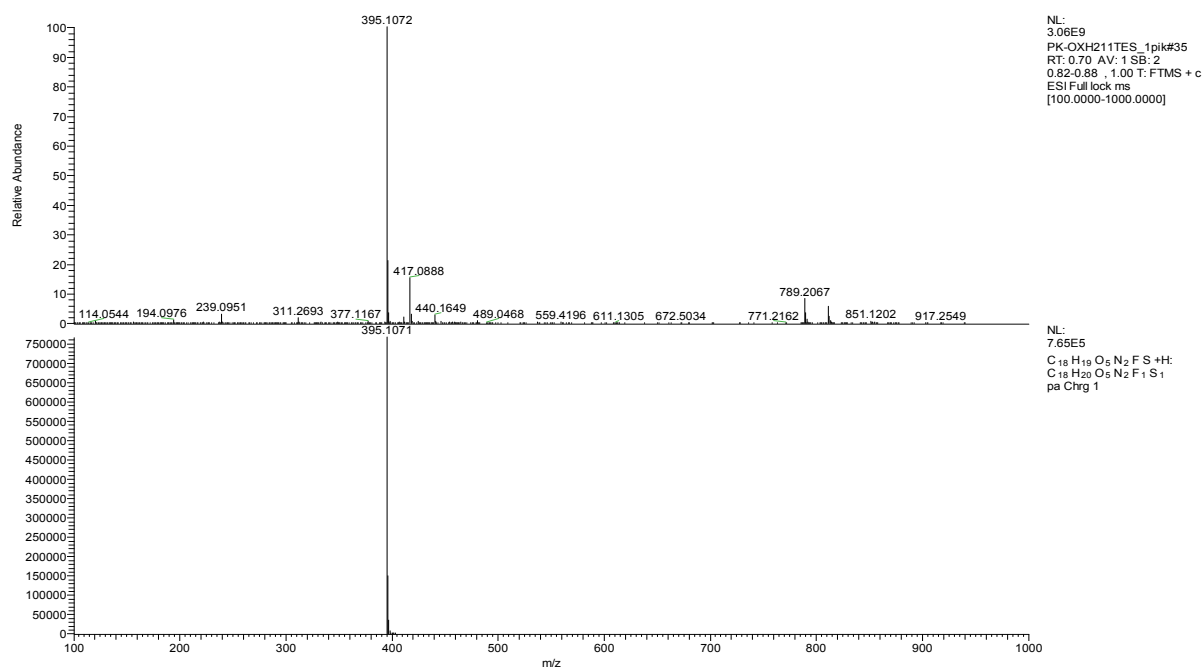
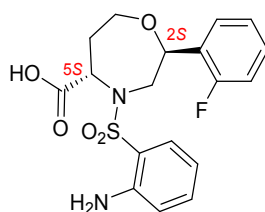


Figure S55. HRMS spectrum of **7i^{2R}**

(-)-(2*S*,5*S*)-4-((2-aminophenyl)sulfonyl)-2-(2-fluorophenyl)-1,4-oxazepane-5-carboxylic acid 7i^{2S}



S31

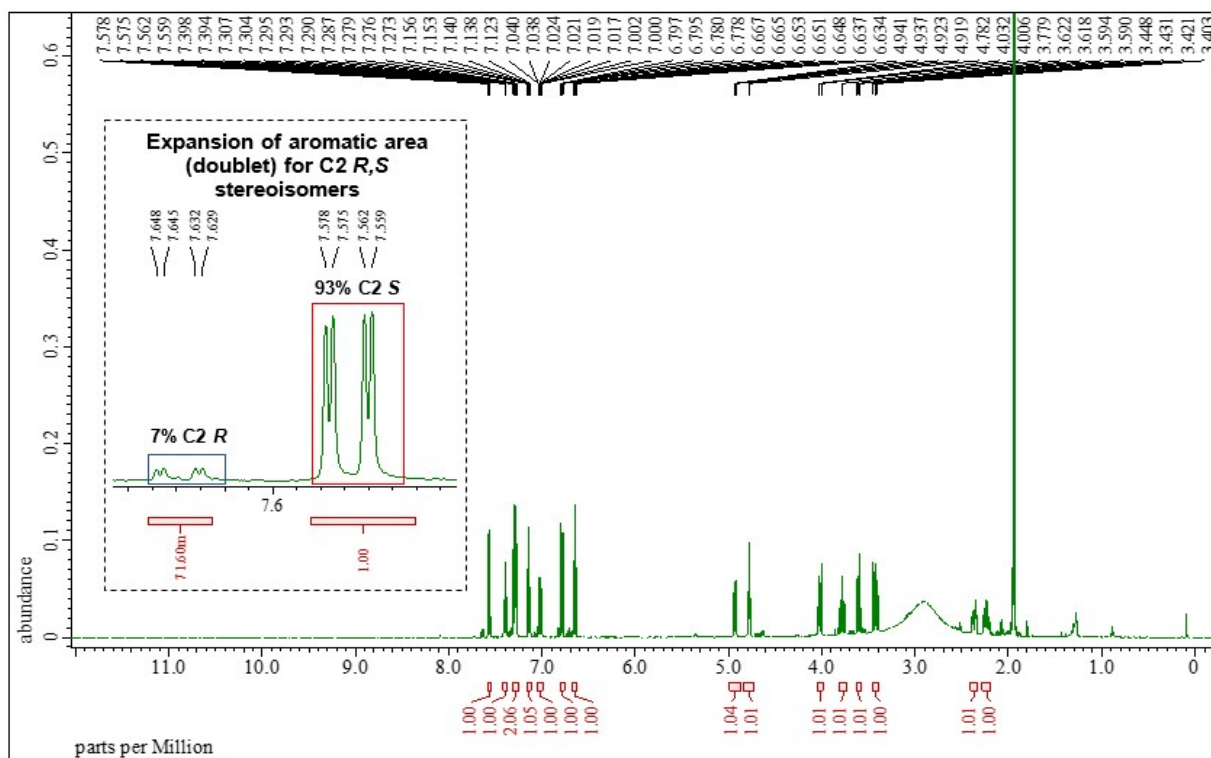


Figure S56. ^1H NMR spectrum of $7i^{2S}$ (500 MHz, $\text{MeCN-}d_3$). Note: Only the signals belonging to the major diastereomer were analyzed.

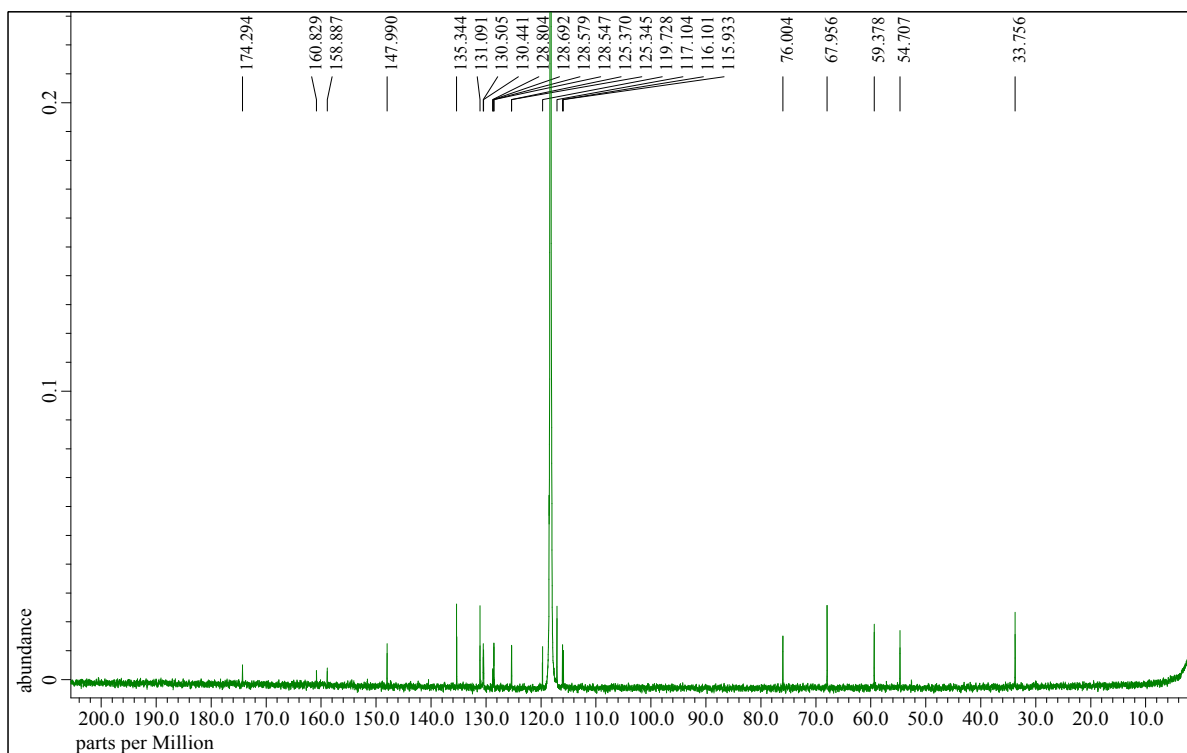


Figure S57. $^{13}\text{C}\{^1\text{H}\}$ NMR spectrum of $7i^{2S}$ (126 MHz, $\text{MeCN-}d_3$). Note: Only the signals belonging to the major diastereomer were analyzed.

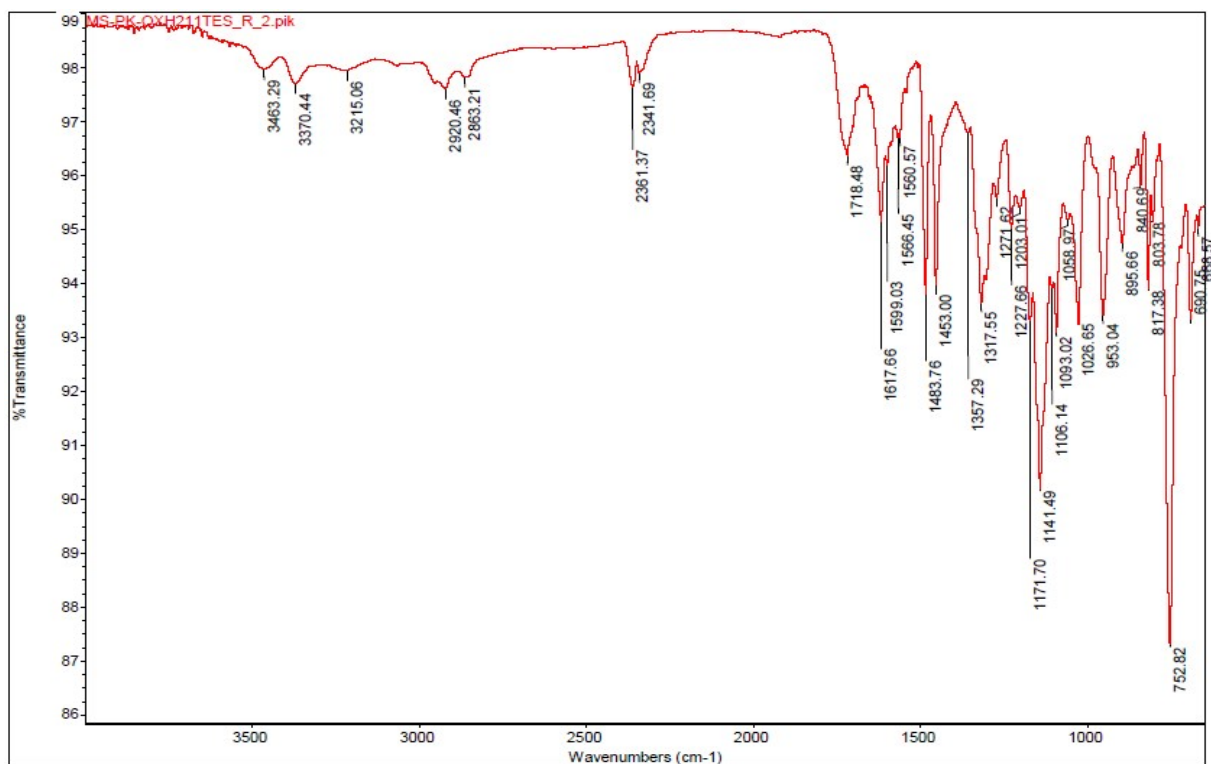


Figure S58. IR spectrum of 7i2S

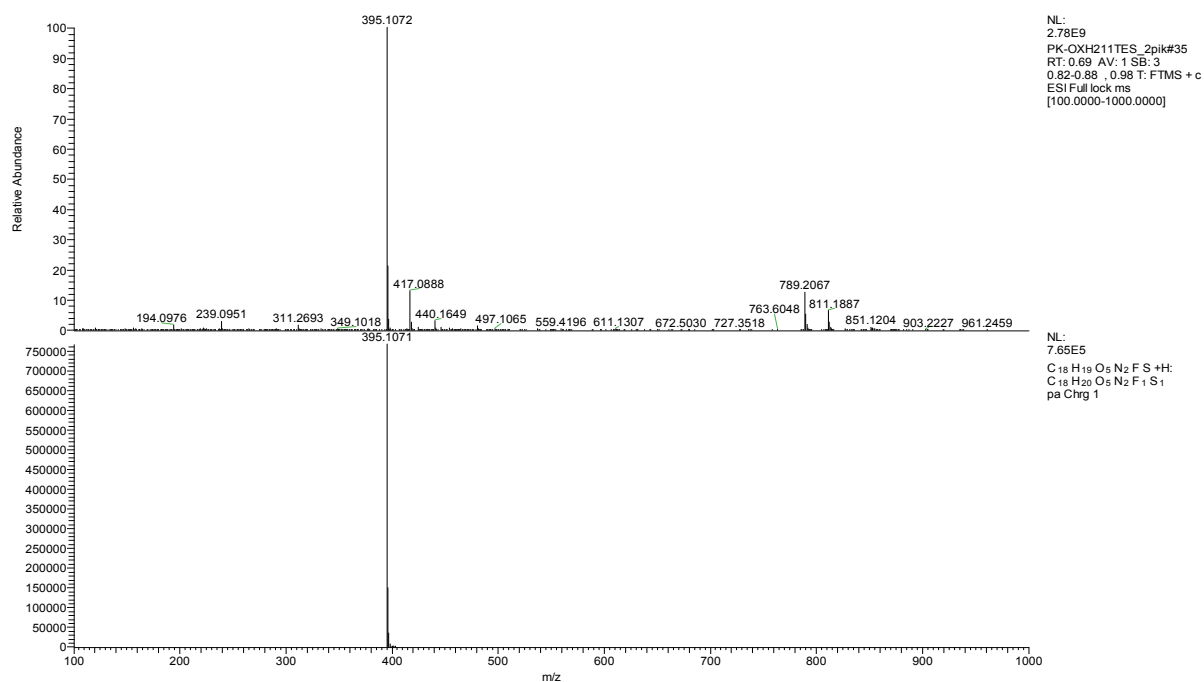
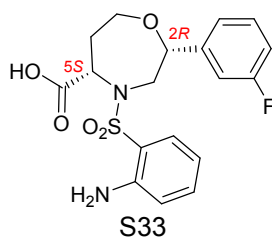


Figure S59. HRMS spectrum of 7i2S

(-)-(2*R*,5*S*)-4-((2-aminophenyl)sulfonyl)-2-(3-fluorophenyl)-1,4-oxazepane-5-carboxylic acid 7k



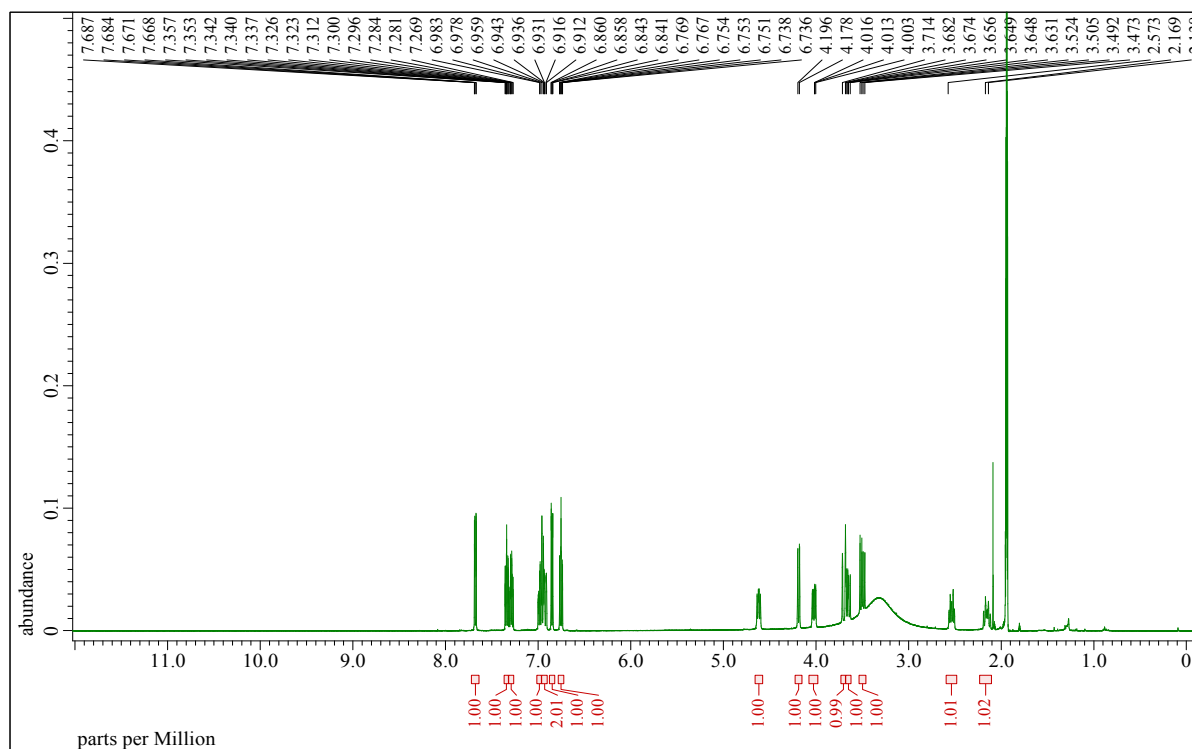


Figure S60. ^1H NMR spectrum of **7k** (500 MHz, $\text{MeCN-}d_3$)

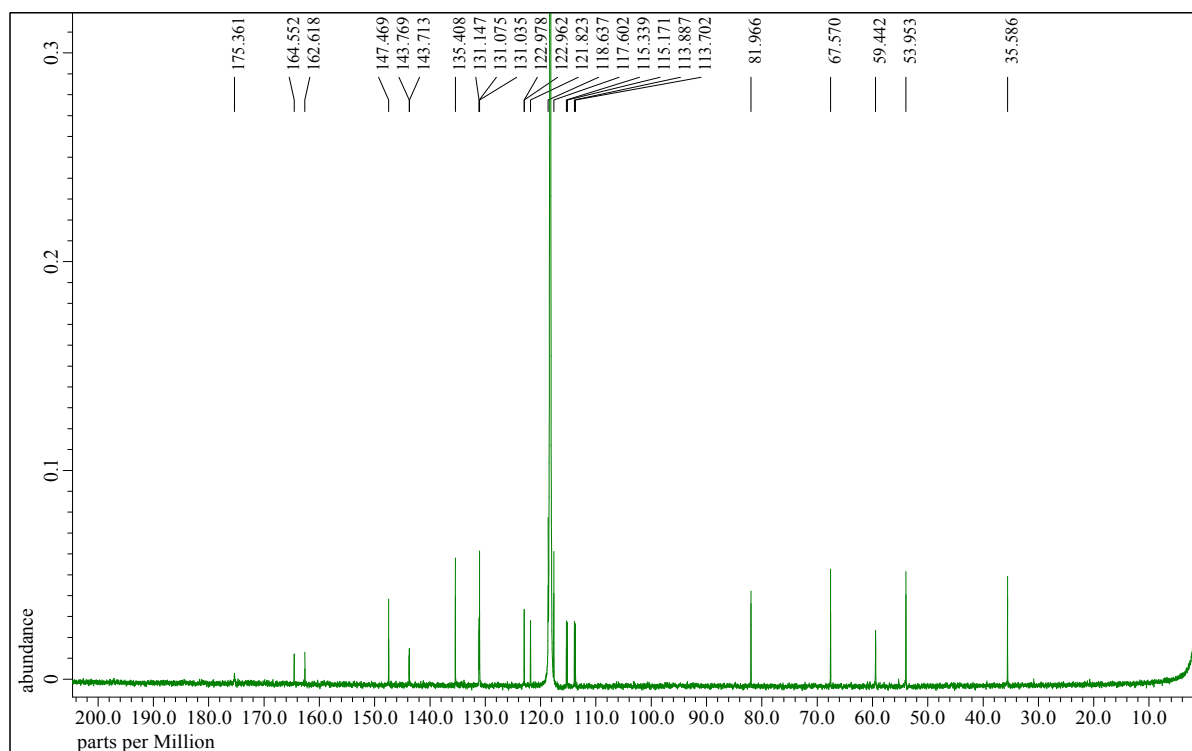


Figure S61. $^{13}\text{C}\{^1\text{H}\}$ NMR spectrum of **7k** (126 MHz, $\text{MeCN-}d_3$)

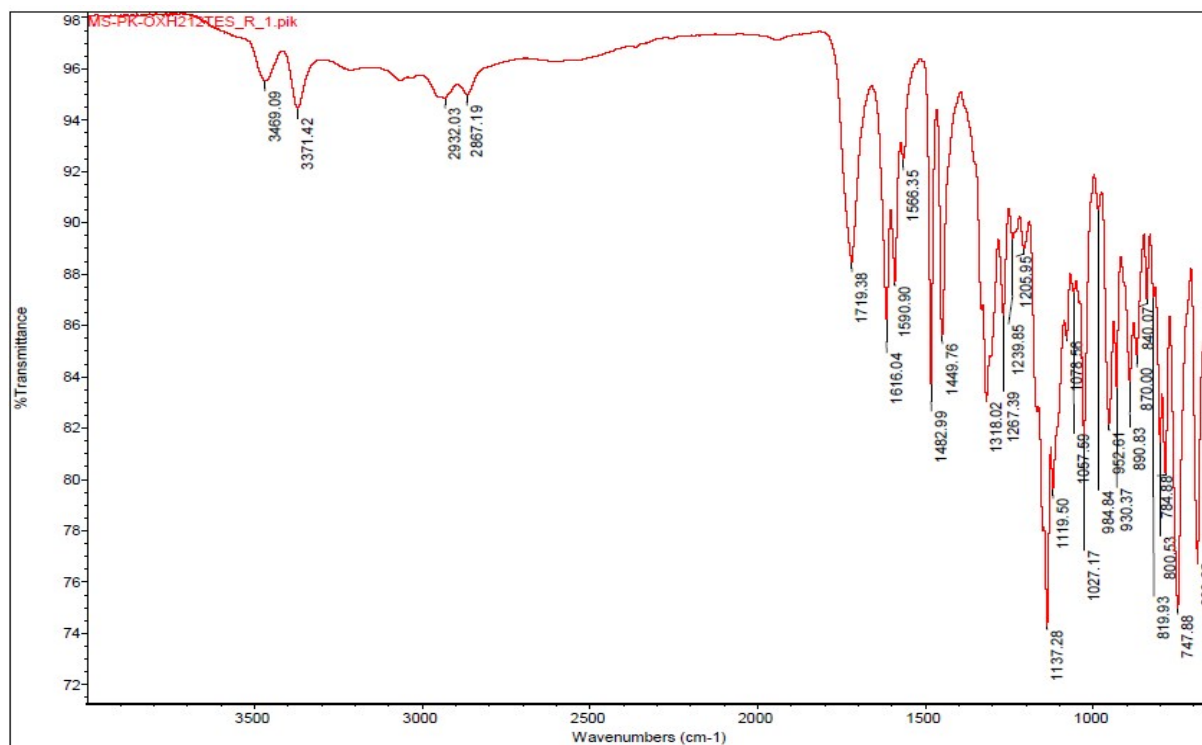


Figure S62. IR spectrum of 7k

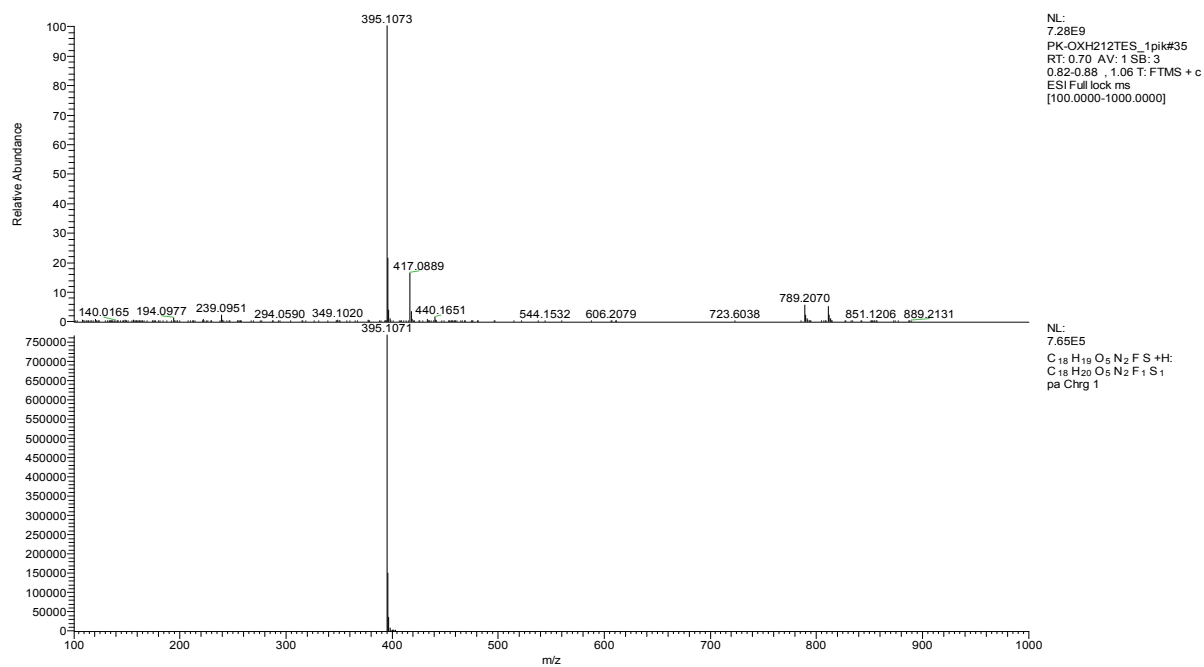
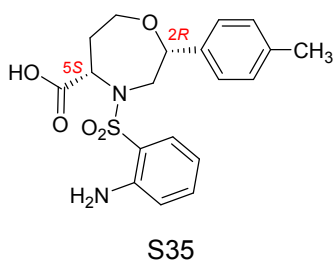


Figure S63. HRMS spectrum of 7k

(+)-(2*R*,5*S*)-4-((2-aminophenyl)sulfonyl)-2-(*p*-tolyl)-1,4-oxazepane-5-carboxylic acid 7m



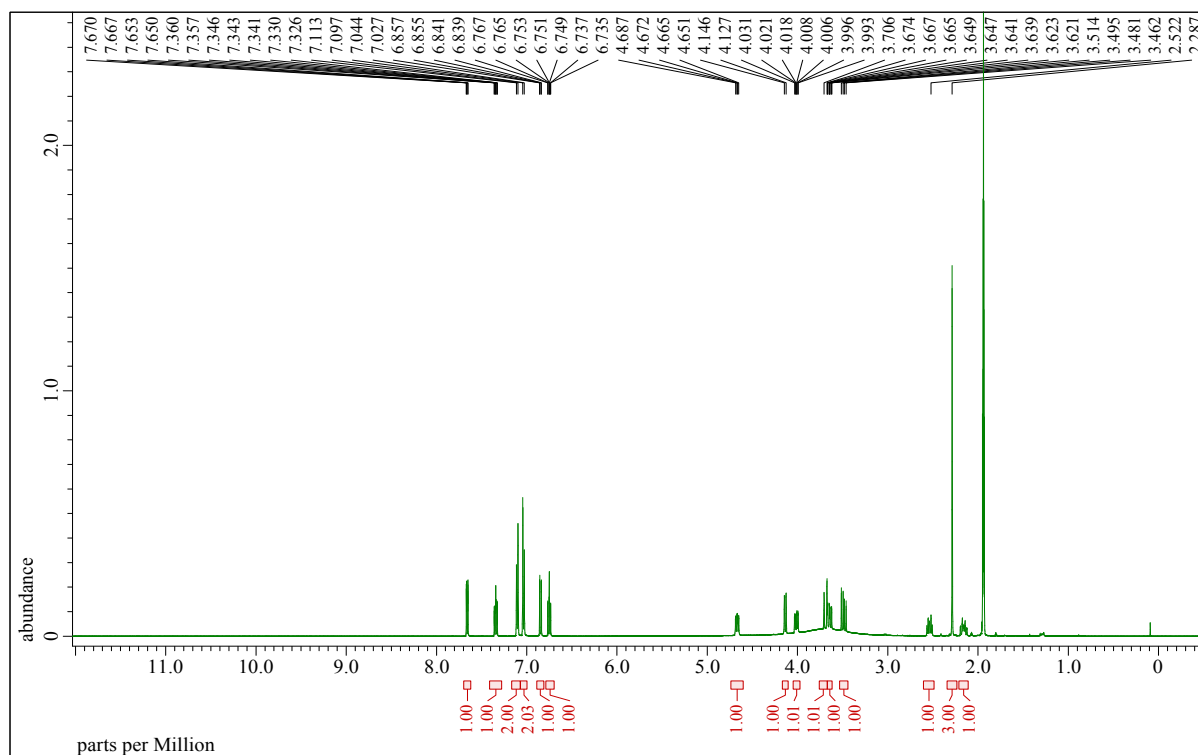


Figure S64. ^1H NMR spectrum of **7m** (500 MHz, MeCN-d_3)

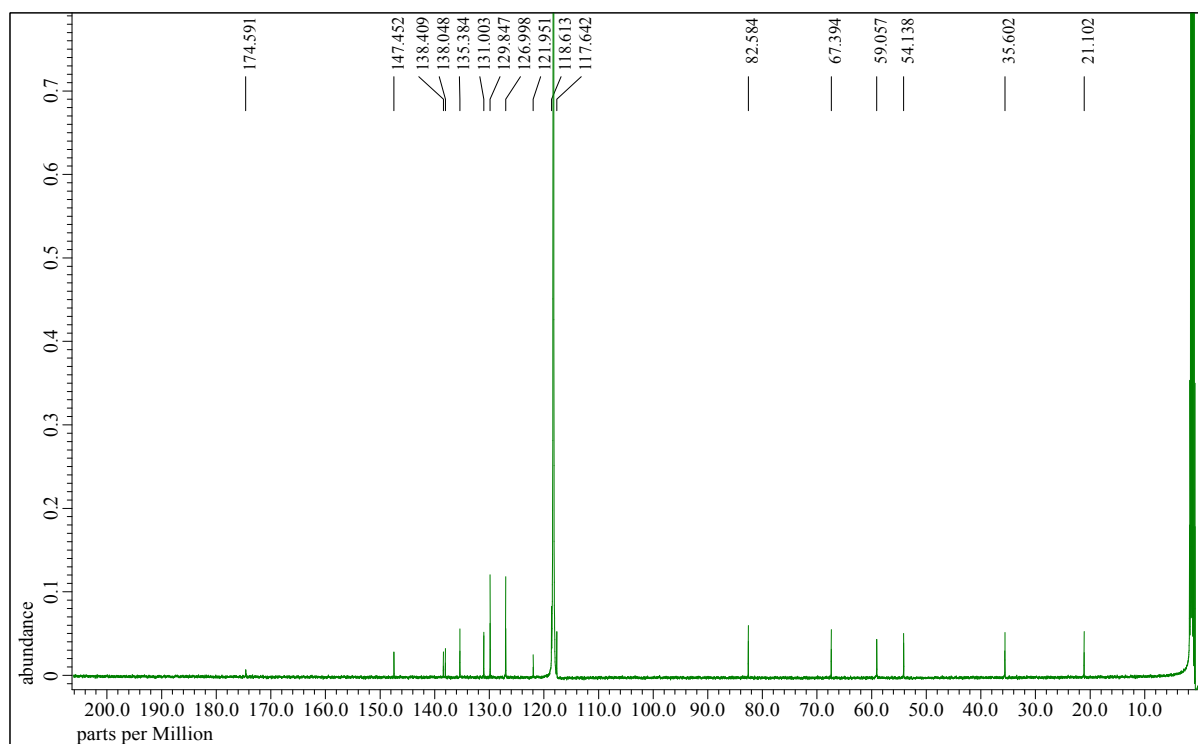


Figure S65. $^{13}\text{C}\{^1\text{H}\}$ NMR spectrum of **7m** (126 MHz, MeCN-d_3)

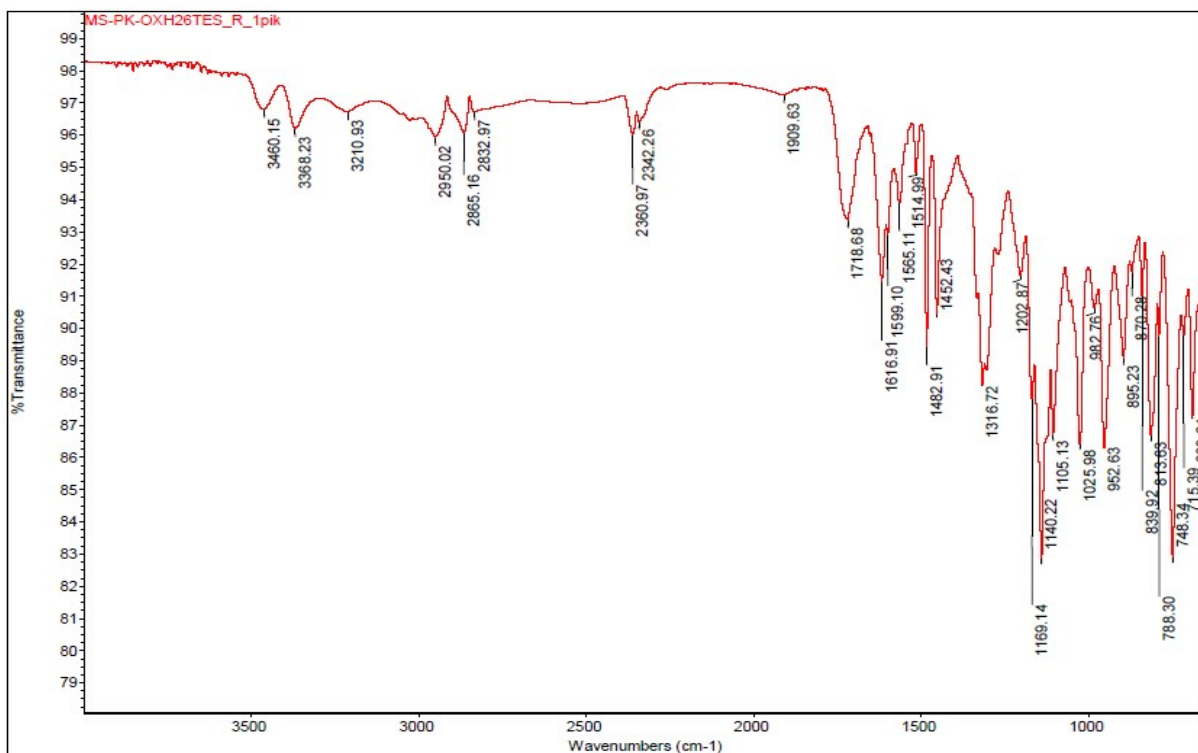


Figure S66. IR spectrum of 7m

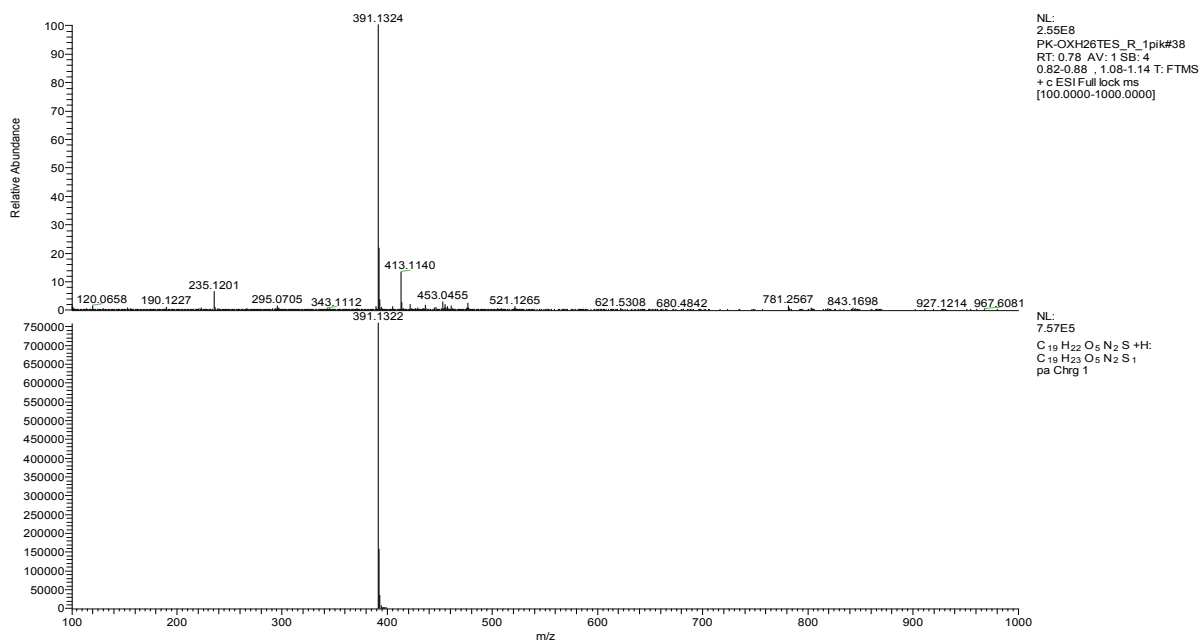
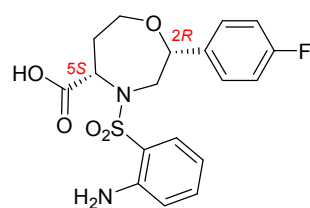
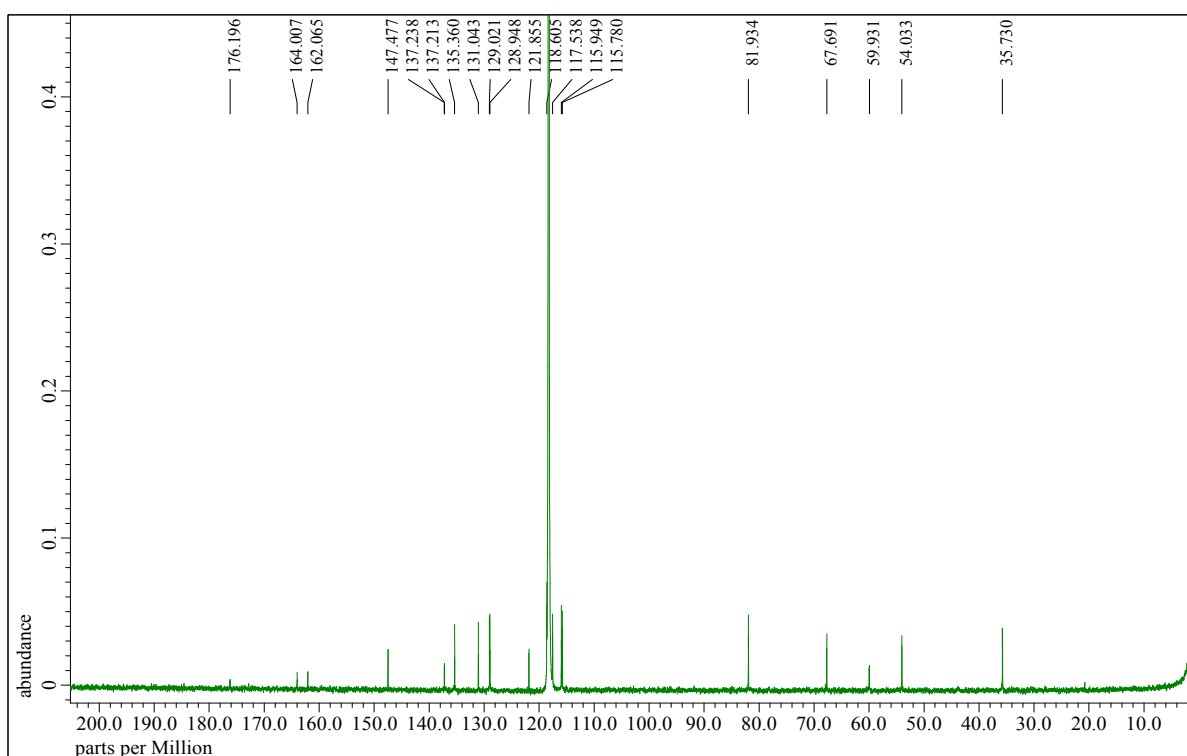
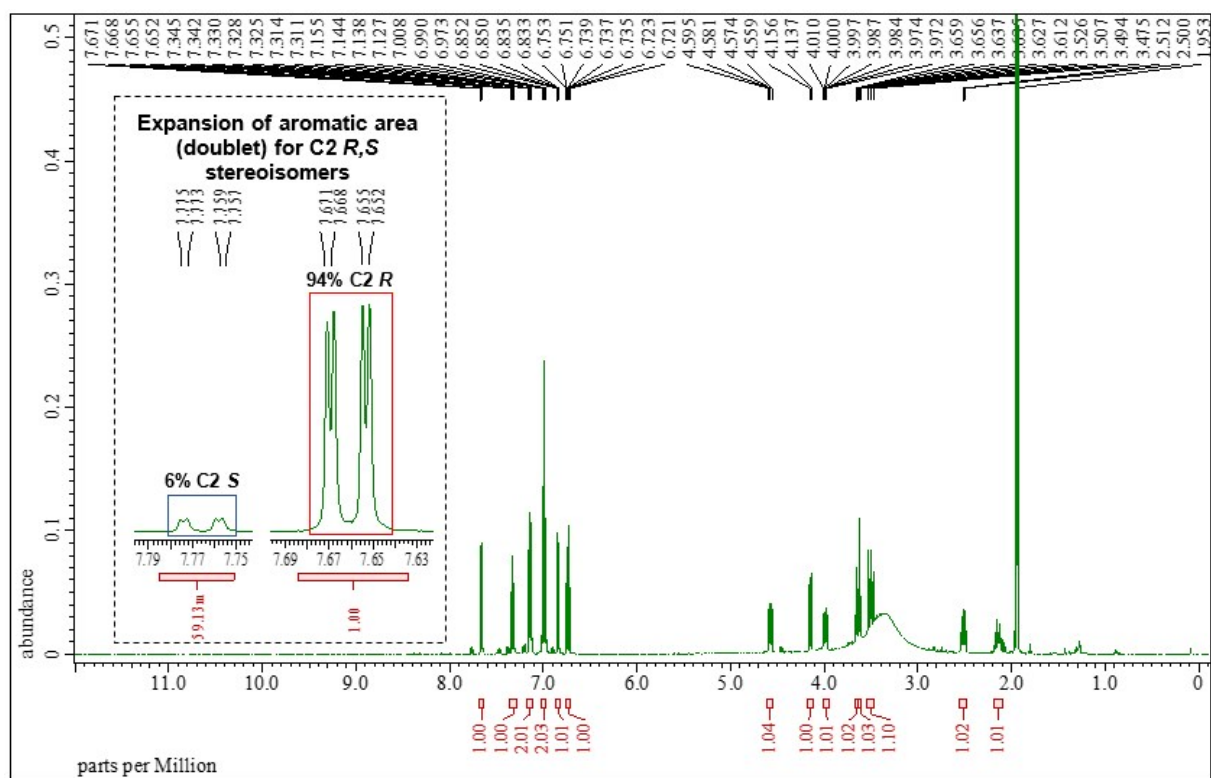


Figure S67. HRMS spectrum of 7m

(+)-(2*R*,5*S*)-4-((2-aminophenyl)sulfonyl)-2-(4-fluorophenyl)-1,4-oxazepane-5-carboxylic acid 7o





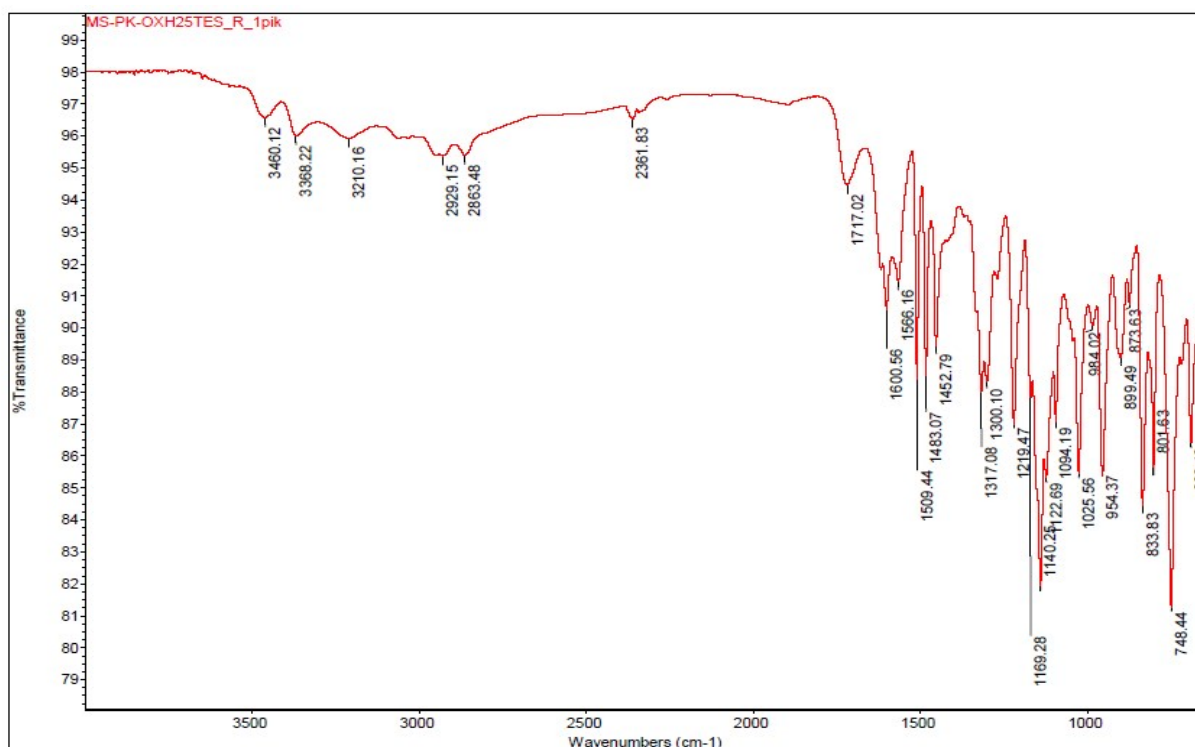


Figure S70. IR spectrum of **7o**

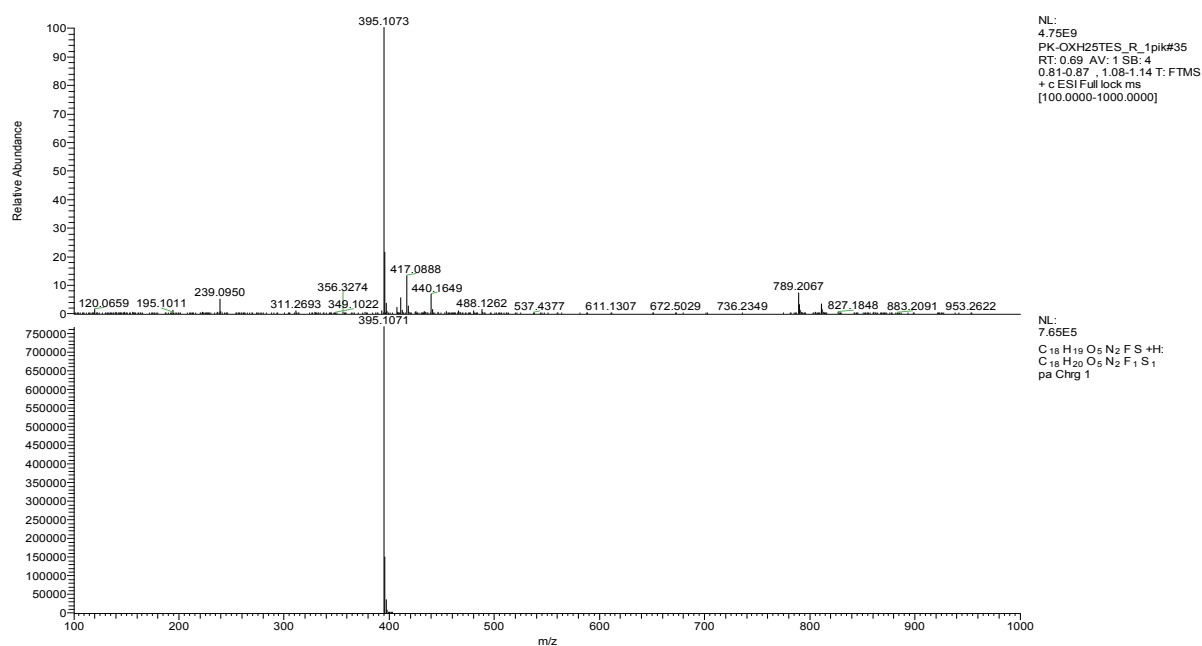
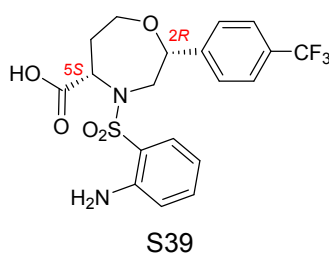


Figure S71. HRMS spectrum of **7o**

(-)-(2*R*,5*S*)-4-((2-aminophenyl)sulfonyl)-2-(4-(trifluoromethyl)phenyl)-1,4-oxazepane-5-carboxylic acid **7q**



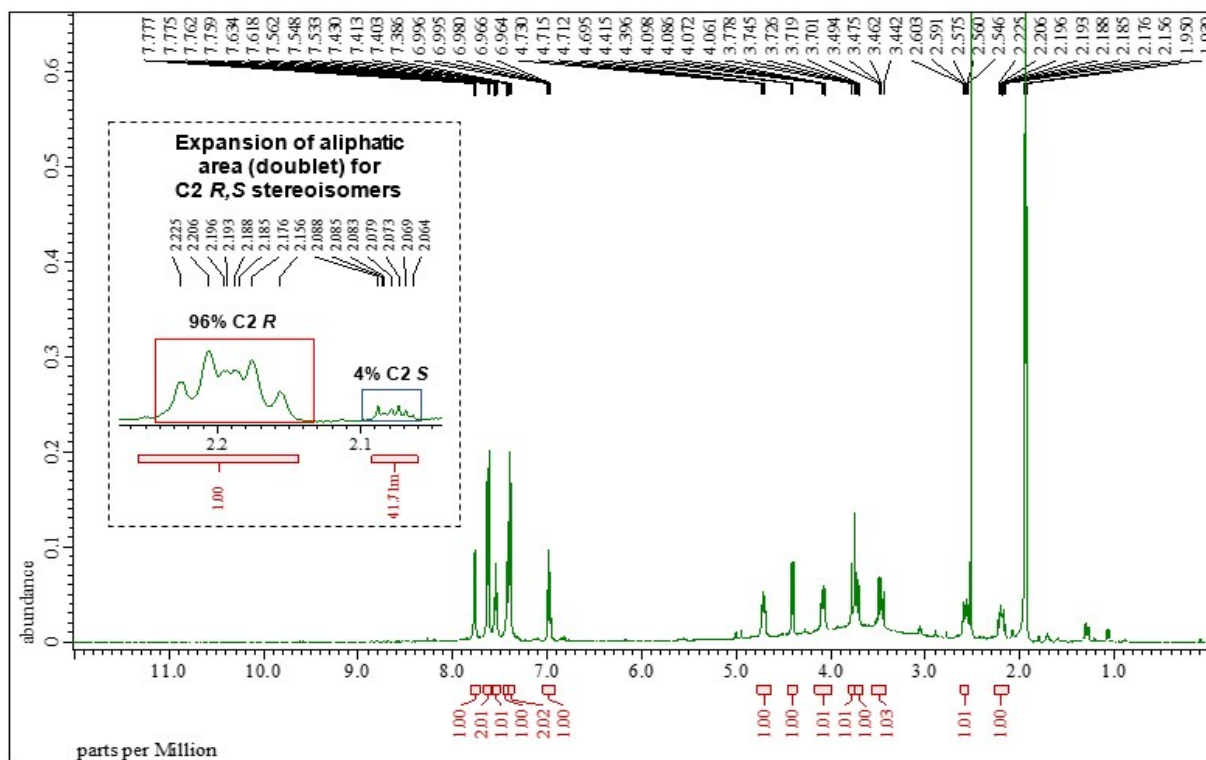


Figure S72. ^1H NMR spectrum of **7q** (500 MHz, $\text{MeCN-}d_3$). Note: Only the signals belonging to the major diastereomer were analyzed.

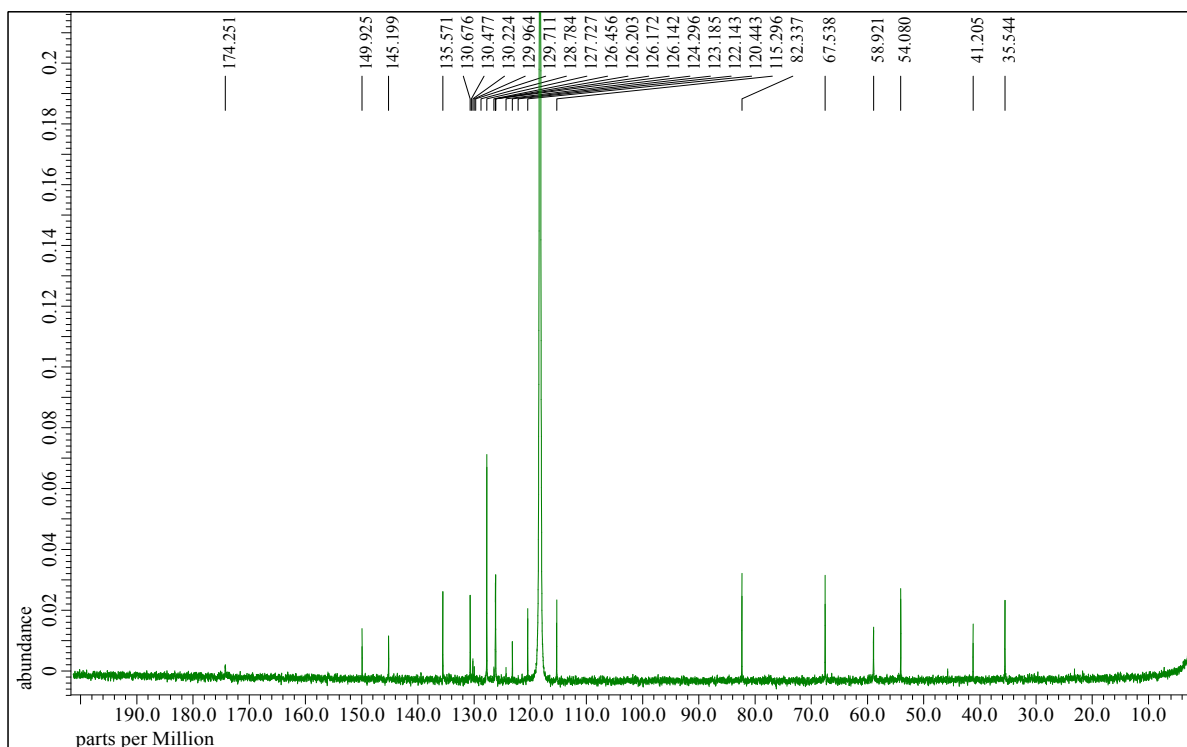


Figure S73. $^{13}\text{C}\{^1\text{H}\}$ NMR spectrum of **7q** (126 MHz, $\text{MeCN-}d_3$). Note: Only the signals belonging to the major diastereomer were analyzed.

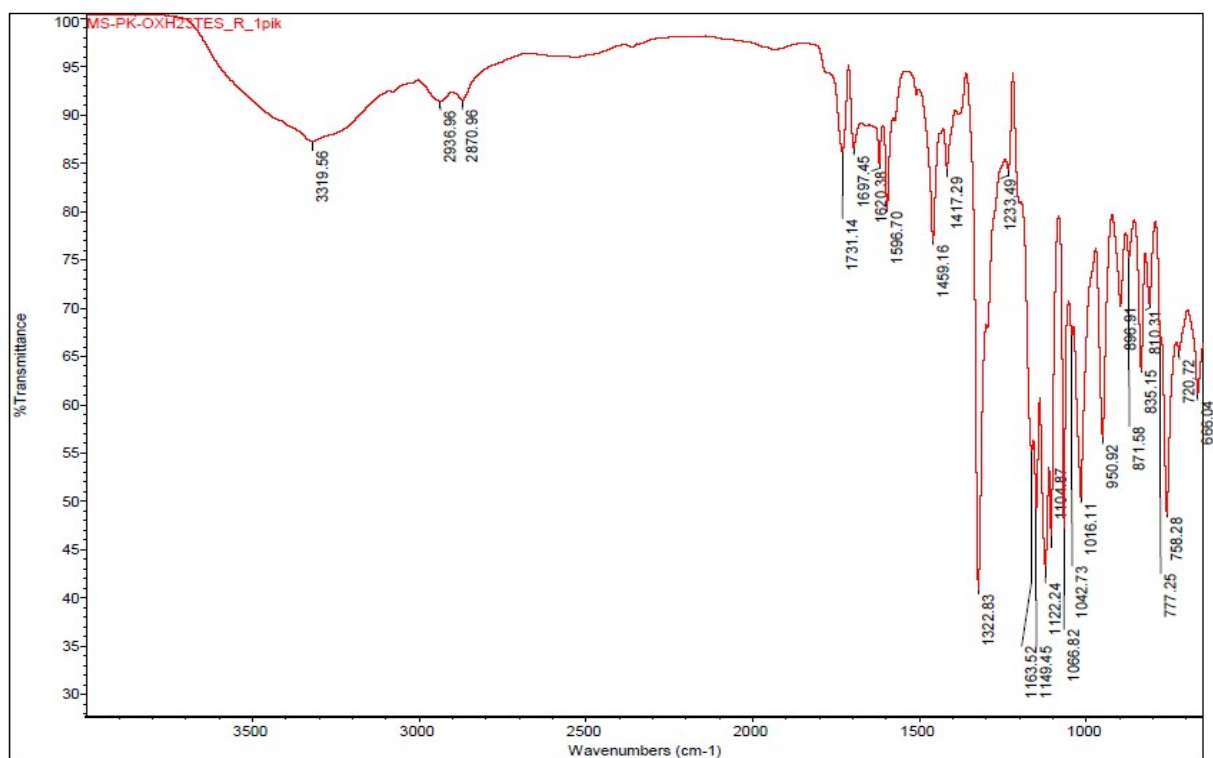


Figure S74. IR spectrum of 7q

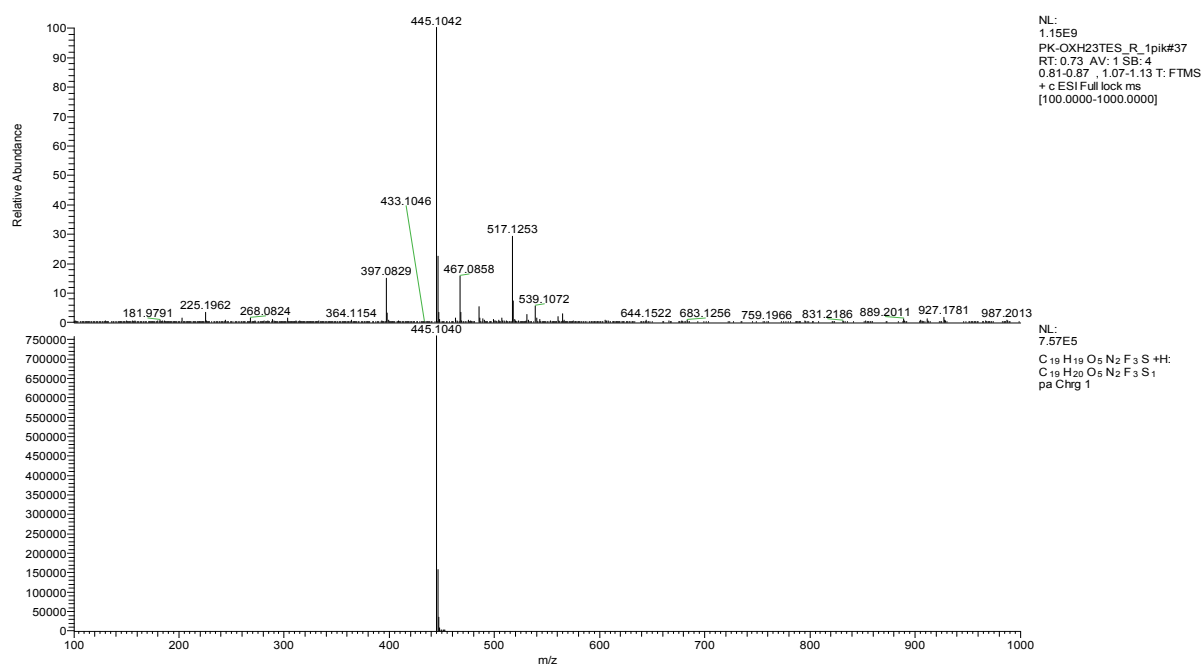
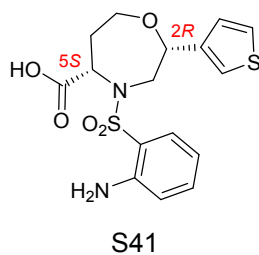


Figure S75. HRMS spectrum of 7q

(-)-(2R,5S)-4-((2-aminophenyl)sulfonyl)-2-(thiophen-3-yl)-1,4-oxazepane-5-carboxylic acid 7t



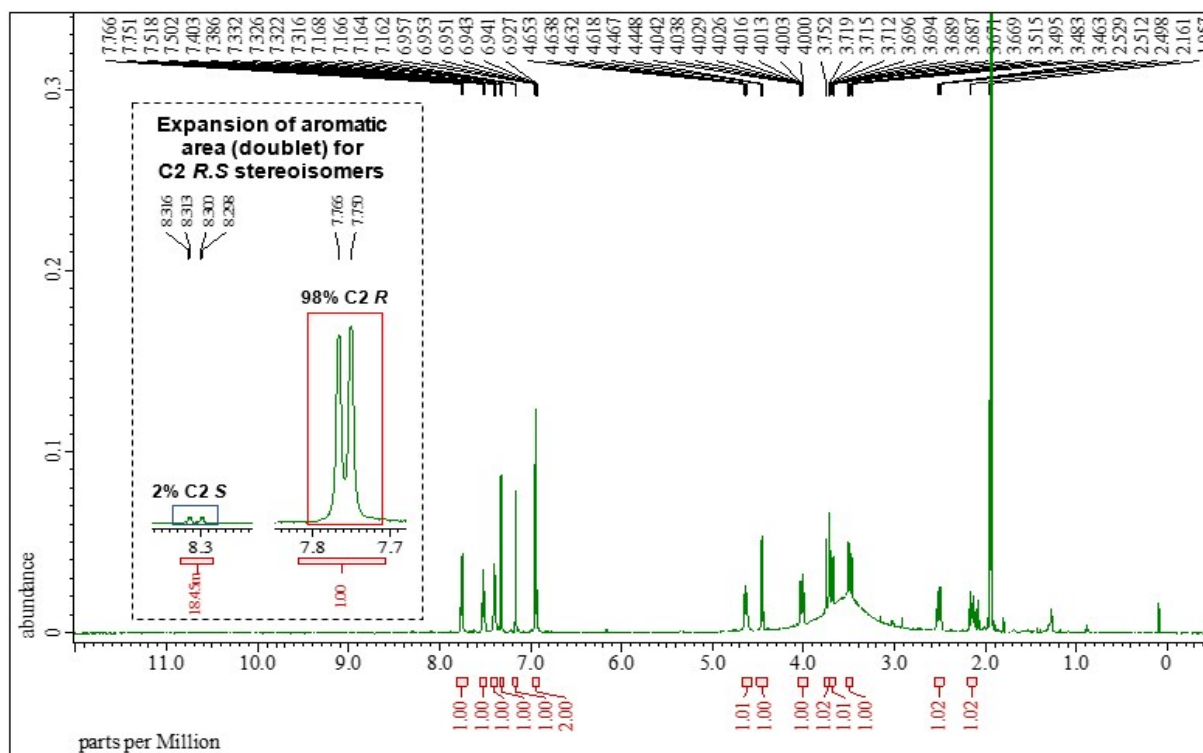


Figure S76. ^1H NMR spectrum of **7t** (500 MHz, $\text{MeCN-}d_3$)

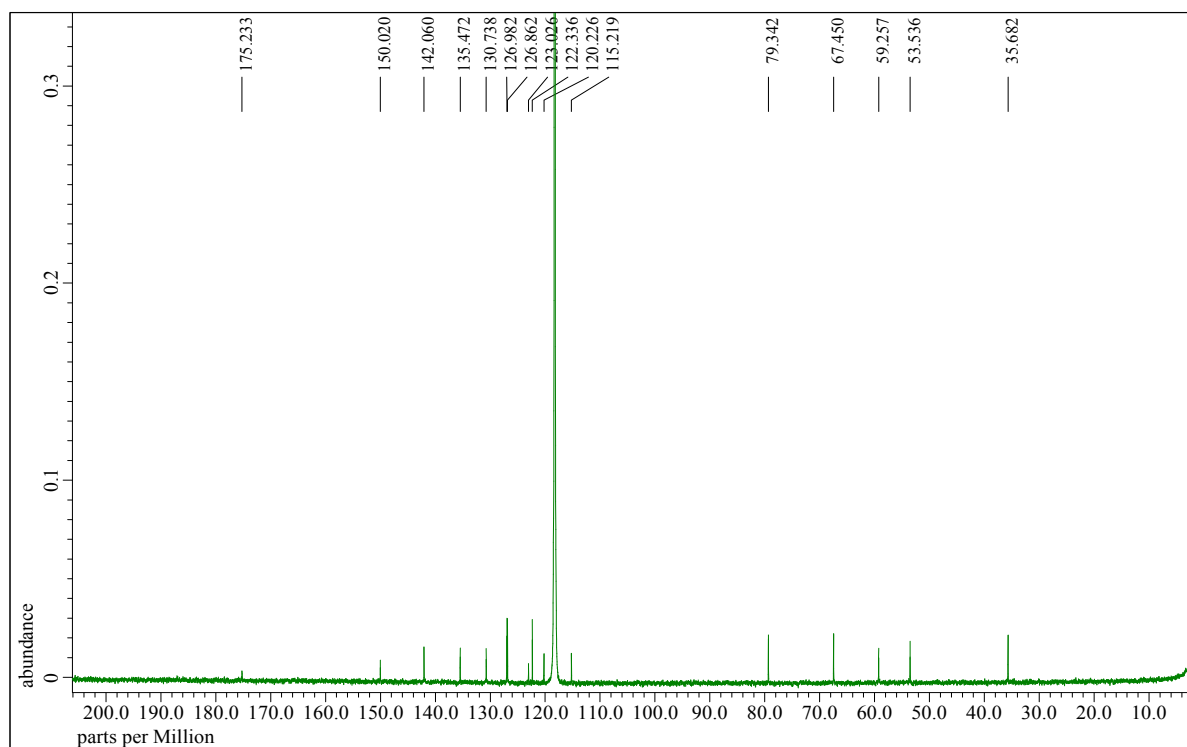


Figure S77. $^{13}\text{C}\{^1\text{H}\}$ NMR spectrum of **7t** (126 MHz, $\text{MeCN-}d_3$)

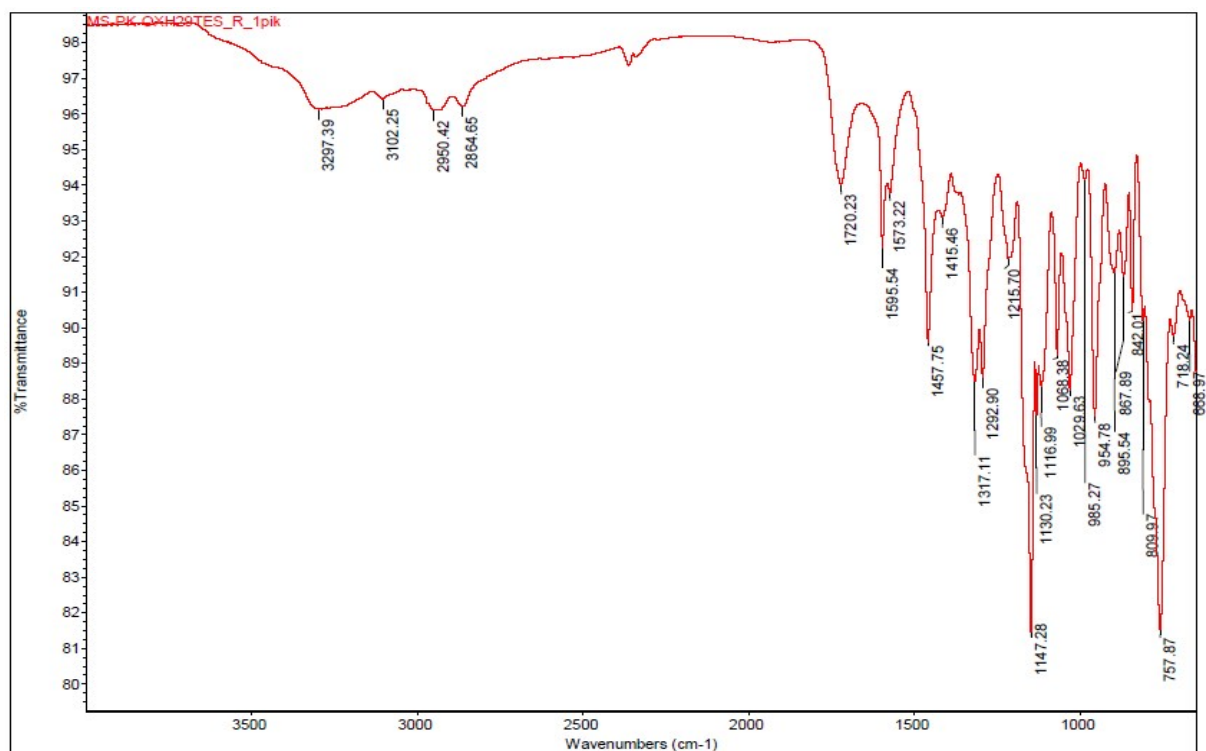


Figure S78. IR spectrum of 7t

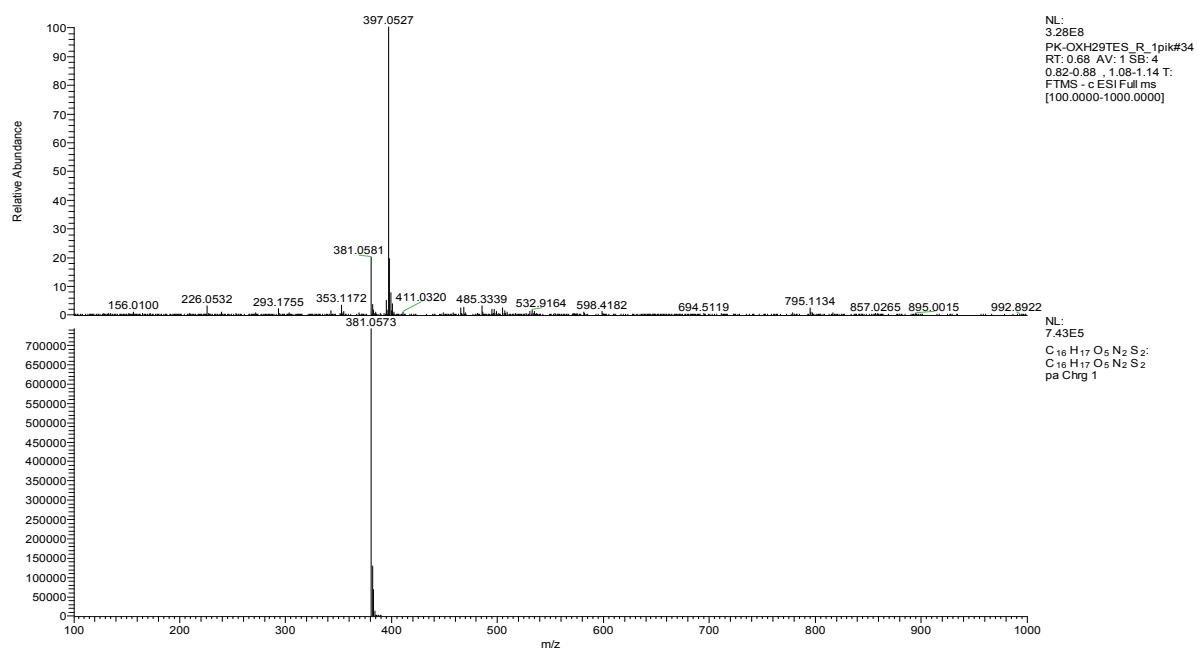
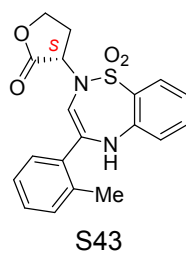


Figure S79. HRMS spectrum of 7t. Note: ion 397 belongs to the ammonium adduct originating from mobile phase.

(-)-(S)-3-(1,1-dioxo-4-(*o*-tolyl)benzo[*f*][1,2,5]thiadiazepin-2(5*H*)-yl)dihydrofuran-2(3*H*)-one 9h



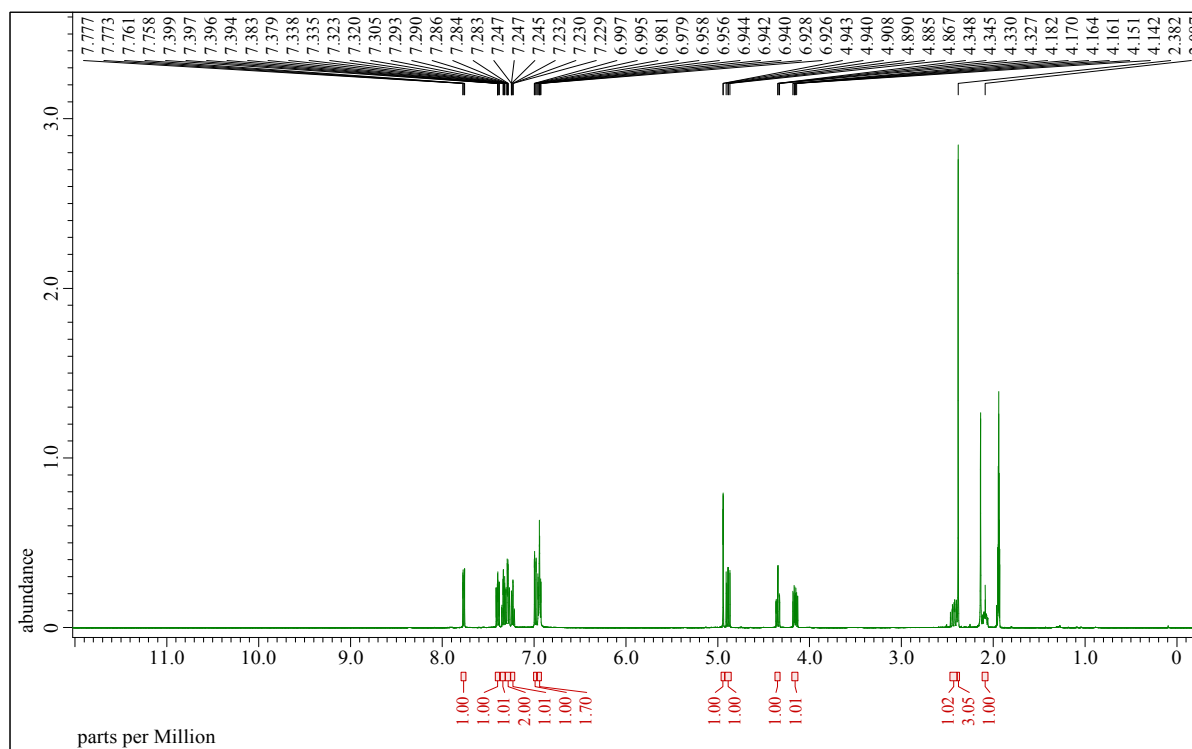


Figure S80. ^1H NMR spectrum of **9h** (500 MHz, $\text{MeCN-}d_3$)

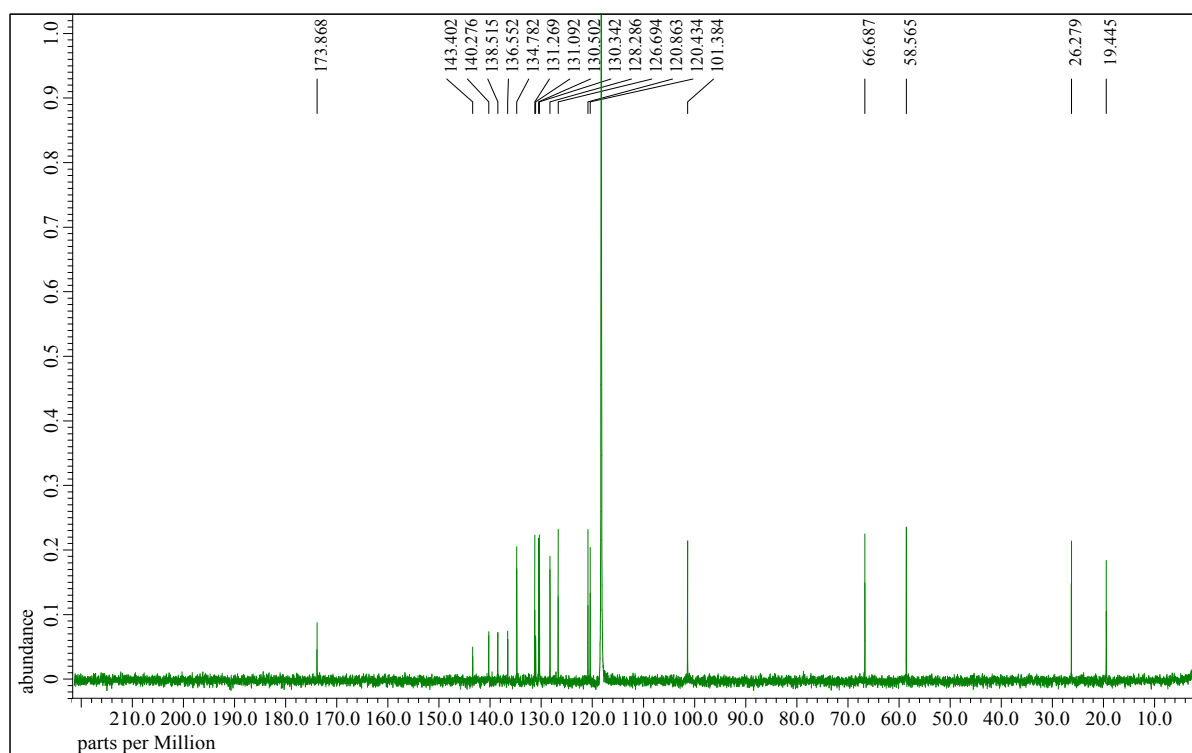


Figure S81. $^{13}\text{C}\{^1\text{H}\}$ NMR spectrum of **9h** (126 MHz, $\text{MeCN-}d_3$)

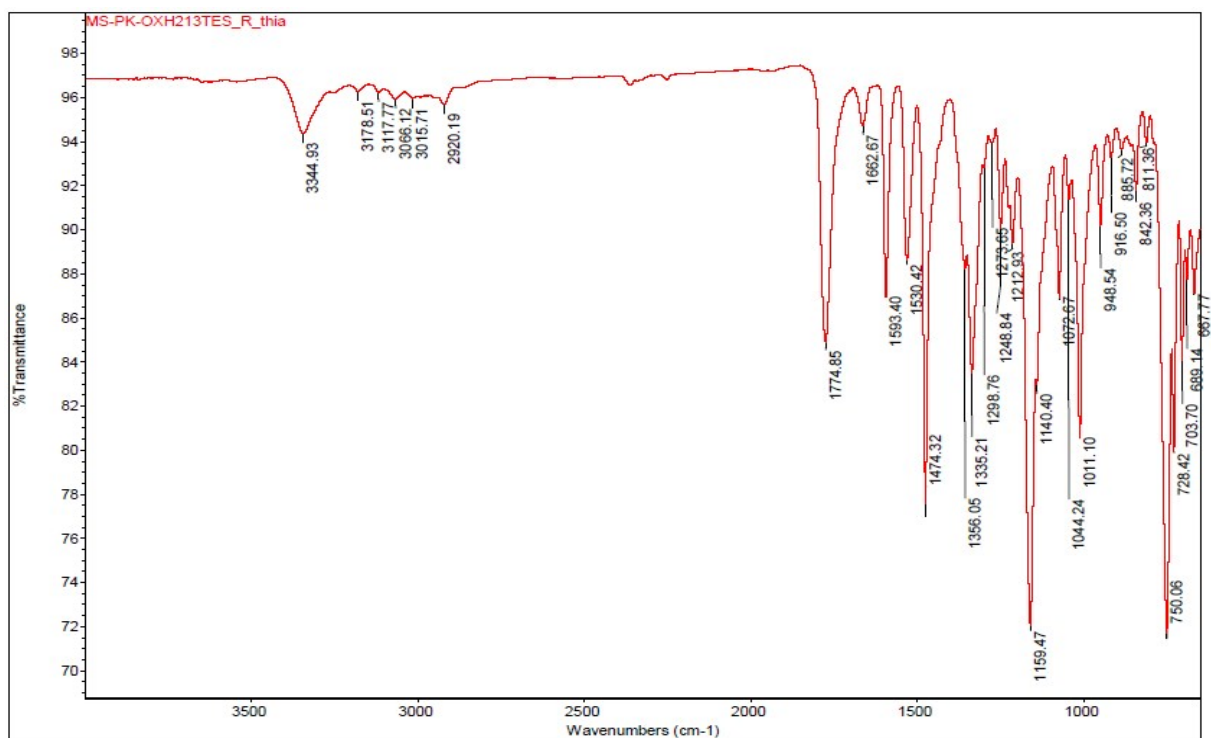


Figure S82. IR spectrum of 9h

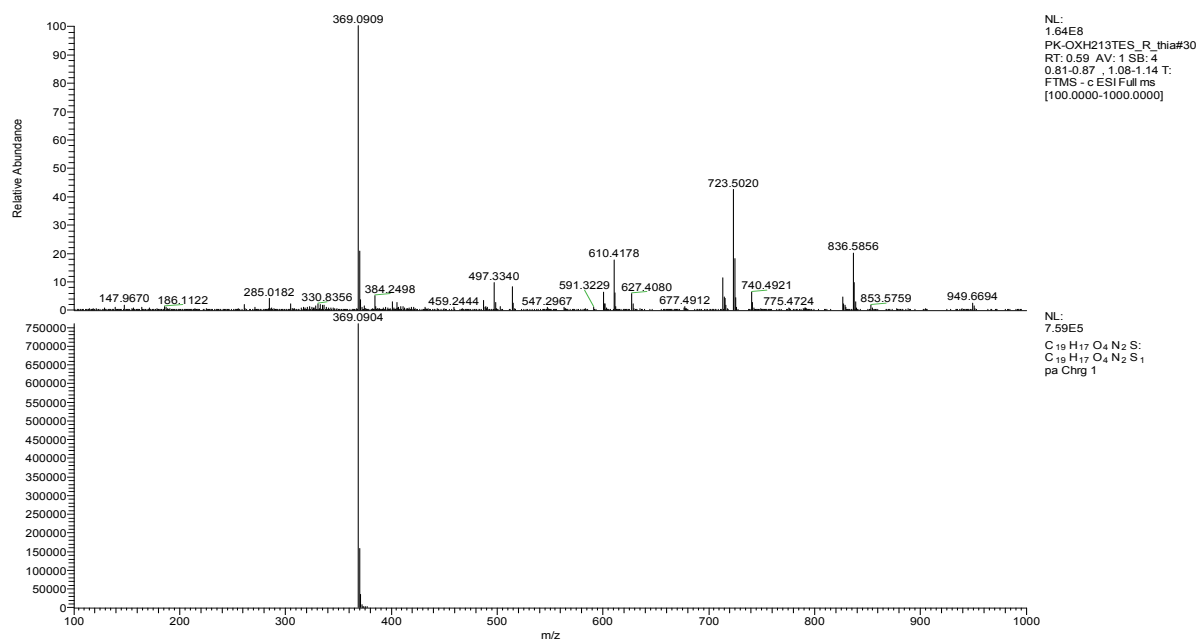
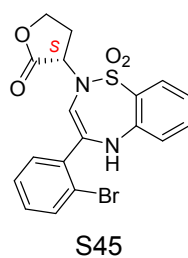


Figure S83. HRMS spectrum of 9h

(-)-(S)-3-(4-(2-bromophenyl)-1,1-dioxobenzo[*f*][1,2,5]thiadiazepin-2(5*H*)-yl)dihydrofuran-2(3*H*)-one 9j



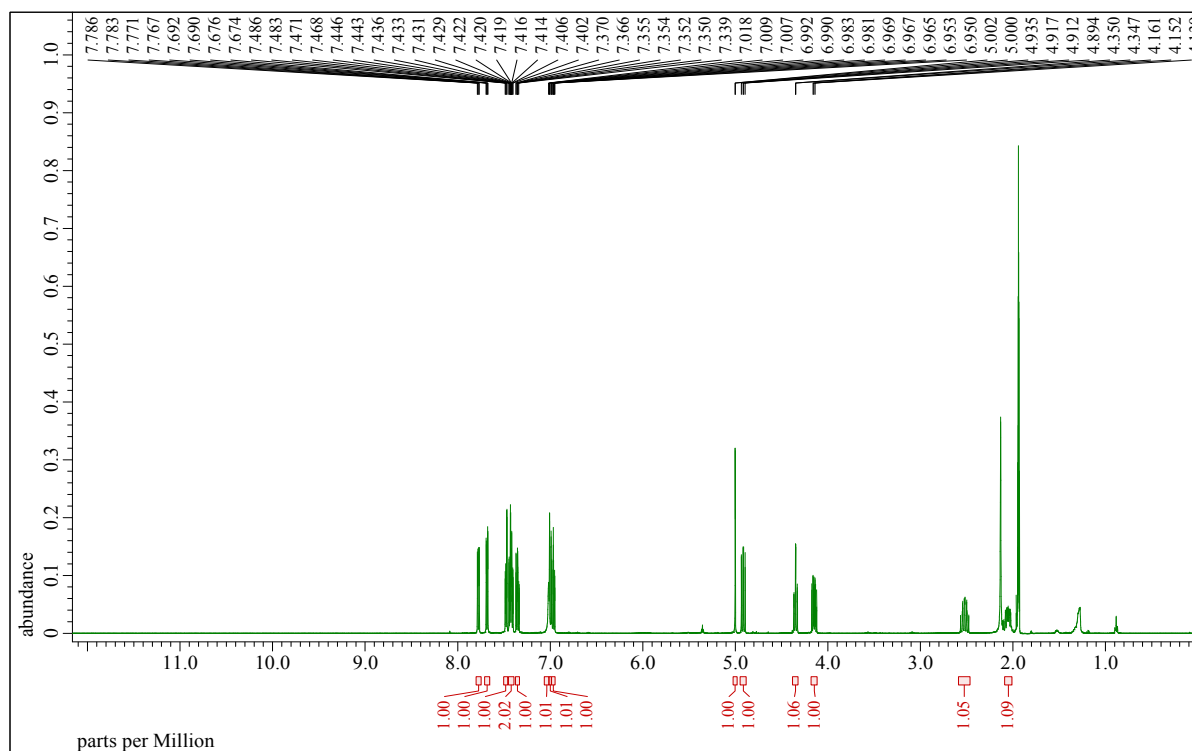


Figure S84. ^1H NMR spectrum of **9j** (500 MHz, $\text{MeCN-}d_3$)

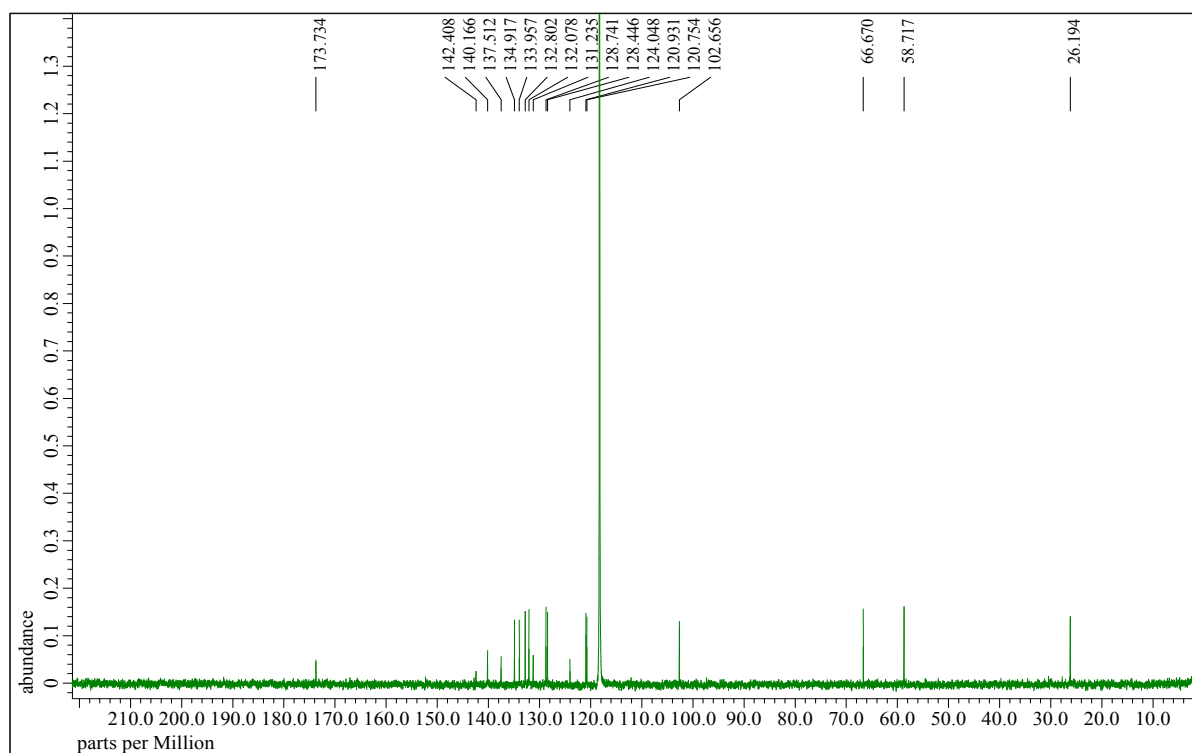


Figure S85. $^{13}\text{C}\{^1\text{H}\}$ NMR spectrum of **9j** (126 MHz, $\text{MeCN-}d_3$)

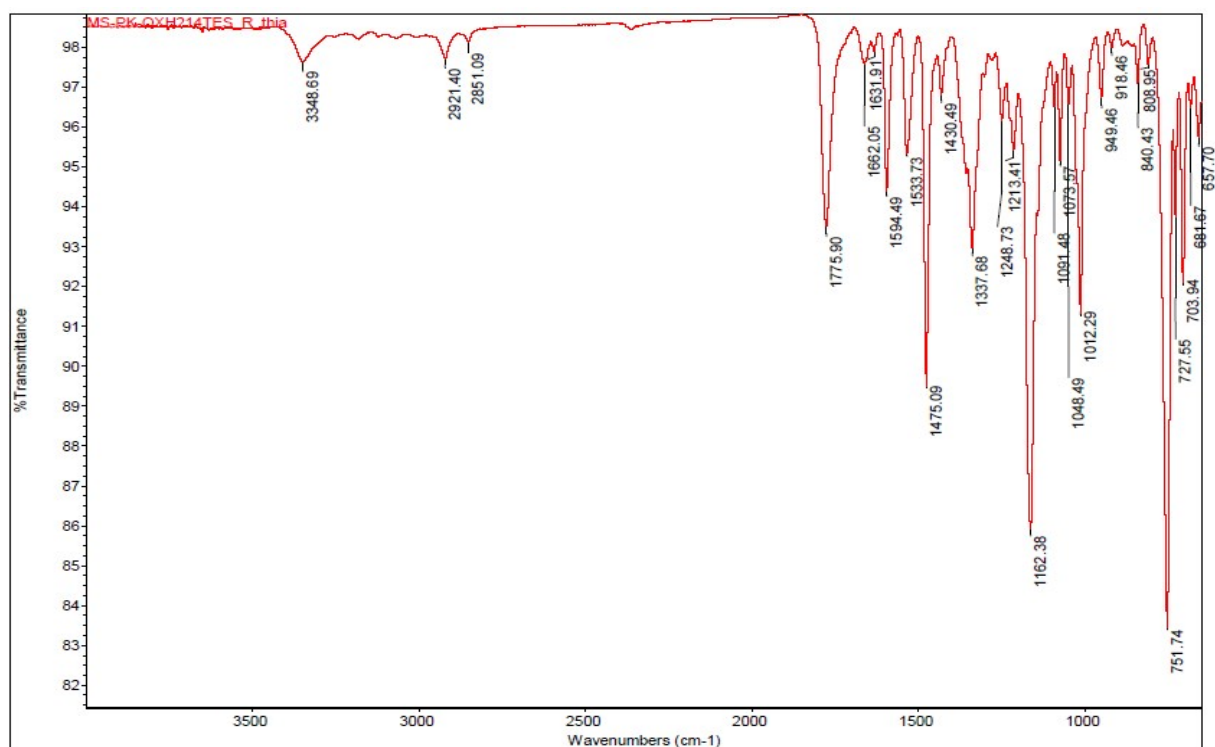


Figure S86. IR spectrum of **9j**

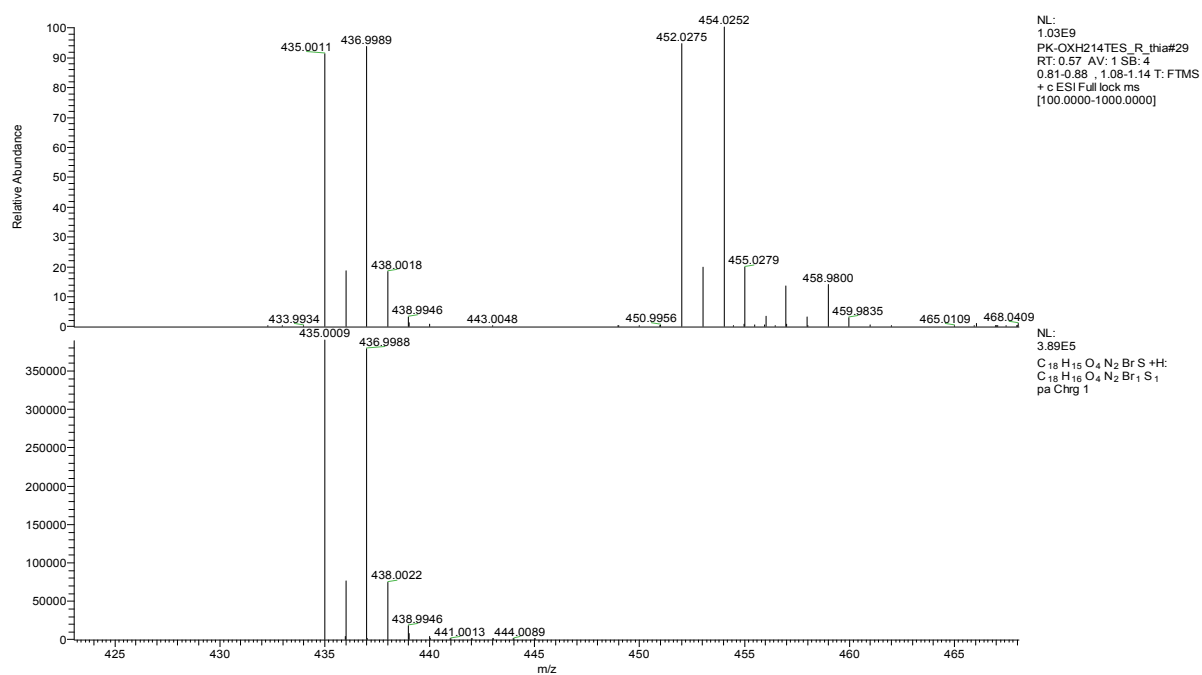
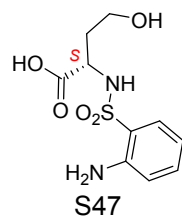


Figure 87. HRMS spectrum of **9j**. Note: ions 452 and 454 belongs to the ammonium adduct originating from mobile phase.

(+)-(S)-((2-aminophenyl)sulfonyl)-L-homoserine 10r



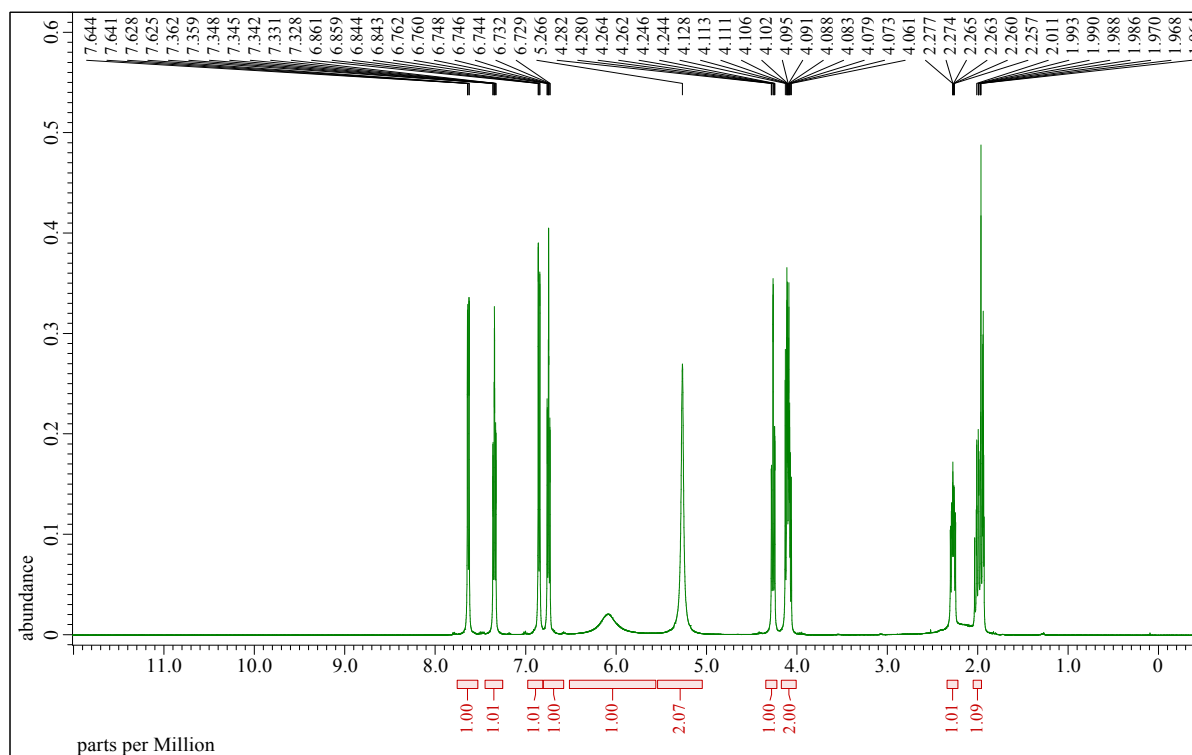


Figure S88. ^1H NMR spectrum of **10r** (500 MHz, $\text{MeCN-}d_3$)

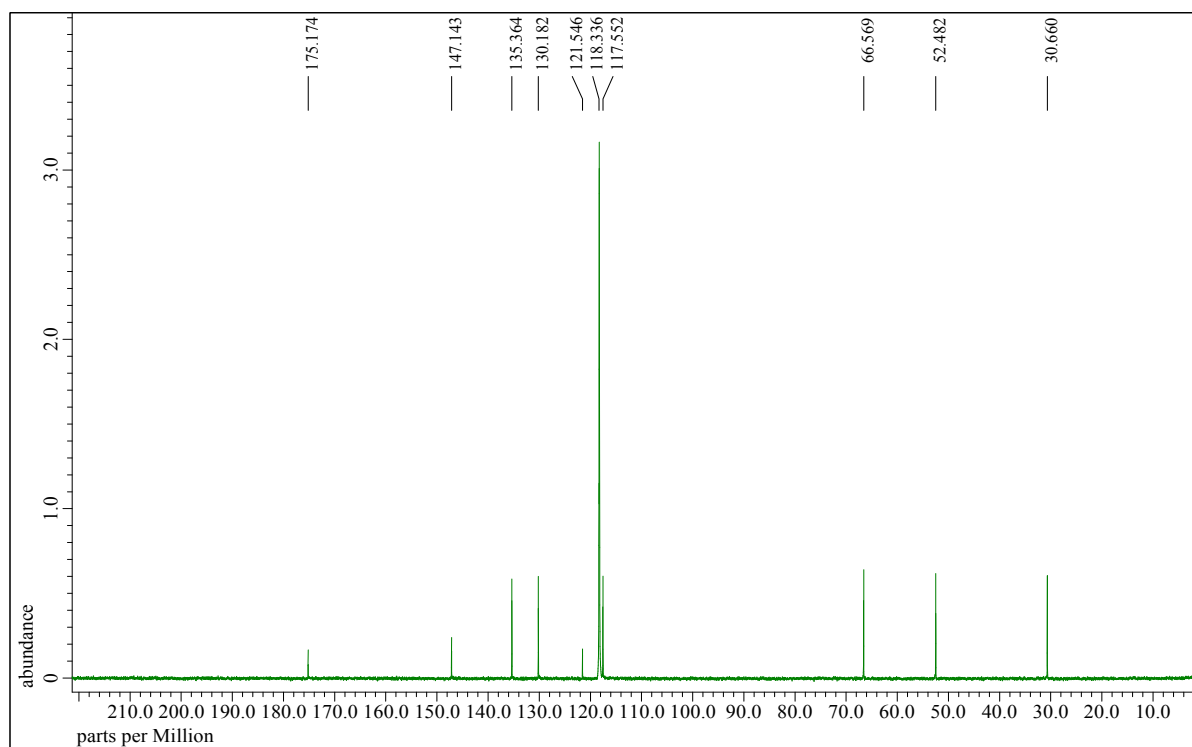


Figure S89. $^{13}\text{C}\{^1\text{H}\}$ NMR spectrum of **10r** (126 MHz, $\text{MeCN-}d_3$)

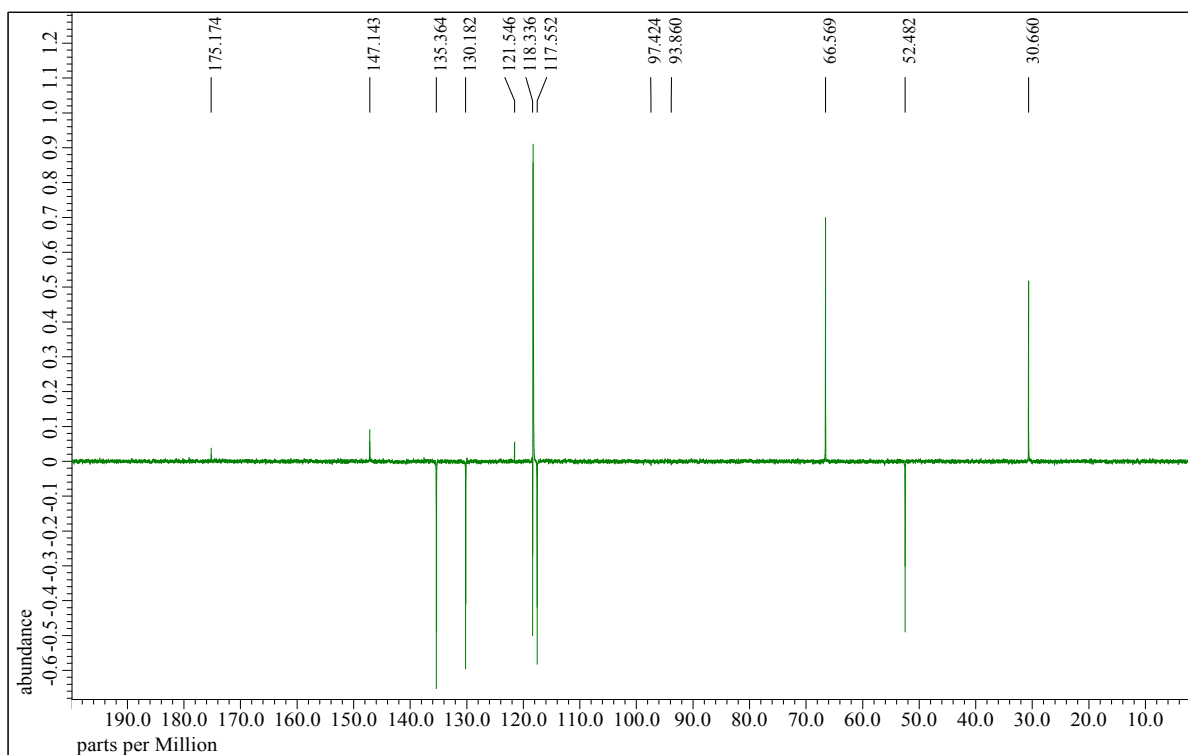


Figure S90. ^{13}C APT NMR spectrum of **10r** (126 MHz, MeCN-d_3)

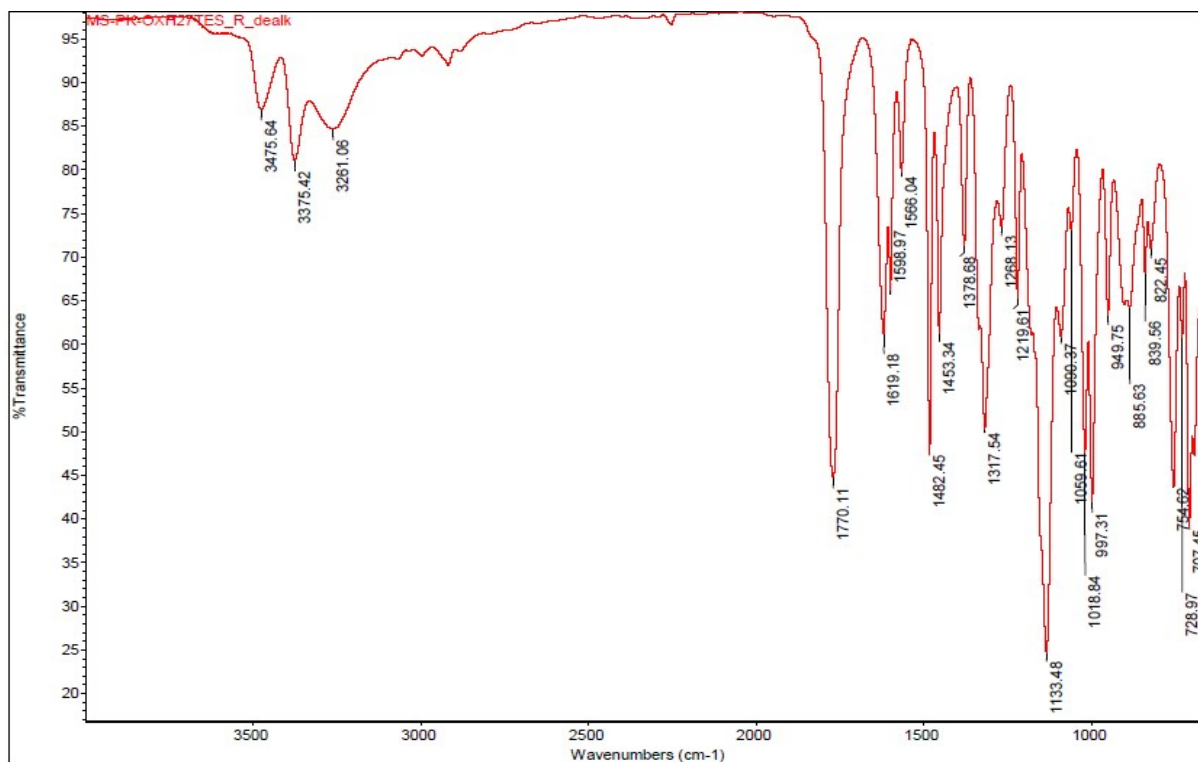


Figure S91. IR spectrum of **10r**

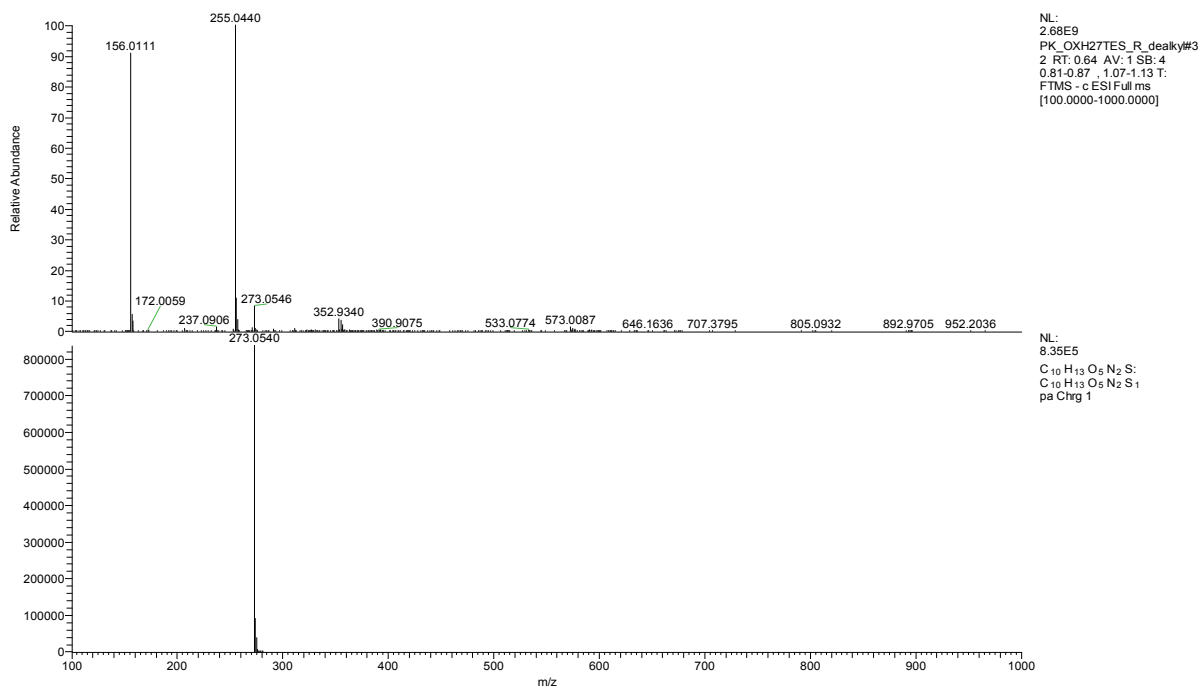


Figure S92. HRMS spectrum of **10r**

(-)-(*S*)-*N*-(4-methoxyphenethyl)-2-nitro-*N*-(2-oxotetrahydrofuran-3-yl)benzenesulfonamide **11n**

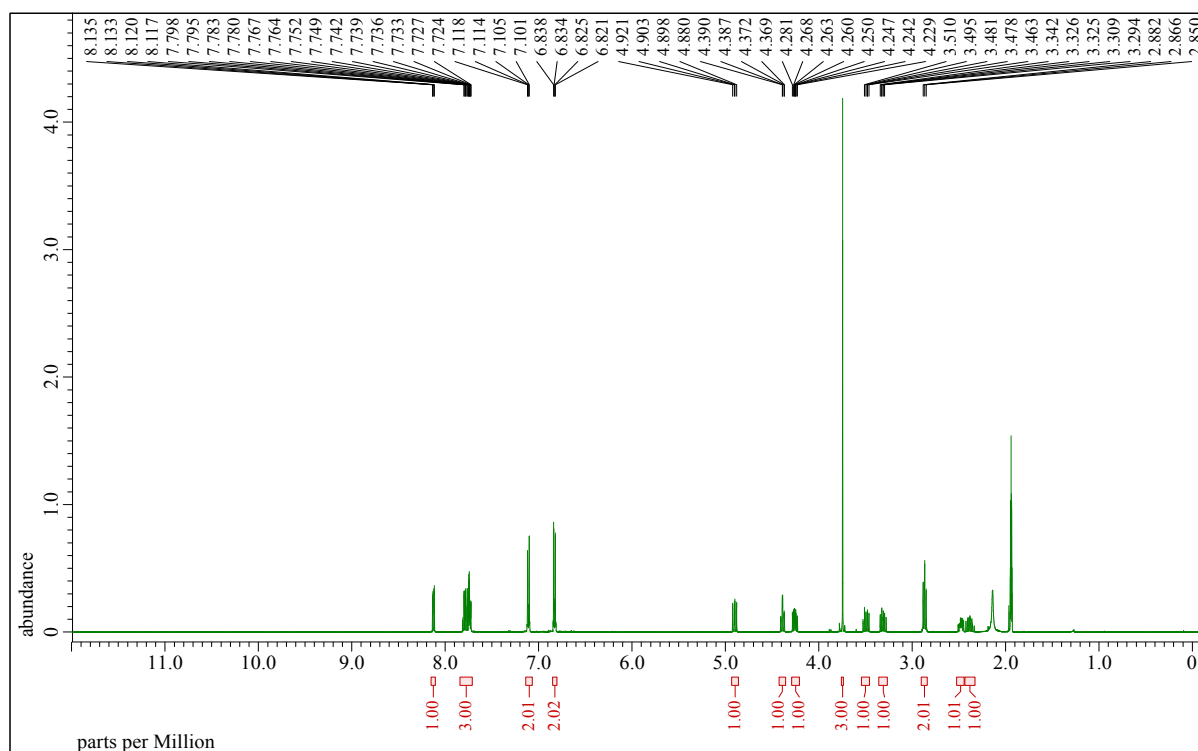
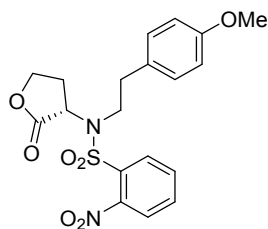


Figure S93. ¹H NMR spectrum of **11n** (500 MHz, MeCN-*d*₃)
S50

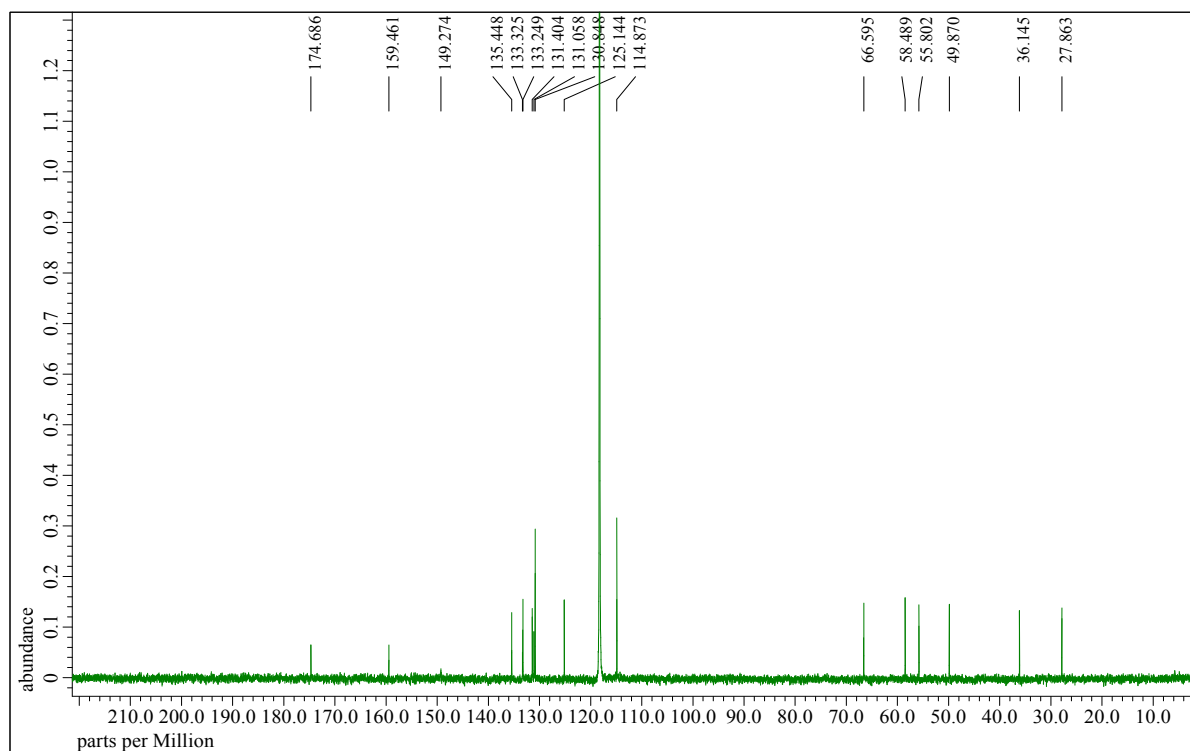


Figure S94. $^{13}\text{C}\{^1\text{H}\}$ NMR spectrum of **11n** (126 MHz, $\text{MeCN-}d_3$)

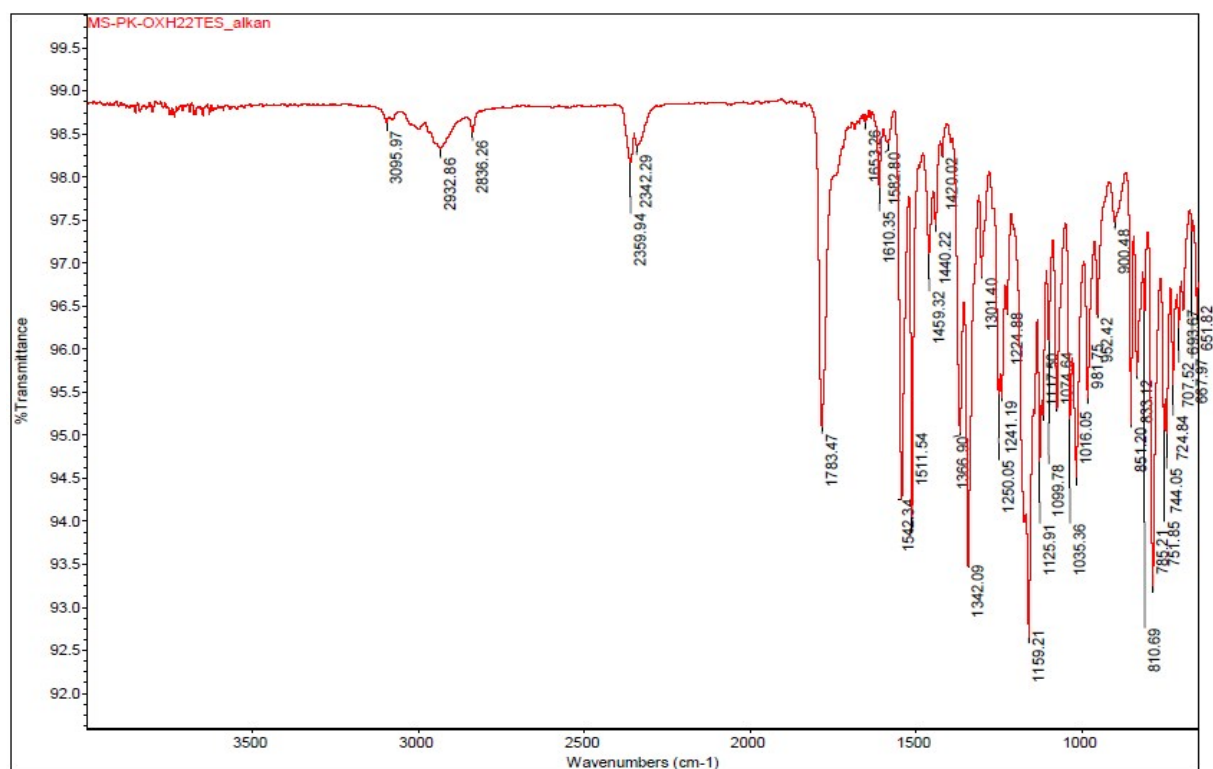


Figure S95. IR spectrum of **11n**

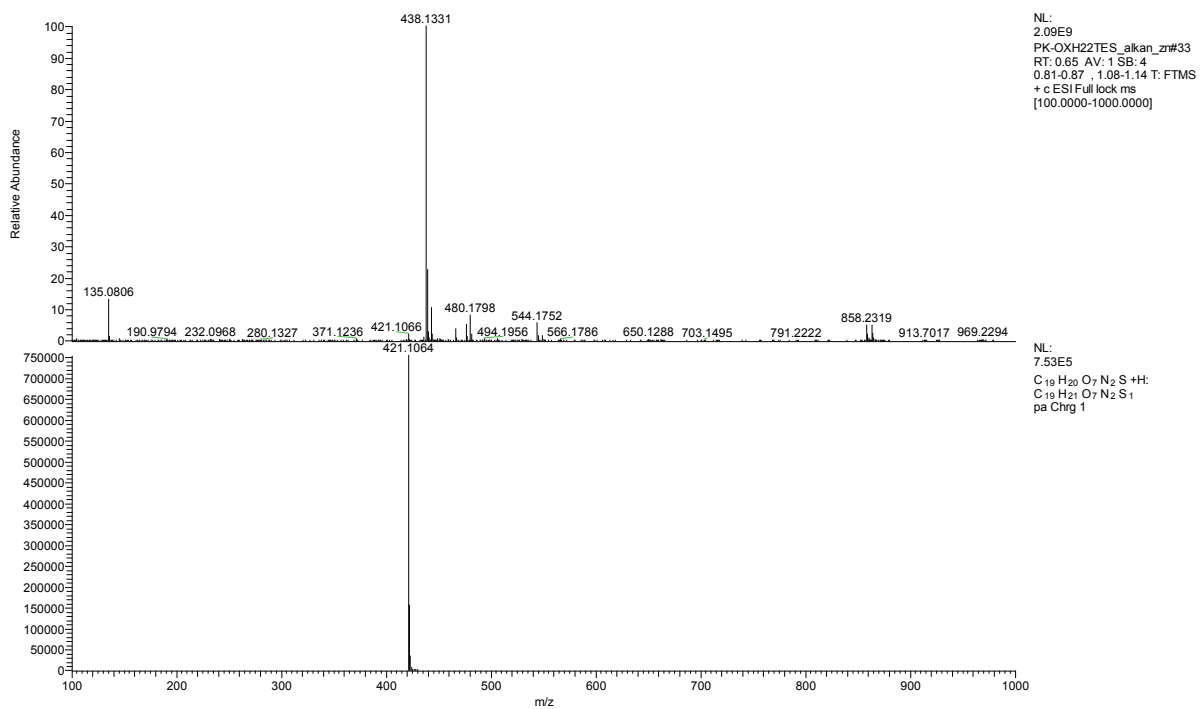


Figure S96. HRMS spectrum of **11n**. Note: ion 438 belongs to the ammonium adduct originating from mobile phase.